

5-2010

Myogenin modulates exercise endurance by altering skeletal muscle metabolism

james eric meadows

Follow this and additional works at: http://digitalcommons.library.tmc.edu/utgsbs_dissertations

 Part of the [Biology Commons](#), [Cell Biology Commons](#), and the [Exercise Physiology Commons](#)

Recommended Citation

meadows, james eric, "Myogenin modulates exercise endurance by altering skeletal muscle metabolism" (2010). *UT GSBS Dissertations and Theses (Open Access)*. Paper 17.

This Dissertation (PhD) is brought to you for free and open access by the Graduate School of Biomedical Sciences at DigitalCommons@The Texas Medical Center. It has been accepted for inclusion in UT GSBS Dissertations and Theses (Open Access) by an authorized administrator of DigitalCommons@The Texas Medical Center. For more information, please contact laurel.sanders@library.tmc.edu.

**MYOGENIN MODULATES EXERCISE ENDURANCE BY ALTERING SKELETAL
MUSCLE METABOLISM**

by

James Eric Meadows, M.S.

APPROVED:

William H. Klein, PhD, Supervisory Professor

Sharon Dent, PhD

Randy Johnson, PhD

Robert Schwartz, PhD

Marta Fiorotto, PhD

APPROVED:

**Dean, The University of Texas
Health Science Center at Houston
Graduate School of Biomedical Sciences**

**MYOGENIN MODULATES EXERCISE ENDURANCE BY ALTERING SKELETAL
MUSCLE METABOLISM**

**A
DISSERTATION**

**Presented to the Faculty of
The University of Texas
Health Science Center at Houston**

**And
The University of Texas
M.D. Anderson Cancer Center
Graduate School of Biomedical Sciences
in Partial Fulfillment**

**of the Requirements
for the Degree of
DOCTOR OF PHILOSOPHY**

**by
James Eric Meadows, M.S.
Houston, Texas**

May, 2010

Acknowledgements

I owe a great debt of gratitude to my advisor, William H. Klein, PhD, for his confidence, guidance, and patience as I matured as a scientist in his laboratory. I would also like to thank my supervisory committee: Sharon Dent, PhD, Marta Fiorotto, PhD, Randy Johnson, PhD, and Robert Schwartz, PhD. Their advice and guidance during my years as a graduate student have taught me how to think critically and stay focused on the most important of my aims. All experiments in this dissertation were performed as a collaborative effort with my friend and colleague, Jesse Flynn. He has helped make it possible to achieve a level of productivity and happiness in the lab that is unforgettable. Many thanks to my lovely fiancé, Annalisa Gradassi, whose invaluable input and feedback made this dissertation much easier to understand. Lastly, I'd like to thank my parents for their support and encouragement as I found my way to doing something I really enjoy – the biological sciences.

MYOGENIN MODULATES EXERCISE ENDURANCE BY ALTERING SKELETAL MUSCLE METABOLISM

PROJECT I – ABSTRACT

The function of myogenic regulatory factors (MRFs) during adult life is not well understood. The requirement of one of these MRFs, myogenin (*Myog*), during embryonic muscle development suggests an equally important role in adult muscle. In this study, we have determined the function of myogenin during adult life using a conditional allele of *Myog*. In contrast to embryonic development, myogenin is not required for adult viability, and *Myog*-deleted mice exhibited no remarkable phenotypic changes during sedentary life. Remarkably, sedentary *Myog*-deleted mice demonstrated enhanced exercise endurance during involuntary treadmill running. Altered blood glucose and lactate levels in sedentary *Myog*-deleted mice after exhaustion suggest an enhanced glycolytic metabolism and an ability to excessively deplete muscle and liver glycogen stores. Traditional changes associated with enhanced exercise endurance, such as fiber type switching, and increased oxidative potential, were not detected in sedentary *Myog*-deleted mice. After long-term voluntary exercise, trained *Myog*-deleted mice demonstrated an enhanced adaptive response to exercise. Trained *Myog*-deleted mice exhibited superior exercise endurance associated with an increased proportion of slow-twitch fibers and increased oxidative capacity. In a parallel experiment, dystrophin-deficient young adult mice showed attenuated muscle fatigue following the deletion of *Myog*. These results demonstrate a novel and unexpected role for myogenin in modulating skeletal muscle metabolism.

MYOGENIN TARGET GENE ACTIVATION IN ADULT MUSCLE STEM CELLS

PROJECT II - ABSTRACT

Skeletal muscle development is a complex biological process that is regulated by the expression of myogenic regulatory factors (MRFs). Myogenin (*Myog*) is one of these MRFs, which is involved in the differentiation and fusion of embryonic myoblasts and adult satellite (stem) cells into myofibers. Knockout of *Myog* during embryonic development results in perinatal death due to the loss of properly differentiated and fused muscle fibers (Hasty et al., 1993; Nabeshima et al., 1993). *MyoD* is a related MRF with broad functions during myogenesis, including involvement in myoblast specification and differentiation (Berkes and Tapscott, 2005). My hypothesis is that genes can be identified whose expression is strictly dependent on *Myog* versus *MyoD*. The aim of this project is to distinguish the differences in transcriptional activation by myogenin compared to MyoD. Regardless of the outcome, our experiments will provide a better understanding of the mechanisms underlying myoblast differentiation and muscle gene expression.

TABLE OF CONTENTS

Approval Page	i
Title Page	ii
Acknowledgements	iii
Abstract – Project I	iv
Abstract – Project II	v
Table of Contents	vi
List of Illustrations	ix
List of Tables	xii
Abbreviations	xiii

PROJECT I - MYOGENIN MODULATES EXERCISE ENDURANCE BY ALTERING SKELETAL MUSCLE METABOLISM	1
Chapter 1 – Introduction	2
Section 1.1 – Section 1.1 – Skeletal muscle fiber type and metabolism	2
Section 1.2 – Section 1.2 – The MRFs orchestrate skeletal muscle development	9
Section 1.3 – Section 1.3 – The MRFs and muscular dystrophy	16
Hypothesis & Specific Aims	21
Chapter 2 – Results	23
Section 2.1 - Myogenin is not essential for viability or maintaining normal weight during adult life	23
Section 2.2 - Lack of myogenin during adult life confers enhanced exercise endurance	23

Section 2.3 - Lack of myogenin alters blood metabolite concentrations during exhaustive exercise	34
Section 2.4 - Myogenin is not necessary to maintain normal muscle fiber type, aerobic potential, or expression of genes involved in fatty-acid metabolism	41
Section 2.5 – Mice lacking myogenin do not consume more food	50
Section 2.6 - The hypoglycemic state abolishes the enhanced exercise endurance of mice lacking myogenin	50
Section 2.7 - Mice lacking myogenin do not voluntarily run more than wild-type during running-wheel exercise	59
Section 2.8 - Superior adaptation to exercise training in mice lacking myogenin	70
Section 2.9 - Lack of myogenin during long-term exercise training increases slow-twitch fiber-type proportion and oxidative capacity of skeletal muscle	70
Section 2.10 - Myogenin regulates the expression of genes involved in metabolism and signal transduction during adult life	73
Section 2.11 - Myogenin is not essential for viability in dystrophin-deficient adult mice	78
Section 2.12 - Dystrophin-deficient mice exhibit reduced exercise endurance	78
Section 2.13 - Lack of myogenin in dystrophin-deficient adult mice attenuates reduced exercise endurance	84
Chapter 3 – Discussion	89
Section 3.1 - Myogenin modulates exercise endurance by altering skeletal muscle metabolism	89
Section 3.2 – The lack of myogenin enhances adaptation to exercise training	95
Section 3.3 – The lack of myogenin attenuates muscle fatigue associated with muscular dystrophy	101

PROJECT II - MYOGENIN TARGET GENE ACTIVATION IN ADULT MUSCLE STEM CELLS	103
Chapter 4 – Introduction	104
Hypothesis & Specific Aims	114
Chapter 5 – Results	119
Section 5.1 - Inducible myogenin expression in Tet-On- <i>Myog</i> -GFP adult muscle stem cells	119
Section 5.2 - Myogenin expression is doxycycline dose-dependent	119
Section 5.3 - Adult myogenin-target gene activation in myogenin-induced adult muscle stem cells	126
Chapter 6 – Discussion	133
Chapter 7 – Materials and Methods	138
References	152
Curriculum Vitae	162

LIST OF ILLUSTRATIONS

Page #

Project I

Figure 1 – Metabolism, fiber-type, and exercise performance	4
Figure 2 – The lactate shuttle (Cori Cycle)	7
Figure 3 – MRFs coordinate skeletal muscle development	10
Figure 4 – The requirement for myogenin throughout life	12
Figure 5 – <i>Myog</i> ^{flox} conditional allele	14
Figure 6 – Dystrophin and the dystrophin-associated complex	19
Figure 7 – Efficient deletion and viability of adult <i>Myog</i> -deleted mice	24
Figure 8 – Columbus Instruments Exer 3/6 Treadmill	26
Figure 9 – Low- and high-intensity running regimes	28
Figure 10 – <i>Myog</i> -deleted mice run significantly farther than wild-type mice during low-intensity exercise	30
Figure 11 – <i>Myog</i> -deleted mice consistently run farther than wild-type mice during high-intensity exercise	32
Figure 12 – <i>Myog</i> -deleted mice exhibit enhanced exercise capacity shortly after the deletion of <i>Myog</i> .	35
Figure 13 – <i>Myog</i> -deleted mice have normal blood lactate levels after low-intensity running	37
Figure 14 – <i>Myog</i> -deleted mice have reduced blood glucose levels after low-intensity running	39
Figure 15 – <i>Myog</i> -deleted mice exhibit a trend towards increased blood ketone levels after low-intensity running	42
Figure 16 – <i>Myog</i> -deleted mice have lower blood glucose levels after high-intensity exercise compared to wild-type mice	44

Figure 17 – <i>Myog</i> -deleted mice have higher blood lactate levels after high-intensity exercise compared to wild-type mice	46
Figure 18 – <i>Myog</i> -deleted mice exhibit normal proportions of Type-I and Type II-fibers in soleus muscle	48
Figure 19 – <i>Myog</i> -deleted mice exhibit normal expression of major myosin isoforms in gastrocnemius muscle	51
Figure 20 – <i>Myog</i> -deleted mice exhibit no difference in SDH activity in gastrocnemius	53
Figure 21 – <i>Myog</i> -deleted mice exhibit normal expression of fatty-acid metabolism genes in gastrocnemius muscle	55
Figure 22 – <i>Myog</i> deleted mice do not consume more food	57
Figure 23 – <i>Myog</i> -deleted mice do not run more than wild-type mice during high-intensity running in the fasted state	60
Figure 24 – <i>Myog</i> -deleted mice have normal blood lactate levels after high-intensity running in the fasted state	62
Figure 25 – <i>Myog</i> -deleted mice have normal blood glucose levels after high-intensity running in the fasted state	64
Figure 26 – The Klein Lab Voluntary Exercise Running Wheel	66
Figure 27 – Trained <i>Myog</i> -deleted mice do not voluntarily run farther or faster than trained wild-type mice	68
Figure 28 – Superior adaptation to exercise training in mice lacking myogenin	71
Figure 29 – Trained <i>Myog</i> -deleted mice exhibit an increase in Type-I slow-twitch fibers in soleus muscle	74
Figure 30 – Trained <i>Myog</i> -deleted mice exhibit an increase in Succinate Dehydrogenase enzyme activity in gastrocnemius muscle	76

Figure 31 – Myogenin regulates genes involved in metabolism and signal-transduction during adult life	79
Figure 32 – Dystrophin genotype validation via sequencing	81
Figure 33 – Mdx mice exhibit a reduced exercise capacity	85
Figure 34 – <i>Myog</i> deletion from Mdx mice attenuates reduced exercise capacity	87
Figure 35 – Potential Mechanism	99
Project II	
Figure 36 – Differentially expressed genes in embryonic muscle lacking myogenin	106
Figure 37 – Embryonic <i>Myog</i> -dependent target genes	108
Figure 38 – A global comparison of genes bound by <i>Myog</i> and MyoD reveals many distinct and overlapping target genes.	111
Figure 39 – Hypothesized model of myogenin target gene dependence	115
Figure 40 – Differentially expressed genes in muscle stems cells lacking myogenin	117
Figure 41 – Tet-On inducible myogenin system	120
Figure 42 – Clontech’s pRetroX-Advanced System	122
Figure 43 – Inducible myogenin expression in adult muscle stem cells	124
Figure 44 – <i>Myog</i> Expression is doxycycline dose-dependent	127
Figure 45 – Example experiment #1	129
Figure 46 – Example experiment #2	131
Figure 47 – Conserved E-box motifs are present within the TCRs of adult myogenin target genes	136
Supplemental Figure	
Figure 48 – Co-localized expression of myoglobin and succinate dehydrogenase activity	142

LIST OF TABLES

Table I – Description of selected and validated microarray genes

83

ABBREVIATIONS

bHLH – Basic Helix Loop Helix

DMEM – Dulbecco's Modified Eagle Media

FBS – Fetal Bovine Serum

MRF – Myogenic Regulatory Factor

MEF2 – Myocyte Enhancer Factor 2

Cre-ER – Cre-recombinase fused with an Estrogen Receptor domain.

CAGG(Cre-ER) – the Cre-ER transgene promoter consisting of a chimeric promoter/enhancer of cytomegalovirus immediate-early enhancer and the chicken β -globin promoter/enhancer.

PCR – Polymerase Chain Reaction

RT-qPCR – Reverse Transcription - quantitative PCR

ATP – Adenosine Triphosphate

SDH – Succinate Dehydrogenase

Tet-On – Tetracycline “On”

Dox – Doxycycline

MPC – Myogenic Precursor Cell

ChIP – Chromatin Immunoprecipitation

rtTA – reverse tetracycline transactivator protein

TRE – Tetracycline response element

IRES – Internal ribosomal entry site

PROJECT I

Myogenin modulates exercise endurance by altering skeletal muscle metabolism

Chapter 1 - Introduction

The regulation of gene expression in skeletal muscle is critical to orchestrating muscle exercise adaptation and regeneration upon injury. The ability of skeletal muscle to enhance exercise endurance and to resist fatigue are key adaptive mechanisms (Holloszy and Coyle, 1984). Skeletal muscle wasting and degeneration are commonly associated with the muscular dystrophies. Progressive muscle weakness and muscle degeneration occur when essential proteins that transmit force from within the skeletal muscle fiber to the extracellular matrix are dysfunctional (Wallace and McNally, 2009).

Section 1.1 – Skeletal muscle fiber type and metabolism

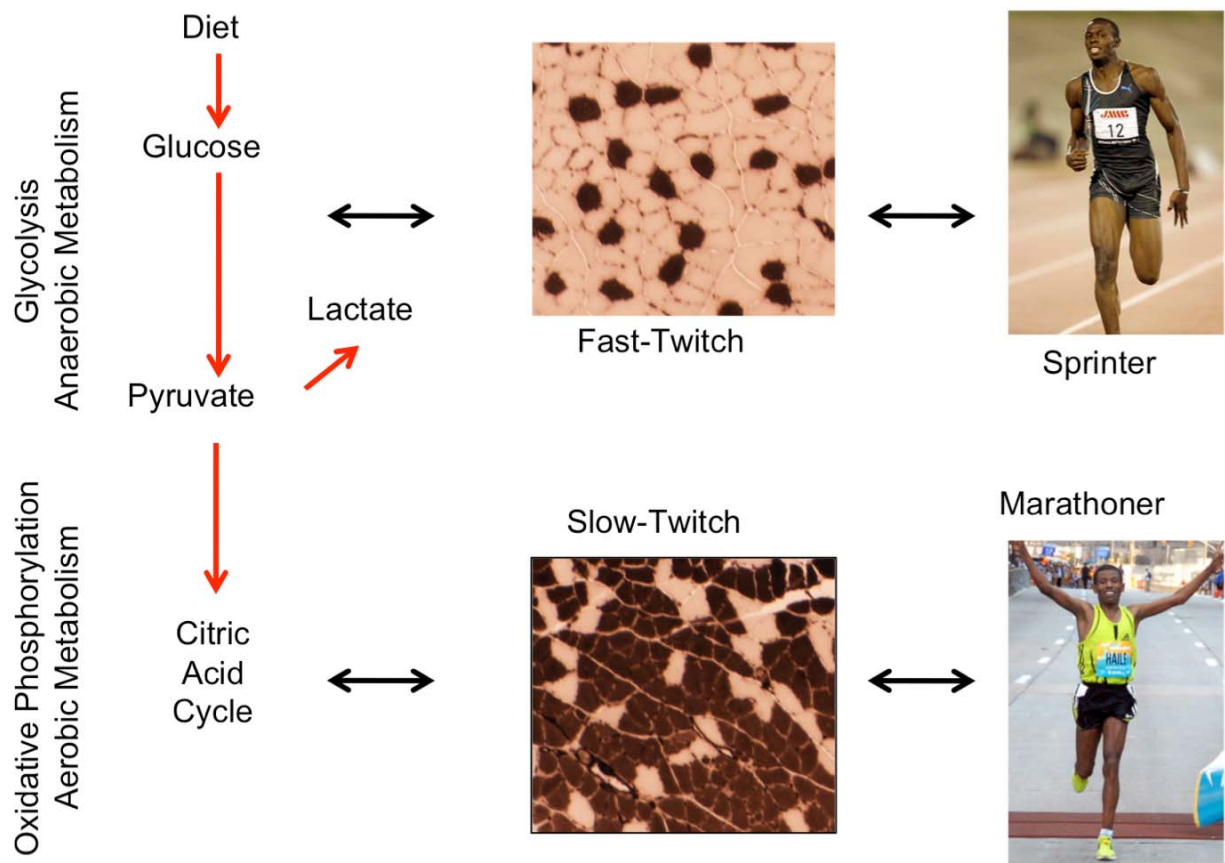
Skeletal muscle is composed of various types of myofibers, each exhibiting unique characteristics that allow contraction under low- and high-intensity loads and that perform work under aerobic and anaerobic conditions (Schiaffino et al., 2007). Although there are no widely accepted rules about defining muscle fiber types, classifications are often made using fiber color, expression of myosin isoforms, or metabolic profile (Schiaffino et al., 2007). In addition, different fiber types vary in their myoglobin content, mitochondrial density, vascularization, and resistance to fatigue. Muscle fibers are broadly separated into the following categories: Type-I slow-twitch oxidative, Type-IIa fast-twitch oxidative/glycolytic, and Type IIb fast-twitch glycolytic. Type IIx, and not Type-IIb is the major fast-twitch glycolytic muscle fiber in humans. Myosin isoforms are readily distinguished from one another by their ATP hydrolysis activity. Myoglobin content helps maintain oxygen consumption in exercising muscle (Cole, 1982). Mitochondrial content ultimately determines the oxidative capacity of skeletal muscle (Gnaiger, 2009). Increasing oxidative capacity has a direct relationship with the degree of

vascularization within the muscle. Type-I fibers represent a population of muscle fibers with high content of myoglobin and mitochondria, reliance on oxidative metabolism to perform work, and expression of myosin Type-I as the primary myosin isoform (Schiaffino et al., 2007) (Figure 1). Type-I fibers efficiently use oxidative metabolism to derive 36 molecules of ATP per glucose molecule via the TCA cycle from fatty acid oxidation. The muscles in marathon runners have an enriched proportion of Type-I muscle fibers and are fatigue resistant (Booth and Thomason, 1991). Type-IIa fibers represent a population of muscle fibers with a high content of myoglobin and mitochondria, reliance on both oxidative and glycolytic metabolism to perform work, and expression of myosin Type-IIa as the primary myosin isoform (Schiaffino et al., 2007). Like Type-I fibers, Type-IIa fibers efficiently produce ATP over long periods. Type-IIb and IIx fibers represent a population of muscle fibers with a low content of myoglobin and mitochondria, reliance on glycolysis to produce ATP for muscle contraction, and expression of myosin Type-IIb as the primary myosin isoform (Schiaffino et al., 2007) (Figure 1). The reliance of IIb and IIx fibers on glycolysis indicates they have a lower requirement for oxygen, however, due to incomplete oxidation, they yield of ATP is only 2. Type-IIb and IIx fibers do not require oxygen and make two molecules of ATP per glucose molecule. Although glycolytic metabolism is less efficient at ATP production than oxidative metabolism, it can generate ATP much faster overall. Sprinters have an enriched proportion of Type-IIx muscle fibers and are less fatigue resistant (Booth and Thomason, 1991).

The unique ability of Type-I and Type-II fibers to make ATP under various conditions also makes their substrates and metabolites unique. In general, Type-I and Type-IIa muscle fibers efficiently metabolize glucose and fatty acids to produce ATP. Type-IIb muscle fibers primarily metabolize glucose due to a low abundance of mitochondria (Hamilton and Booth, 2000; Schiaffino et al., 2007). Lactate is a major by-product of exercise metabolism, accumulating when only glycolysis can sustain the energy demand (i.e. high-intensity exercise)

Figure 1 – Metabolism, fiber-type, and exercise performance

Sprinters and marathoners have very different physical abilities that are primarily determined by muscle metabolism and fiber-type. Sprinters have enrichment in fast-twitch muscle fibers, which primarily derive ATP by glycolytic metabolism. Fast-twitch fibers using glycolytic metabolism allow sprinters to perform high-intensity work, but for only short periods of time prior to exhaustion. Sprinters primarily use glucose as an energy source. The onset of exhaustion is typically associated with the excess accumulation of lactate, which is produced when oxygen availability is limited (anaerobic conditions). Marathoners have enrichment in slow-twitch muscle fibers, which primarily utilize oxidative metabolism to perform work. Slow-twitch fibers using oxidative metabolism allow marathoners to perform low-intensity work, but for very long periods of time prior to exhaustion. Marathoners use fatty acids as an energy source, while efficiently conserving glucose. The onset of exhaustion in marathoners is typically associated with the depletion of liver and muscle glycogen stores (glucose). In marathoners, lactate is not created in excess because oxygen is plentiful (aerobic conditions). Myosin ATPase fiber-typing shown. Dark fibers represent Type-I slow fibers; Light fibers represent Type-II fibers.

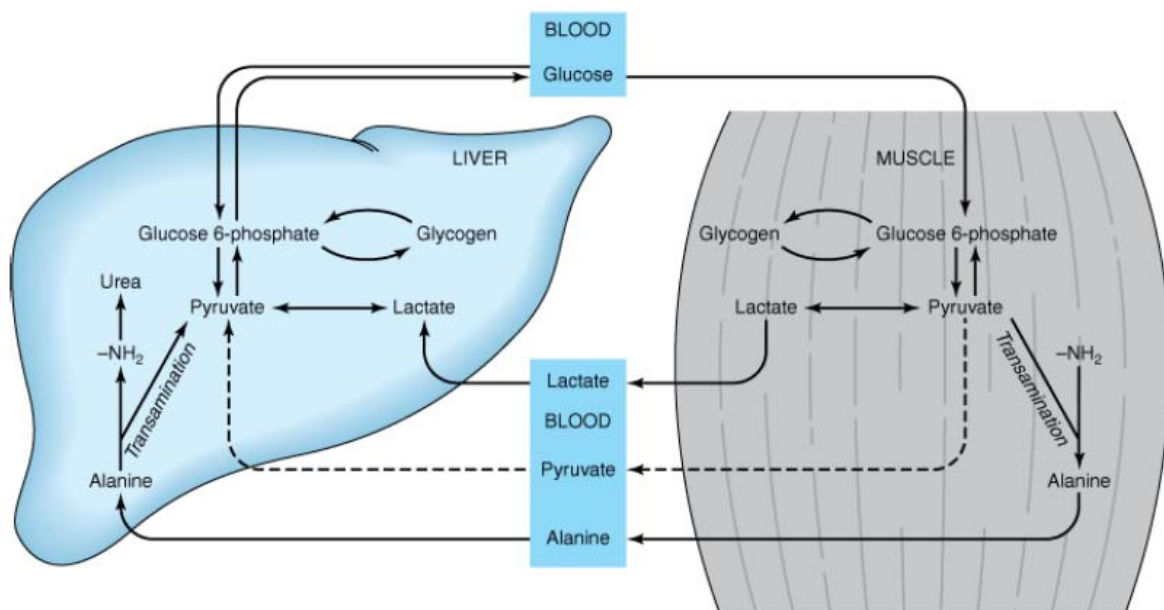


(Gladden, 2008). The lactate shuttle (Cori Cycle) is a metabolic pathway that involves skeletal muscle and liver (Figure 2). As glycolytic pathways are stressed in skeletal muscle (i.e. high-intensity exercise), pyruvate increases in the absence of oxygen, thus favoring lactate formation. Lactate is transported from working skeletal muscle into the bloodstream and is taken up by non-working skeletal muscle and the liver. Non-working skeletal muscle and liver convert lactate back into pyruvate, which is either metabolized via the TCA cycle or the liver converts the pyruvate into glucose (or glycogen) through gluconeogenesis and releases the glucose into the bloodstream. The working skeletal muscle will use the circulating blood glucose for energy production (Gladden, 2000).

Blood lactate concentration is arguably the most well-studied and often-measured metabolite associated with exercise performance. The production of lactate is not only an indication of glycolytic activity, but has been long argued to be directly associated with muscle fatigue and exhaustion (Asmussen, 1956; Fitts, 1994). While the onset of muscle fatigue is controversial, fatigue is generally thought to be due to the production of excess hydrogen ion (associated with lactic acid production) and the resultant drop in intramuscular pH levels (Fitts, 2004). Lactic acid ultimately breaks down within the skeletal muscle to form hydrogen and lactate ions. The clearance of these metabolites is essential to normal muscle function. Traditionally, the increased acidic environment is believed to be detrimental to sarcomeric contractile protein function (Fitts, 2004). Recently, however, other studies have shown that lactic acid production does not cause muscle fatigue and may actually enhance exercise performance (Allen and Westerblad, 2004; Allen et al., 2008; Pedersen et al., 2004). Thus, the ability to increase lactic acid production during exercise may confer enhanced high-intensity exercise endurance.

Figure 2 – The lactate shuttle (Cori Cycle)

As skeletal muscle performs work under anaerobic conditions, intramuscular lactate concentration increases. Lactate diffuses into the bloodstream and is taken up by the liver and non-working skeletal muscle. In the liver, lactate is converted back into pyruvate and is ultimately converted back into glucose through gluconeogenesis. The glucose is released back into the bloodstream and taken up by the working skeletal muscle, thus completing the cycle (Bender DA, 2009). Used with permission from McGraw Hill Publishers.



Section 1.2 – The MRFs orchestrate skeletal muscle development

Normal muscle development and function is dependent on the cooperation of all skeletal muscle components, and the proper expression of these components requires the activity of the Myogenic Regulatory Factors (MRFs). To better understand the mechanisms underlying muscle adaptation to exercise and muscular dystrophies during adult life, the precise function of MRFs in adult skeletal muscle must be determined. MRFs generally help coordinate the development, maintenance, and repair of skeletal muscle fibers (Charge and Rudnicki, 2004) (Figure 3). Myogenin is a basic-Helix-Loop-Helix (bHLH) skeletal muscle-specific transcription factor and a member of the MRF family. To efficiently activate the expression of muscle-expressed genes, myogenin heterodimerizes with ubiquitously expressed E-proteins in order to bind to the consensus E-box motif (Berkes and Tapscott, 2005; Olson and Klein, 1994). The Mef2 class of proteins also cooperate with MRFs to provide a synergistic effect on muscle gene activation (Black and Olson, 1998). When *Myog* expression is knocked out during embryonic myogenesis, mice die at birth due to the absence of skeletal muscle fibers, and thus leading to asphyxiation caused by poor diaphragm development (Hasty et al., 1993; Meadows et al., 2008; Nabeshima et al., 1993) (Figure 4). Importantly, *Myog* is the only single MRF knockout that exhibits gross skeletal muscle defects and no other factors compensate for its loss (Venuti et al., 1995). To better understand the role of MRFs during postnatal life, mice harboring *Myog*^{flox} conditional alleles were generated (Knapp et al., 2006) (Figure 5). Upon deletion of *Myog* immediately after birth, *Myog*-deleted mice reach adulthood with normal skeletal muscle (consistent myofiber area and non-centrally located nuclei) but proportionally smaller body size (Knapp et al., 2006; Meadows et al., 2008) (Figure 4).

Depending on environmental pressures (i.e. exercise training), mature skeletal muscle can undergo phenotypic changes that allow adaptation. Environmental cues lead to changes in

Figure 3 – MRFs coordinate skeletal muscle development

During embryonic myogenesis, myogenic precursor cells (MPCs) are specified to the myogenic fate with the expression of Pax3 or Pax7. Pax3-expressing MPCs go on to upregulate the myogenic program; in turn Myf5, MyoD, and Mrf4 commit the MPCs to the myogenic fate and coordinate their proliferation as myoblasts. Myogenin and MRF4 are next upregulated, causing the cells to differentiate and fuse with one another to form multi-nucleated myofibers. During postnatal and adult life, satellite (muscle stem) cells arise from Pax7-expressing MPCs, specifying them to the myogenic fate. Satellite cells reside alongside each myofiber in a quiescent state. Inductive cues, such as muscle growth or injury/repair, will initiate the myogenic program to contribute additional myofibers to the skeletal muscle. Modified from (Charge and Rudnicki, 2004).

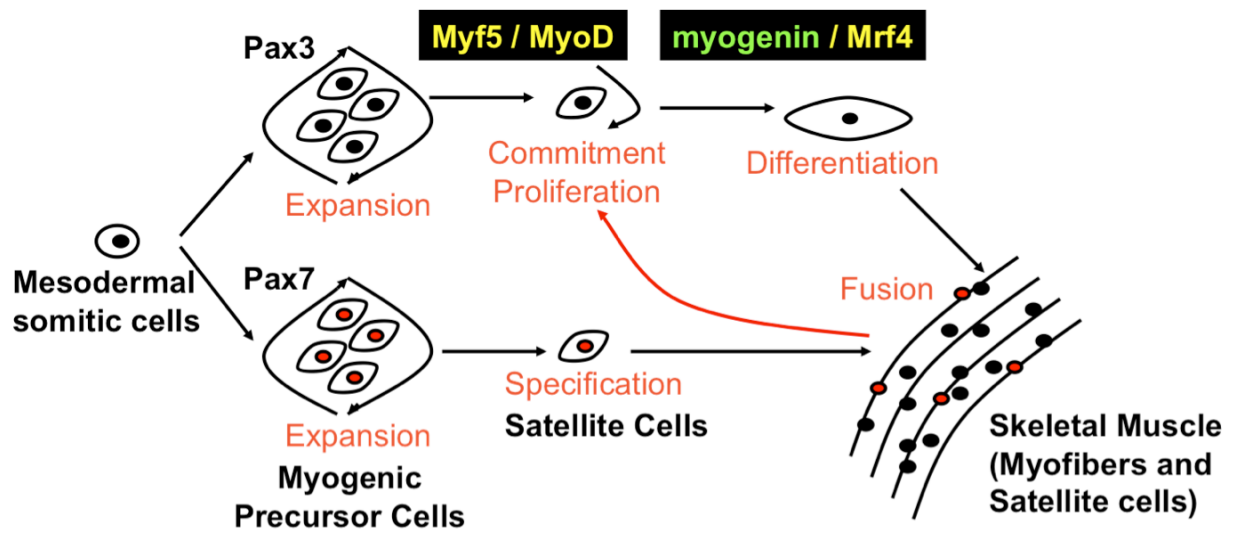


Figure 4 – The requirement for myogenin throughout life

Myogenin is required during embryonic and fetal myogenesis, and must be properly expressed until birth. The absence of myogenin after birth leads to proportionally reduced myofiber size and body mass (Meadows et al., 2008). The function of myogenin during adult life is addressed in this study.

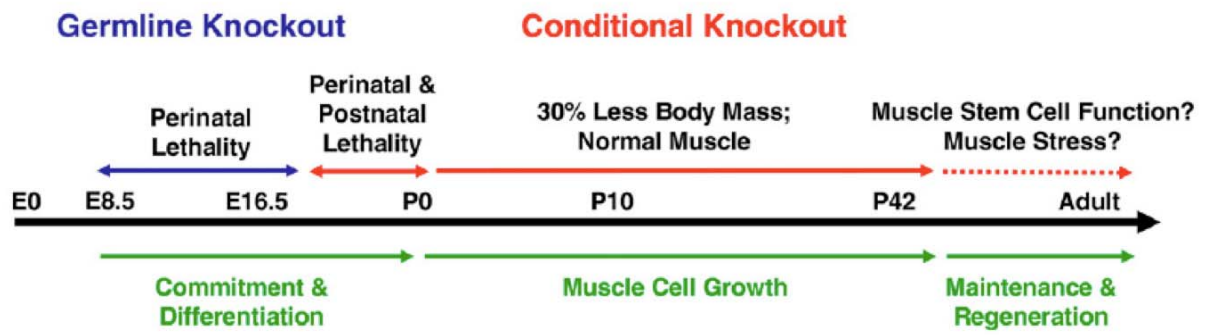
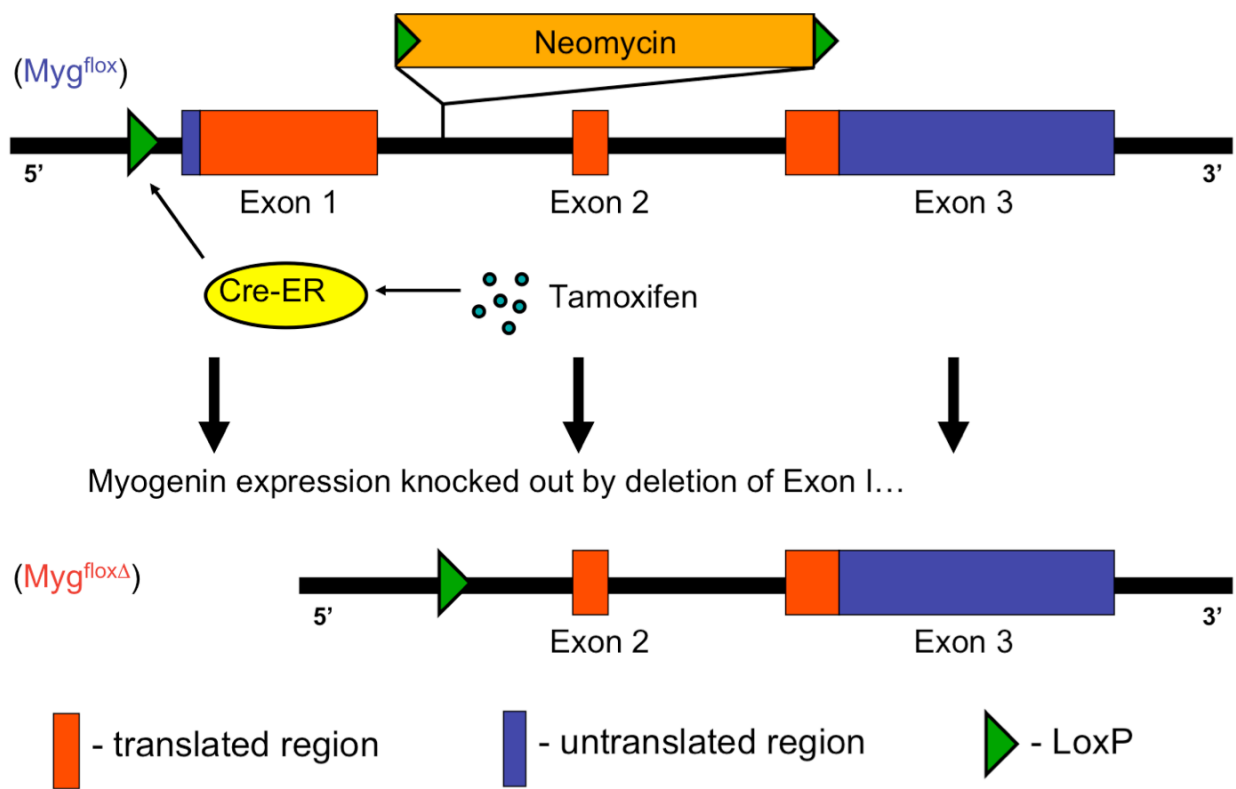


Figure 5 – *Myog*^{fllox} conditional allele

A conditional allele of *Myog* incorporates LoxP sites upstream of exon I and flanking a neomycin cassette inserted within intron I. A tamoxifen-inducible Cre-recombinase is utilized to conditionally mediate a site-specific recombination event at the LoxP sites. Following tamoxifen treatment, exon I of the *Myog*^{fllox} allele is recombined, giving a *Myog*-deleted locus.



nerve-dependent electrical activity and vascularization that ultimately determines muscle fiber characteristics. While dramatic changes in fiber type have been experimentally induced (Mayne et al., 1993; Windisch et al., 1998), less dramatic changes have been observed in mammals that have undergone exercise training (Fitts, 1996). Exercise training induces changes in metabolism that may be associated with changes in fiber type proportion (i.e. Type IIb/IIx to Type IIa) (Abdelmalki et al., 1996; Kraemer et al., 1995; Schluter and Fitts, 1994; Wang et al., 1993). Although the plasticity of muscle under experimentation and exercise training is well-described, the intramuscular pathways that link the changes in environmental demand to the necessary changes in contractile and metabolic proteins are poorly understood.

Section 1.3 – The MRFs and muscular dystrophy

The MRFs play a role in coordinating changes in gene expression with innervation-dependent electrical activity. For example, myogenin and MyoD expression were found to selectively accumulate in slow- and fast-twitch skeletal muscle fibers, respectively. This relationship is controlled by muscle innervation, as cross-reinnervation of a slow-twitch muscle by a nerve from a fast-twitch muscle shifts gene expression patterns towards a fast-twitch profile (Hughes et al., 1993). Yet, when myogenin was over-expressed in fast-twitch muscles, muscle enzyme activity shifted from glycolytic towards oxidative metabolism independent of changes in myosin isoform expression (Hughes et al., 1999). These results demonstrate that myogenin expression mediates the effects of muscle innervation on slow-twitch muscle fibers and activates properties associated with oxidative metabolism.

The role of MRFs in maintaining normal muscle gene expression in the presence of a muscular dystrophy is not well understood. Muscle-expressed proteins normally organize to form skeletal muscle's basic contractile apparatus, the sarcomere (Gordon et al., 2000).

Transmission of force from the sarcomere to the surrounding connective tissue is essential to survival. Muscle proteins involved in the generation and transmission of force are regularly turned over or damaged throughout adult life and require MRF activity for regeneration (Charge and Rudnicki, 2004). Absent or defective sarcomere components or neighboring dystrophin complex components lead to a multitude of muscular dystrophies, some of which are well understood but have no available cures (Blake et al., 2002; Kontrogianni-Konstantopoulos et al., 2009). Given that the development of these muscle components is dependent on MRF activity, understanding the precise requirement of each MRF (i.e. myogenin) in maintaining normal muscle gene expression in muscular dystrophies is essential to understanding muscle regeneration and developing therapies.

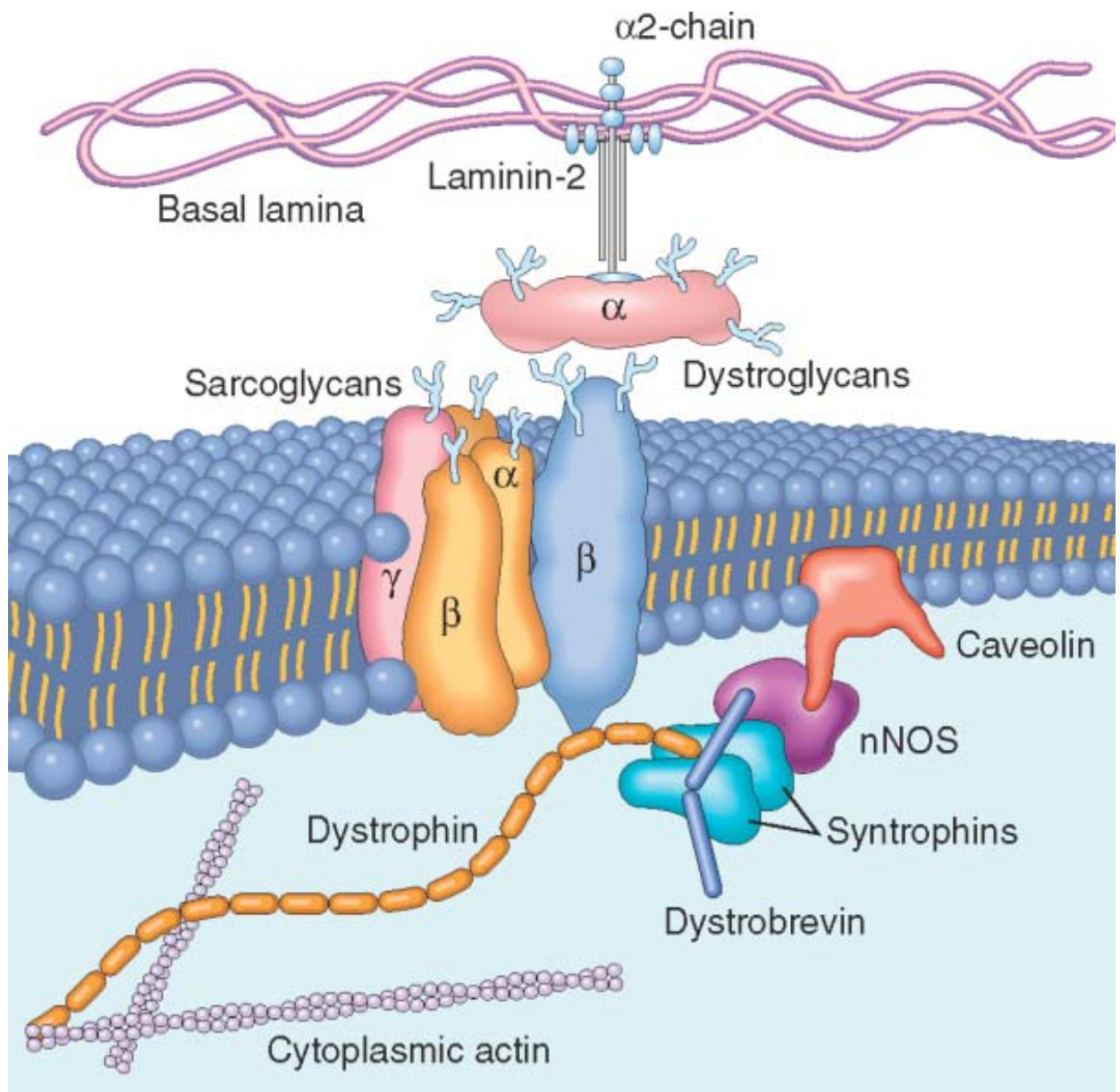
Duchenne Muscular Dystrophy, caused by dystrophin deficiency, is the most prevalent muscular dystrophy in humans, affecting 1 in 3500 newborn males (Blake et al., 2002). Dystrophin is the largest gene in the human genome at 2.4MB and is the major constituent of the dystrophin complex. The dystrophin complex serves to connect the cytoskeleton of the muscle fiber to the extracellular matrix and to functionally transmit forces produced at the sarcomere to the tendons and bones (Figure 6). Mice lacking dystrophin are not severely affected due to compensation by a homolog of dystrophin, utrophin (Grady et al., 1997). The severity of the dystrophin-deficiency in mice is highly dependent on background strain, although age and muscle use also plays a significant factor (Chamberlain et al., 2007; Heydemann et al., 2005). Exercise training mice with muscular dystrophy proves to be beneficial or deleterious, depending on the severity of the dystrophy, animal age, exercise intensity, exercise duration, and exercise type (aerobic vs resistive strength) (Carter et al., 2002).

This study aims to identify functions for myogenin during adult life and to determine whether exercise endurance and muscular dystrophy are affected by the loss of myogenin. We hypothesize that myogenin is required for muscle function and maintenance of normal skeletal

muscle metabolism during adult life. If the hypothesis is correct, the lack of myogenin should adversely affect exercise endurance and dystrophic skeletal muscle by disrupting the normal expression of critical skeletal muscle enzymes and components.

Figure 6 – Dystrophin and the dystrophin-associated complex

Dystrophin is a protein that helps hold together the muscle cell wall (sarcolemma). Dystrophin anchors actin filaments within the myofiber to the sarcolemmal membrane, providing both structural support and a means for force transduction. Other proteins, such as laminin, dystroglycan, and sarcoglycan are found in the dystrophin-associated complex and play similar roles in anchoring myofibers alongside the basal lamina. Robbins & Cotran – Pathologic Basis of Disease, 2010. Used with permission from Elsevier Publishing.



Hypothesis

Myogenin is required for muscle function and maintaining normal skeletal muscle metabolism during adult life. The lack of myogenin will adversely affect exercise endurance and dystrophic skeletal muscle by disrupting the normal expression of critical skeletal muscle metabolic enzymes and structural components.

Specific Aims

- 1.) **Determine whether myogenin is required for adult muscle function.** We will conditionally delete *Myog* and characterize *Myog*-deleted mice. Functional studies such as involuntary and voluntary exercise will be used to test muscle function. Blood metabolite levels, fiber type, oxidative capacity, and gene expression will be analyzed for changes associated with exercise.
- 2.) **Determine whether endurance exercise is dependent on myogenin.** *Myog*-deleted mice will be stressed during adult life using voluntary and involuntary exercise. Muscle function and exercise capacity will be assayed by measuring average distance, average speed, and maximum speed during exercise.
- 3.) **Determine whether muscle maintenance and regeneration occur normally in dystrophic mice lacking myogenin.** *Myog* will first be deleted from dystrophic young adult mice. Exercise performance will then be measured using involuntary treadmill running. Myofiber pathology will be analyzed with H&E staining and dystrophin

antibody staining. In addition, myofiber ultrastructure will be analyzed using Transmission Electron Microscopy (TEM).

Chapter 2 - Results

Section 2.1 - Myogenin is not essential for viability or maintaining normal weight during adult life

To determine whether myogenin is required during adult life, *Myog*^{flox/flox}; *Cre*⁺ mice were injected with tamoxifen between 6 and 8 weeks of age, the age at which mice nearly complete postnatal growth and reach adulthood. Control mice not expressing the tamoxifen-inducible Cre were also injected with tamoxifen. Average deletion of *Myog* obtained was 96% as determined by qPCR (Figure 7A). Skeletal muscle-specific reduction of *Myog* transcripts was determined by RT-qPCR to be less than 1% in gastrocnemius muscle (Figure 7B). By one year of age, *Myog*-deleted mice displayed no observable changes in behavior or mobility and weighed the same as control mice (Figure 7C). These results indicate that sedentary mice do not require myogenin for survival during adult life.

Section 2.2 - Lack of myogenin during adult life confers enhanced exercise endurance

A physiological function for myogenin during adult life was discovered when mice underwent involuntary exercise regimes using a rodent treadmill (Figures 8, 9). Using a low-intensity exercise protocol, *Myog*-deleted mice ran 2.4-fold farther than control mice (Figure 10). On average, wild-type mice ran 4,000 meters until exhaustion while *Myog*-deleted mice ran 10,000 meters until exhaustion. Next, we subjected mice to a high-intensity exercise protocol where we observed that *Myog*-deleted mice consistently ran 1.6-fold farther than control mice during 12 days of treadmill running (Figure 11). On average, wild-type mice ran 382 meters daily until exhaustion while *Myog*-deleted mice ran 599 meters daily until exhaustion. Mice used in these

Figure 7 – Efficient deletion and viability of adult *Myog*-deleted mice

qPCR reveals efficient 96% deletion of *Myog* genomic DNA in adult mice following tamoxifen treatment (n=10 wild-type control, n=12 *Myog*-deleted) (A). At one year of age, hind limb muscle of *Myog*-deleted mice exhibited dramatically reduced expression of *Myog* less than 1% of wild-type control mice, as shown by RT-qPCR (n=3 per group) (B). One-year-old *Myog*-deleted mice weigh the same as wild-type control mice (n=11 per group) (C). Blue bars indicate wild-type control values; red bars indicate *Myog*-deleted values. Error bars represent one standard deviation. *p<0.05

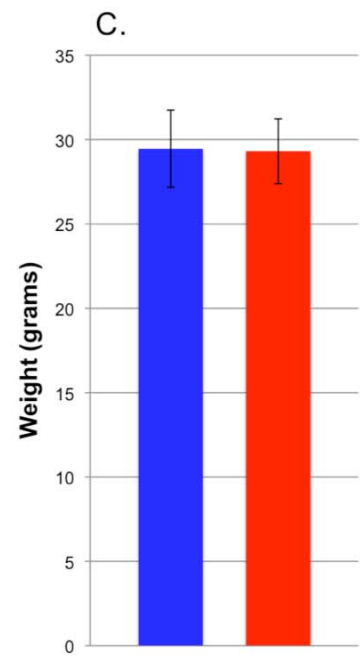
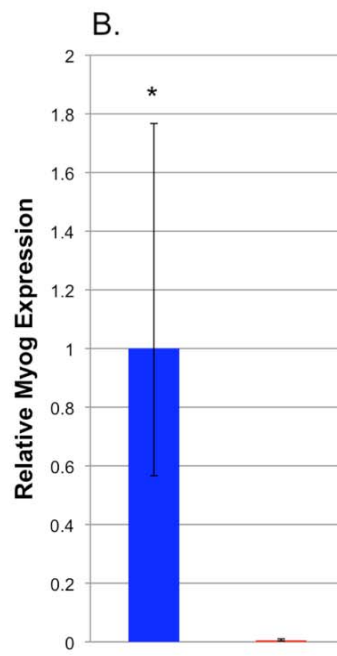
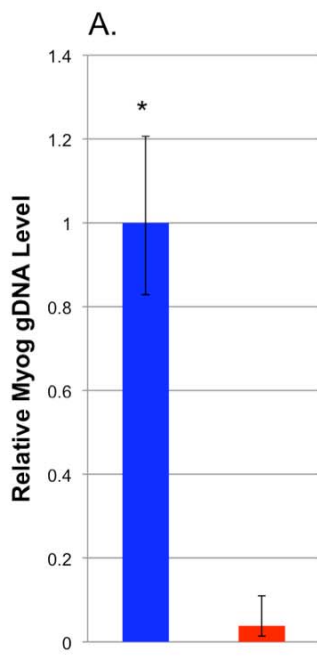


Figure 8 – Columbus Instruments Exer 3/6 Treadmill

To facilitate exercise-induced muscle stress and injury, a Columbus Instruments Exer 3/6 Treadmill was used with low- and high-intensity protocols (see Methods & Figure 9). The treadmill allows for user-defined features such as incline and speed control. An electrical stimulus grid at the rear of the belt provides encouragement to run until exhaustion. Six running lanes accommodate up to 6 mice per running experiment.

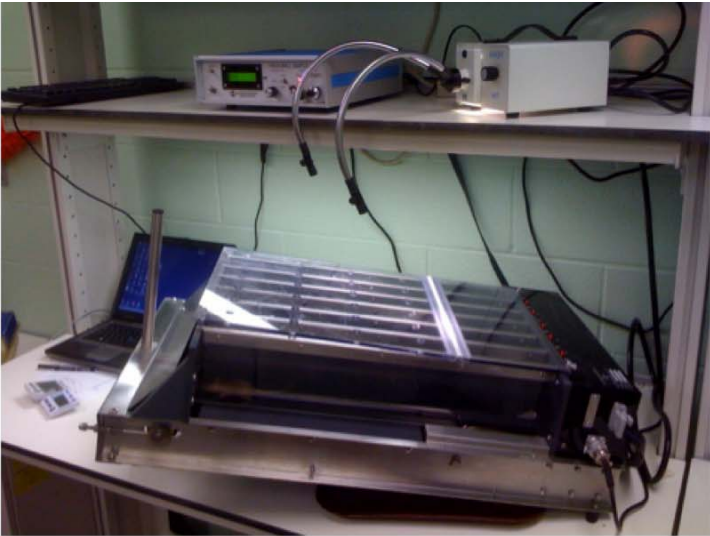


Figure 9 – Low- and high-intensity running regimes

Low-intensity exercise running (green line) consists of a 30 minute warmup period at 10 M/min followed by running at 20 M/min until exhaustion. High-intensity running (red line) consists of a 10 minute warmup period at 10 M/min followed by running at an additional 2 M/min every 2 minutes until exhaustion. Exhaustion is defined when mice prefer to stand on the electrical stimulus grid for 10 seconds rather than run.

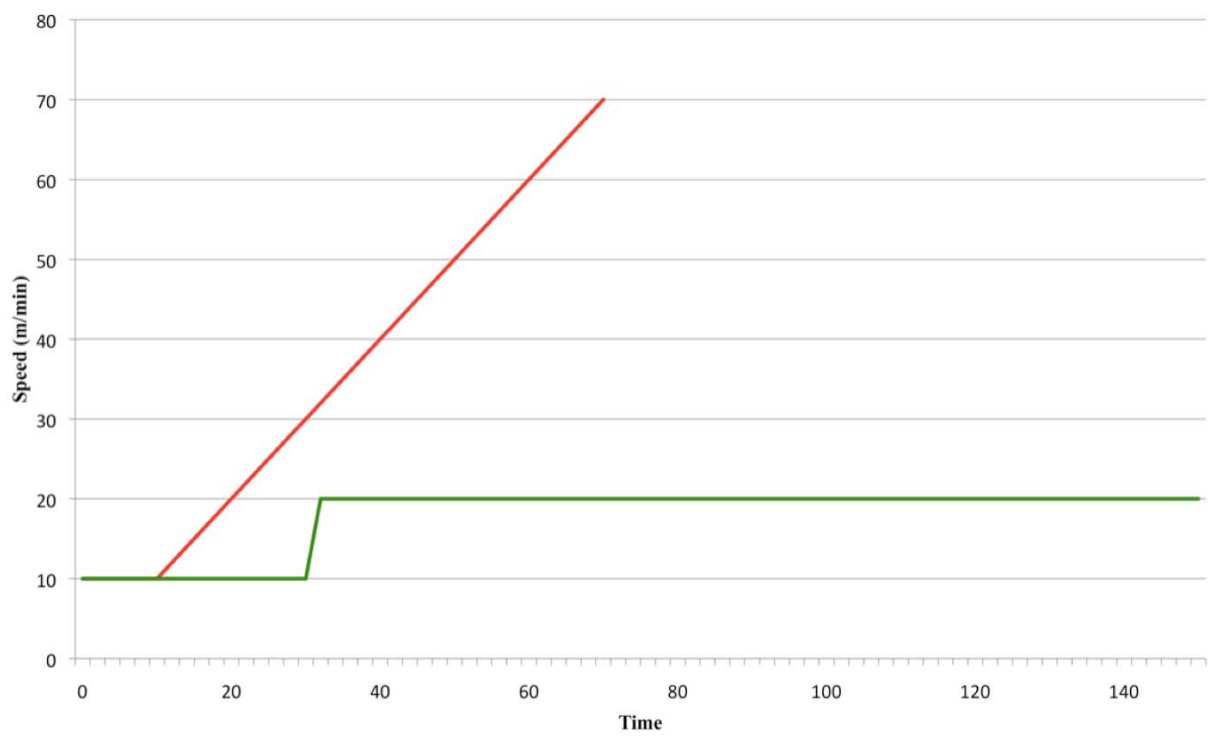


Figure 10 – *Myog*-deleted mice run significantly farther than wild-type mice during low-intensity exercise. During low-intensity exercise, *Myog*-deleted mice ran 2.4-fold farther than wild-type mice (*Myog*-deleted n=4, wild-type n=6). Blue bar indicates wild-type control values; red bar indicates *Myog*-deleted values. Error bars represent one standard deviation. *p<0.05

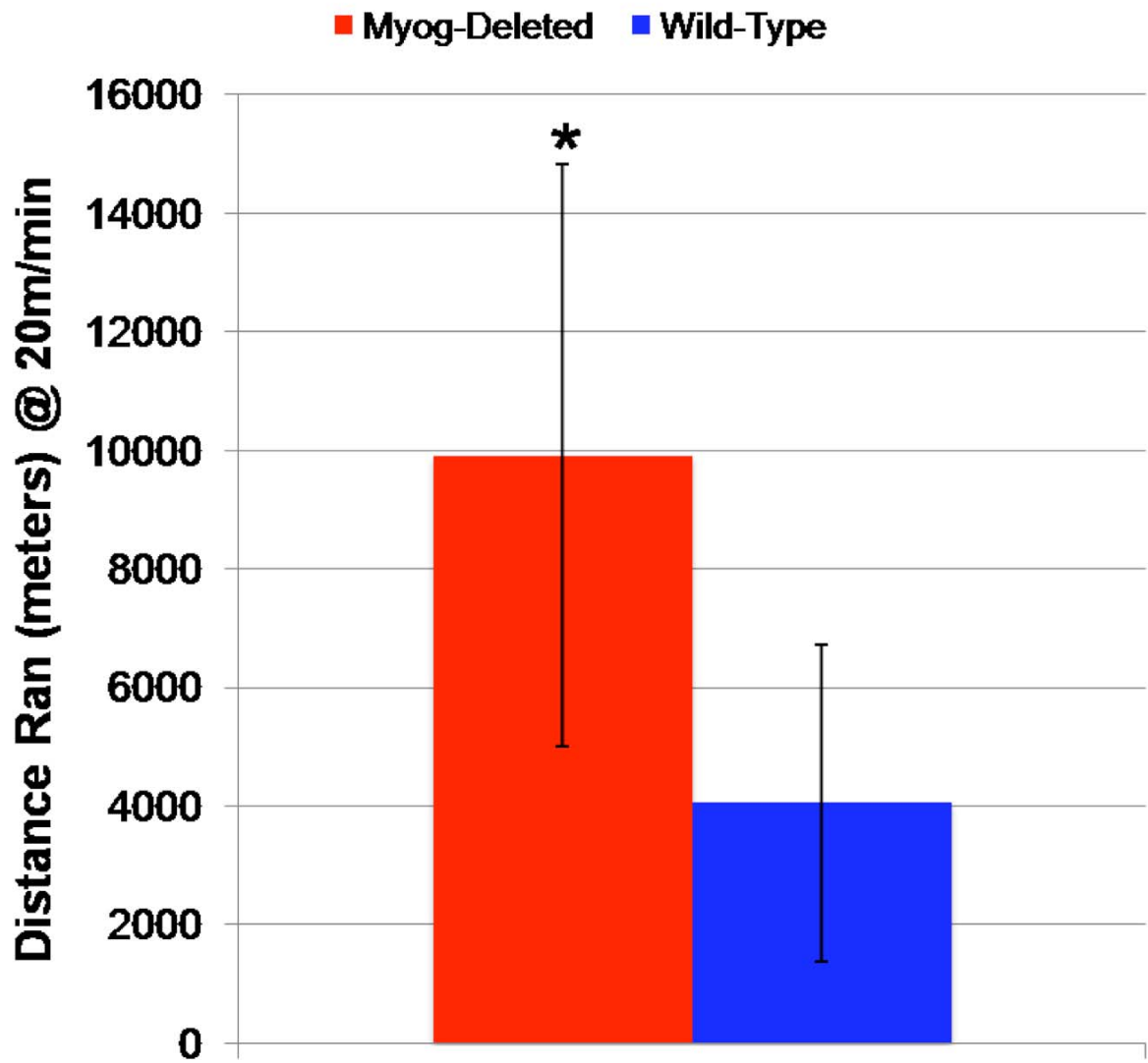
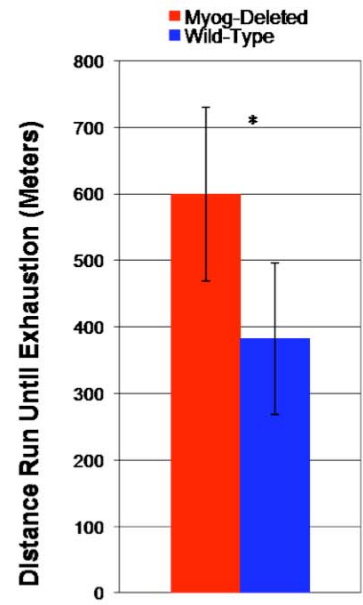
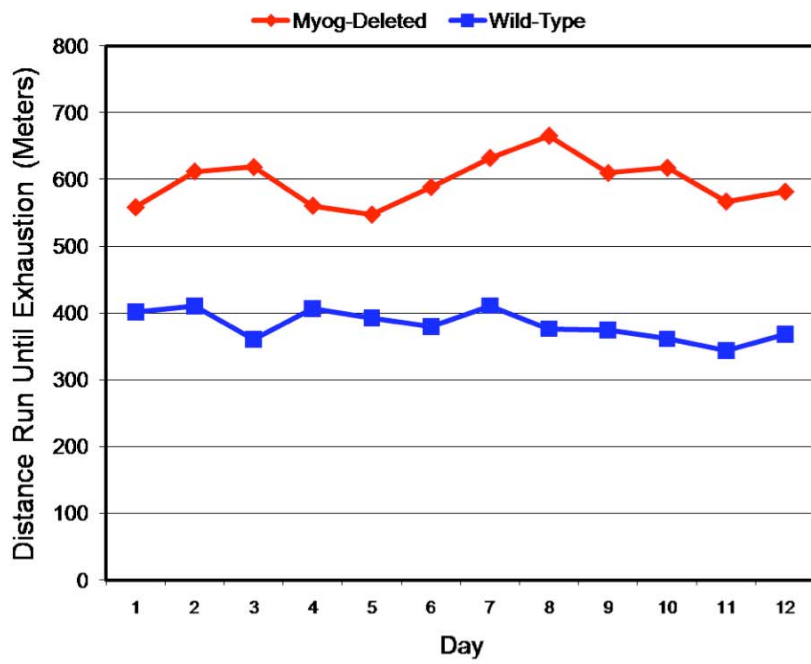


Figure 11 – *Myog*-deleted mice consistently run farther than wild-type mice during high-intensity exercise. During 12 consecutive days of high-intensity exercise, *Myog*-deleted mice ran 1.6-fold farther than wild-type mice on average (*Myog*-deleted 599 meters, wild-type 382 meters) (wild-type n=7, *Myog*-deleted n=8). Blue line and bar indicate wild-type control values; red line and bar indicate *Myog*-deleted values. Error bars represent one standard deviation.

*p<0.01



experiments were approximately six-months of age and all female. *Myog*-deleted mice exhibited a slight trend towards a 15% body weight reduction by 1.5 years of age after repeated treadmill experiments (data not shown). The enhanced exercise capacity during low- and high-intensity running suggests that myogenin may modulate normal skeletal muscle metabolic activity.

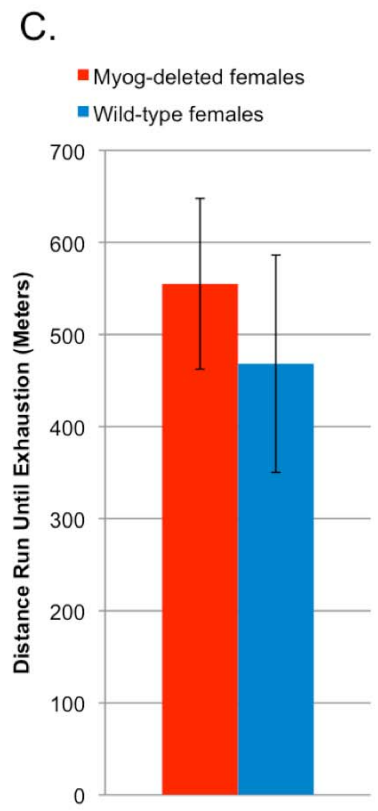
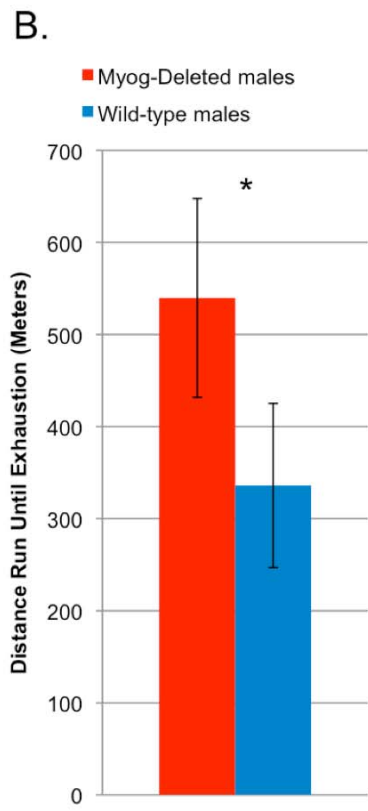
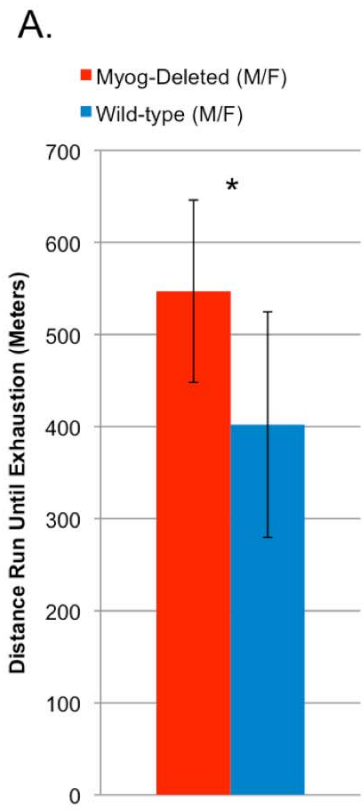
To determine how quickly the phenotype manifests after the deletion of *Myog*, and whether the enhanced exercise capacity is also observed in males, a large cohort of young adult mice were subjected to high-intensity treadmill running within 10 days of tamoxifen injection. On average, *Myog*-deleted mice ran 1.4-fold farther than wild-type mice (*Myog*-deleted 547 meters, wild-type 402 meters) (Figure 12A). *Myog*-deleted males exhibited a greater tendency for enhanced exercise capacity than females, running 1.6-fold farther than wild-type males (*Myog*-deleted 540 meters, wild-type 336 meters) (Figure 12B). *Myog*-deleted females showed a strong trend (not significant) towards running nearly 20% farther than wild-type females (*Myog*-deleted 555 meters, wild-type 468 meters) (Figure 12C). These results demonstrate that the enhanced exercise capacity of *Myog*-deleted mice is observed within a short period of time after the deletion of *Myog*.

Section 2.3 - Lack of myogenin alters blood metabolite concentrations during exhaustive exercise

To better understand the metabolic requirements of *Myog*-deleted mice during exercise and fatigue, blood glucose and blood lactate levels were measured during and after low- and high-intensity treadmill exercise. Blood lactate and glucose baseline levels were measured in

Figure 12 – *Myog*-deleted mice exhibit enhanced exercise capacity shortly after the deletion of *Myog*. Young-adult mice were subjected to high-intensity running 10 days after tamoxifen treatment. *Myog*-deleted mice exhibited a 1.4-fold increase in exercise endurance relative to wild-type control mice (*Myog*-deleted 547 meters, wild-type 402 meters, n=24 mice/group) (12A). *Myog*-deleted males ran 1.6-fold farther than wild-type males (*Myog*-deleted 540 meters, wild-type 336 meters, n=12 mice/group) (12B). *Myog*-deleted females showed a strong trend (p=0.06) towards running nearly 20% farther than wild-type females (*Myog*-deleted 555 meters, wild-type 468 meters, n=12 mice/group) (12C). Blue bars indicate wild-type control values; red bars indicate *Myog*-deleted values. Error bars represent one standard deviation.

*p<1x10⁻⁴



Myog-deleted mice before all low- and high-intensity treadmill runs and determined as normal (3.2 mM Lactate, 149 mg/dL Glucose) (Figures 13, 14, 16, 17). At low-intensity exercise exhaustion, blood lactate was not significantly different from baseline levels or control mice (4.2 mM), while blood glucose levels were reduced 2.4-fold in *Myog*-deleted mice (*Myog*-deleted 33 mg/dL, Wild-type 80 mg/dL) (Figures 13, 14). The 50% reduction of blood glucose levels in wild-type mice at exhaustion is defined herein as a hypoglycemic state. Blood ketone levels were also measured after low-intensity exercise and determined as normal in *Myog*-deleted mice. After low-intensity exercise exhaustion, *Myog*-deleted mice showed a trend towards a 1.5-fold increase in blood ketone levels (*Myog*-deleted 2.9 mM, wild-type 1.9 mM) (Figure 15).

Blood lactate and glucose were next measured during and after high-intensity exercise exhaustion. After wild-type mice reached exhaustion under high-intensity exercise, their blood lactate was elevated to 8.6 mM while blood lactate was only mildly elevated to 4.5 mM in *Myog*-deleted mice at wild-type exhaustion (Figure 17); blood glucose remained unchanged in wild-type mice while blood glucose showed a trend towards reduction in *Myog*-deleted mice at wild-type exhaustion (Figure 16). After *Myog*-deleted mice reached exhaustion, blood lactate was significantly elevated to 12.9 mM while blood glucose was significantly reduced to 105 mg/dL (Figures 16, 17). The excessive production of lactate and increased utilization of glucose as source of fuel suggests that *Myog*-deleted mice exhibit increased glycolytic flux during high-intensity exercise.

Section 2.4 - Myogenin is not necessary to maintain normal muscle fiber type, aerobic potential, or expression of genes involved in fatty-acid metabolism

Figure 13 – *Myog*-deleted mice have normal blood lactate levels after low-intensity running. Blood lactate levels in *Myog*-deleted mice are similar to wild-type mice before and after low-intensity exercise (*Myog*-deleted 3.2 mM, wild-type 4.2 mM). Blue bars indicate wild-type control values; red bars indicate *Myog*-deleted values. Error bars represent one standard deviation.

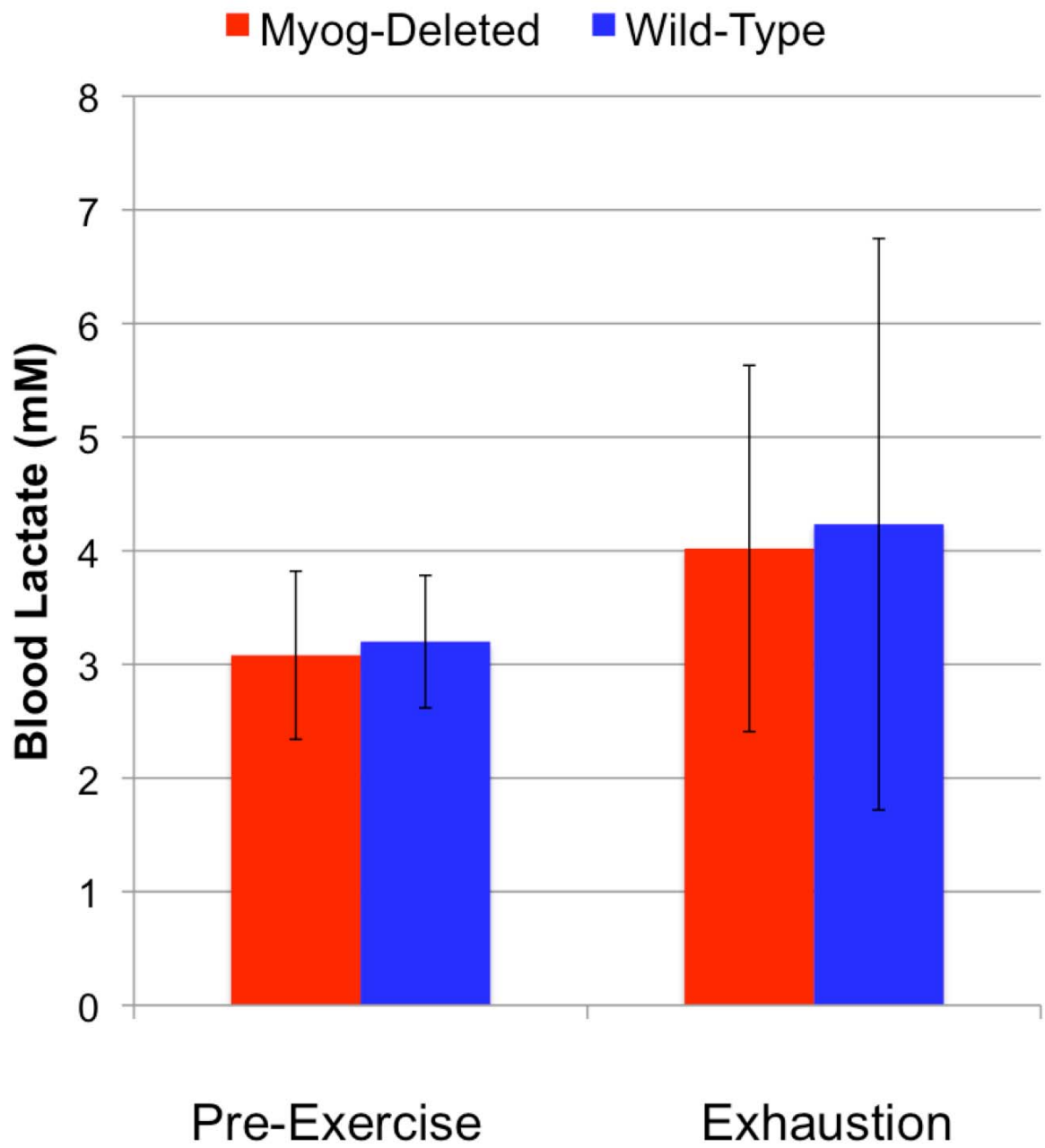


Figure 14 – *Myog*-deleted mice have reduced blood glucose levels after low-intensity running. Blood glucose levels in *Myog*-deleted mice are similar to wild-type prior to low-intensity exercise (149 mg/dL). After low-intensity exercise exhaustion, blood glucose levels were reduced 78% in *Myog*-deleted mice compared to 46% for wild-type controls (*Myog*-deleted 33 mg/dL, wild-type 80 mg/dL). Blue bars indicate wild-type control values; red bars indicate *Myog*-deleted values. Error bars represent one standard deviation. * $p < 0.05$

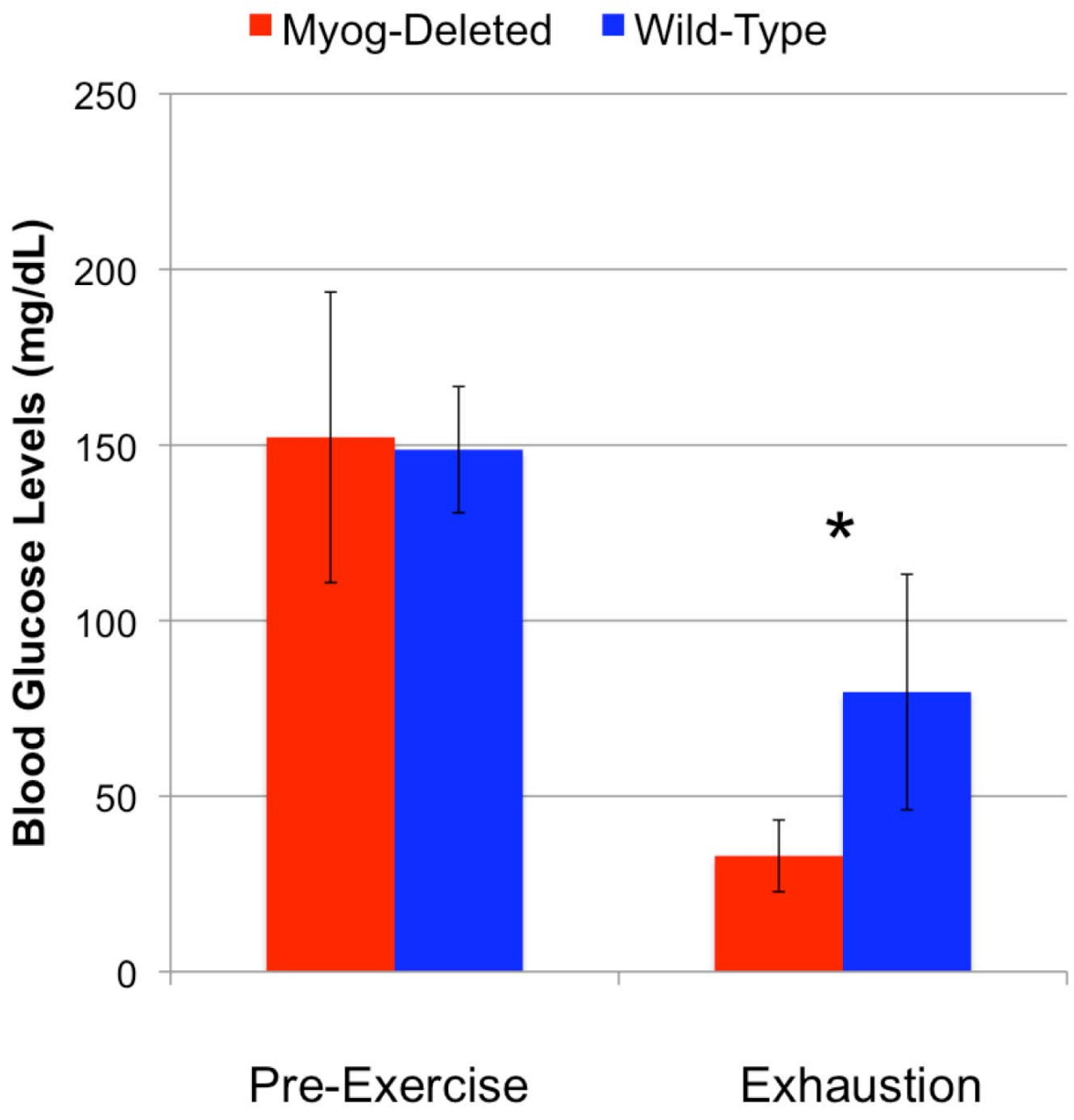


Figure 15 – *Myog*-deleted mice exhibit a trend towards increased blood ketone levels after low-intensity running. *Myog*-deleted mice have normal blood ketone levels prior to exercise (*Myog*-deleted 0.2 mM, wild-type 0.15 mM). After exhaustion, *Myog*-deleted mice exhibit a trend ($p=0.09$) towards a 1.5-fold increase in blood ketone levels relative to wild-type control mice (*Myog*-deleted 2.9 mM, wild-type 1.9 mM). Blue bars indicate wild-type control values; red bars indicate *Myog*-deleted values. Error bars represent one standard deviation.

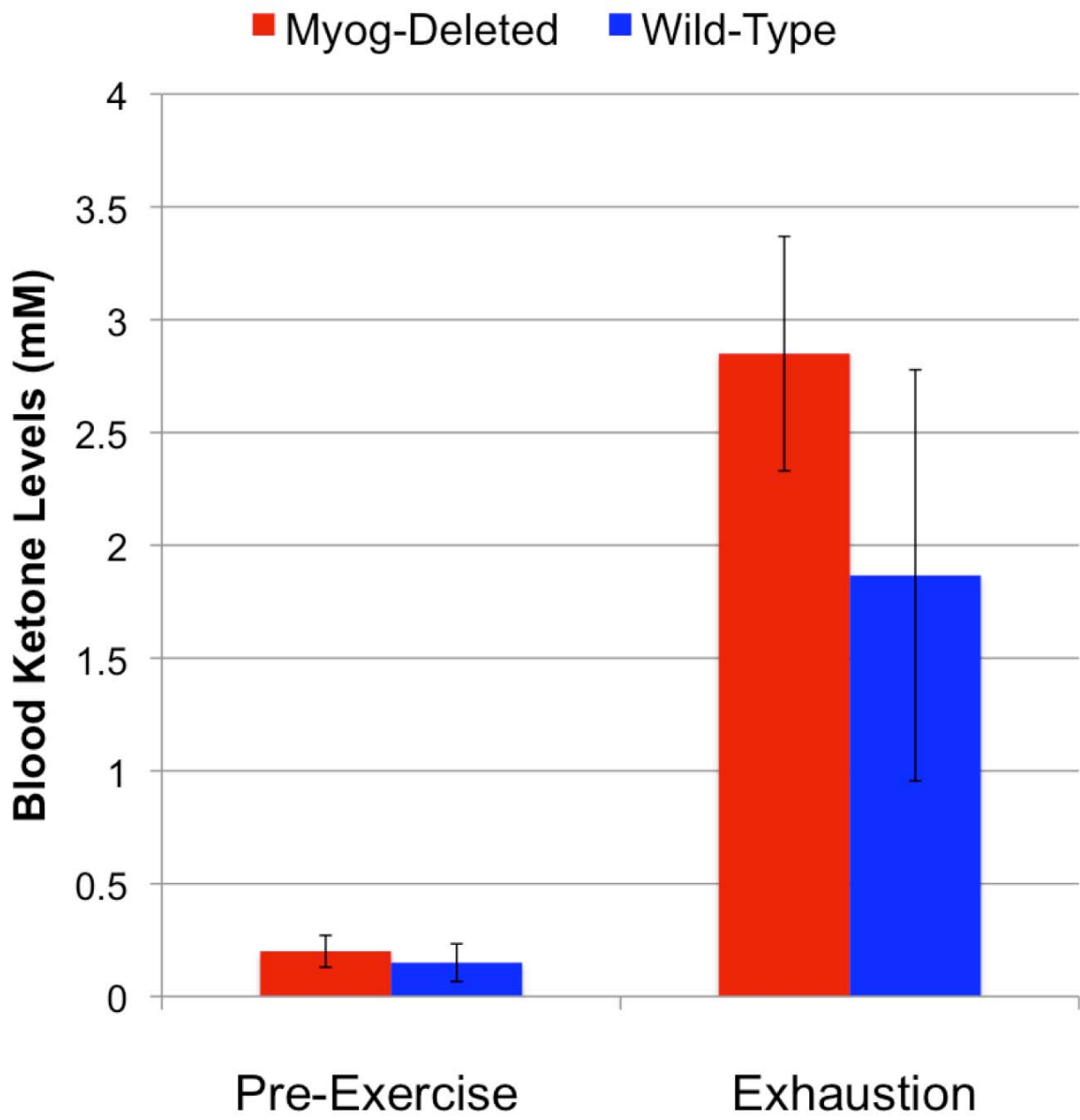


Figure 16 - *Myog*-deleted mice have lower blood glucose levels after high-intensity exercise compared to wild-type mice. Prior to exercise, *Myog*-deleted mice have normal blood glucose levels compared to wild-type control mice (149 mg/dL). As wild-type mice reach exhaustion, their blood glucose levels are elevated, but not significantly different than pre-exercise values (162 mg/dL). At the point of wild-type exhaustion, *Myog*-deleted mice exhibit a trend towards a 29% reduction in blood glucose levels. At exhaustion, *Myog*-deleted mice exhibit a 33% reduction in blood glucose relative to wild-type exhaustion (*Myog*-deleted n=6, wild-type n=6). Blue bars indicate wild-type control values; red bars indicate *Myog*-deleted values. Error bars represent one standard deviation. *p<0.05

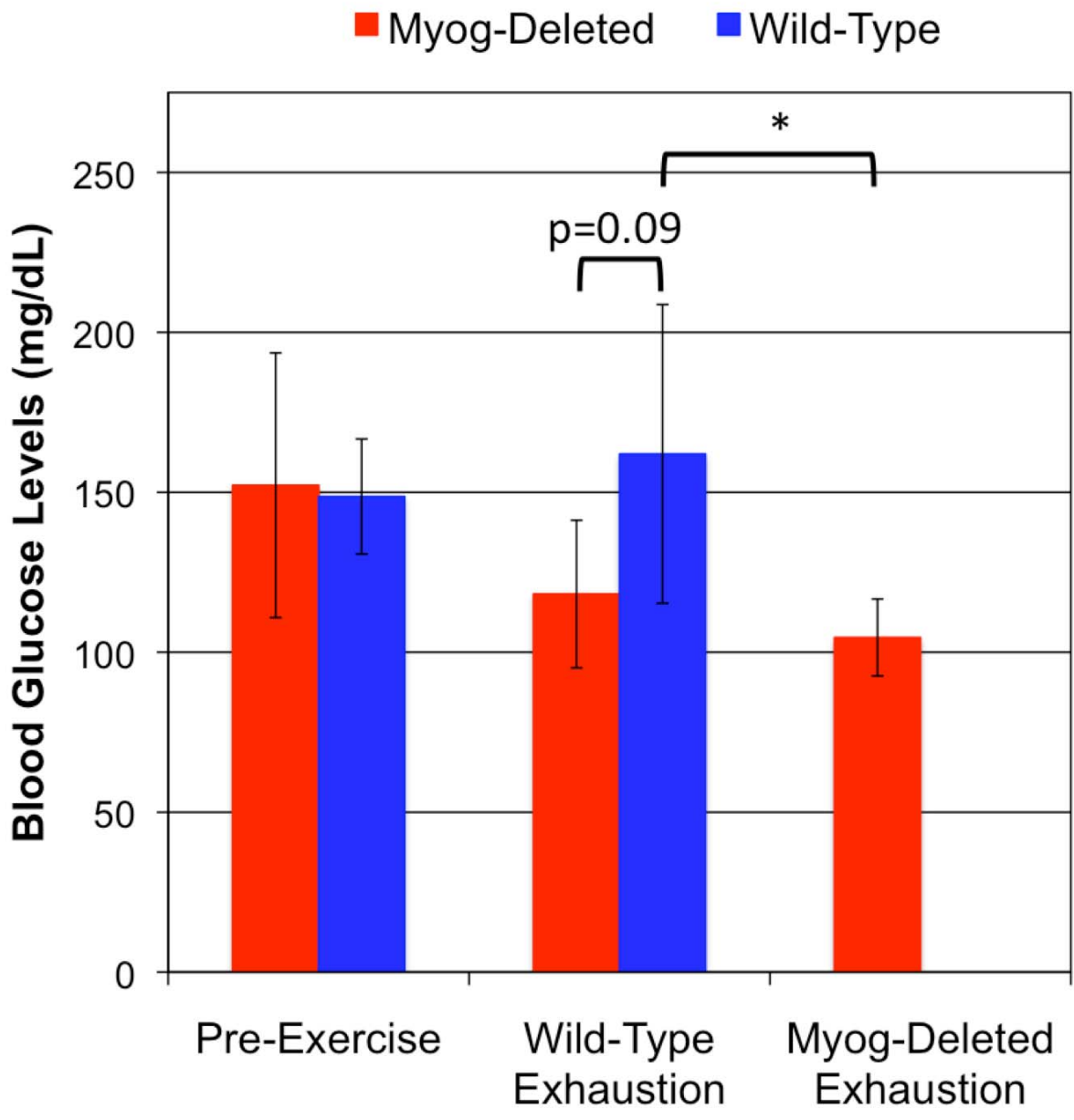
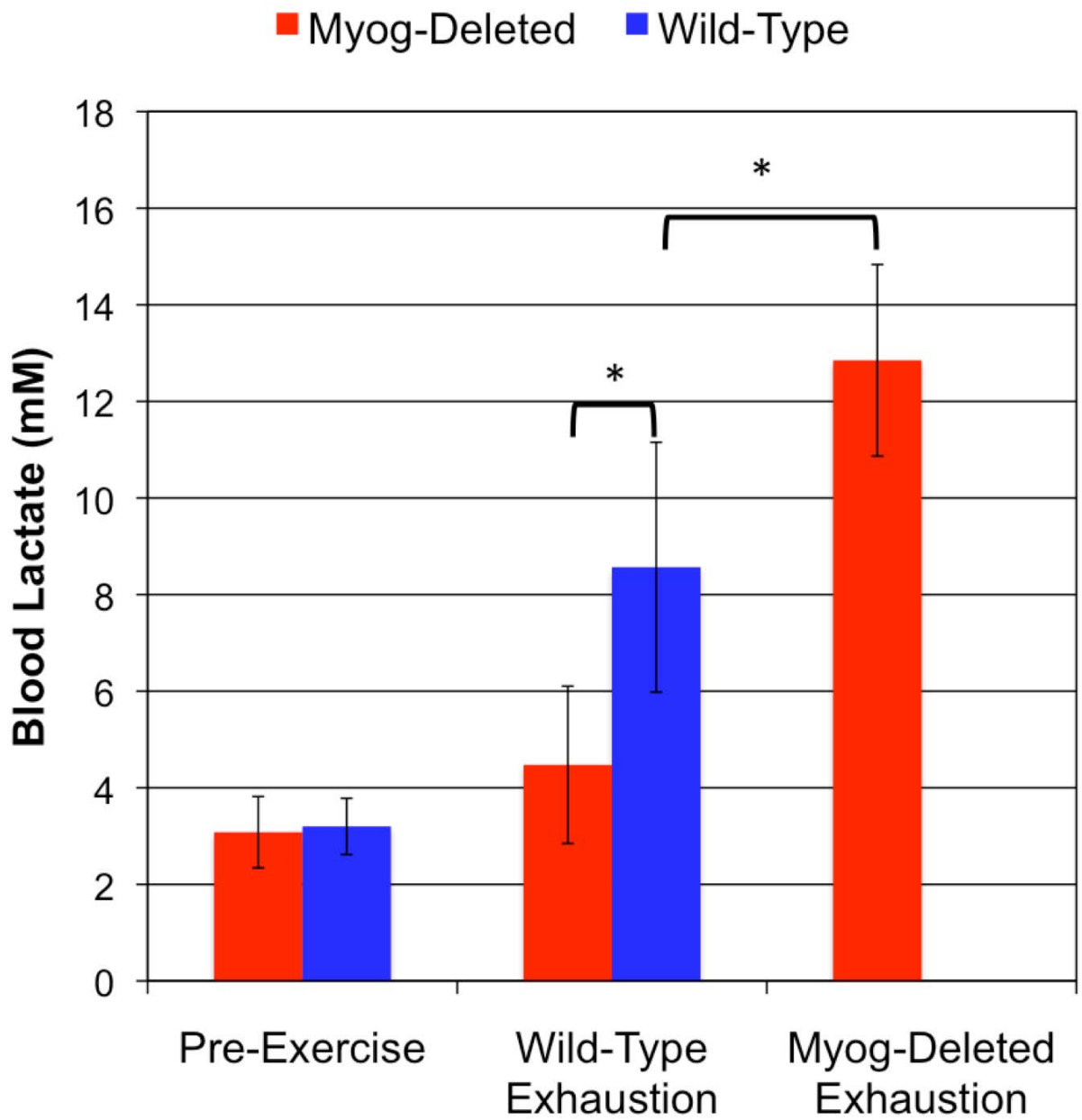


Figure 17 – *Myog*-deleted mice have higher blood lactate levels after high-intensity exercise compared to wild-type mice. Prior to exercise, *Myog*-deleted mice exhibited normal levels of blood lactate (*Myog*-deleted 3.1 mM, wild-type 3.2 mM). Exhausted wild-type mice exhibited elevated blood lactate levels (8.6 mM), 2.7-fold higher than pre-exercise levels. Also at wild-type exhaustion, *Myog*-deleted mice had blood lactate levels similar to pre-exercise levels. Exhausted *Myog*-deleted mice exhibited a dramatic 4.2-fold increase in blood lactate relative to pre-exercise levels, and 1.5-fold higher than exhausted wild-type mice (12.9 mM) (*Myog*-deleted n=6, wild-type n=6). Blue bars indicate wild-type control values; red bars indicate *Myog*-deleted values. Error bars represent one standard deviation. *p<0.05



Myosin-ATPase and Succinate Dehydrogenase (SDH) assays were performed on histological sections of muscle tissue from *Myog*-deleted mice. No difference in the proportion of Type-I and Type-II myofibers was detected by myosin ATPase staining in soleus or gastrocnemius muscles relative to wild-type controls (Figure 18). Myosin Type-I, Type-IIa, and Type IIb isoform expression levels were unchanged in gastrocnemius muscle as shown by RT-qPCR (Figure 19). SDH assays revealed no differences in the proportion of oxidative myofibers in gastrocnemius muscle (Figure 20). Myoglobin expression co-localized with SDH enzymatic activity, further verifying this result (data not shown). Genes involved in fatty-acid metabolism also showed no changes in expression (Figure 21). These genes include: *Acc2*, *CD36*, *Cox8b*, *Cpt-1*, *Ppar-a*, *Ppar-g*, *UCP2* and *UCP3*. Furthermore, *Glut4* expression remained unchanged. These results indicate that the traditional adaptations that accompany enhanced exercise endurance are not found in *Myog*-deleted mice.

Section 2.5 – Mice lacking myogenin do not consume more food

To test whether the enhanced exercise endurance of *Myog*-deleted mice is associated with increased dietary consumption, food weight was measured daily. During a 9-day period of inactivity, *Myog*-deleted mice consumed normal amounts of food relative to wild-type control mice. Similarly, during a 5-day period of daily treadmill running, *Myog*-deleted mice consumed normal amounts of food (Figure 22). These results suggest that *Myog*-deleted mice do not require increased dietary consumption to maintain their enhanced exercise capacity.

Section 2.6 - The hypoglycemic state abolishes the enhanced exercise endurance of mice lacking myogenin

Figure 18 – *Myog*-deleted mice exhibit normal proportions of Type-I and Type II-fibers in soleus muscle. Myosin ATPase staining was used to identify Type-I and Type-II fibers in the soleus muscle (images, left). Average quantitated values reveal normal proportions of these fiber types (graph, right). *Myog*-deleted n=3 (253 myofibers/section), wild-type n=3 (180 myofibers/section). Blue bars indicate wild-type control values; red bars indicate *Myog*-deleted values. Error bars represent one standard deviation.

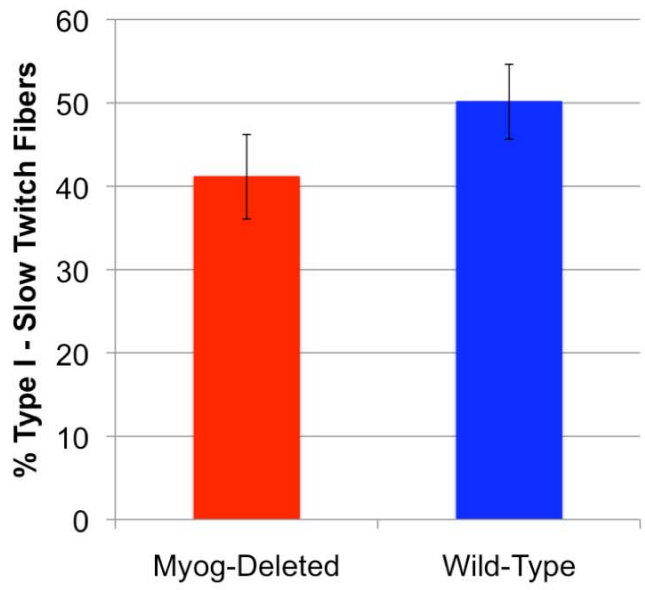
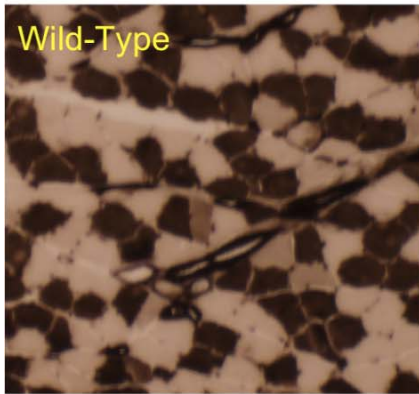
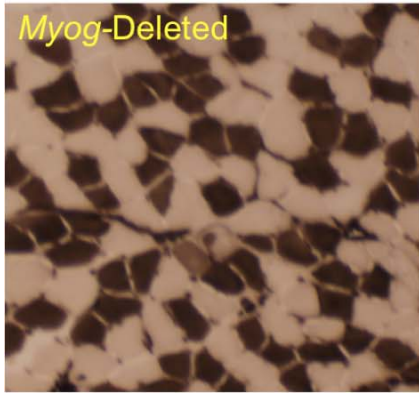


Figure 19 – *Myog*-deleted mice exhibit normal expression of major myosin isoforms in gastrocnemius muscle. Taqman RT-qPCR reveals no changes in the expression of Myosin Type-I, Type-IIA, or Type-IIB. Blue bars indicate wild-type control values; red bars indicate *Myog*-deleted values. Error bars represent one standard deviation.

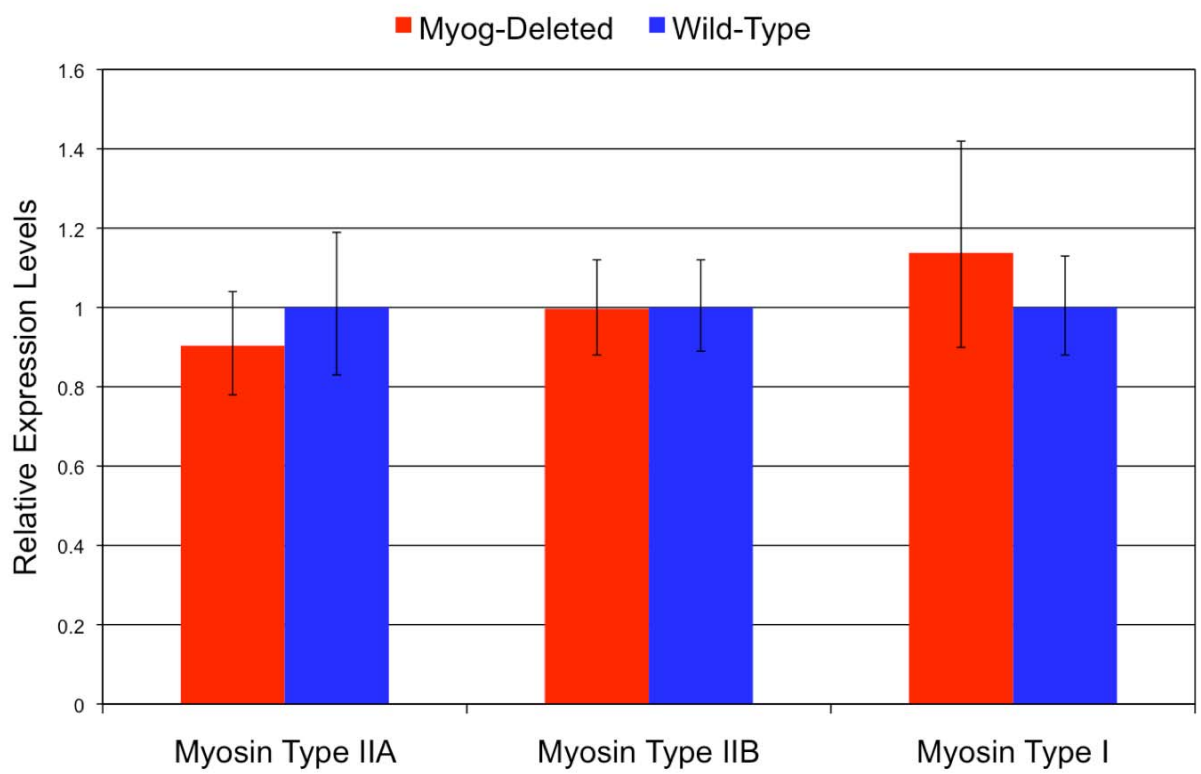


Figure 20 – *Myog*-deleted mice exhibit no difference in SDH activity in gastrocnemius.

Succinate Dehydrogenase (SDH) staining was used to identify oxidative fibers in the medial gastrocnemius (images, left). Average quantitated values reveal normal oxidative activity (graph, right). Blue bars indicate wild-type control values; red bars indicate *Myog*-deleted values. Error bars represent one standard deviation.

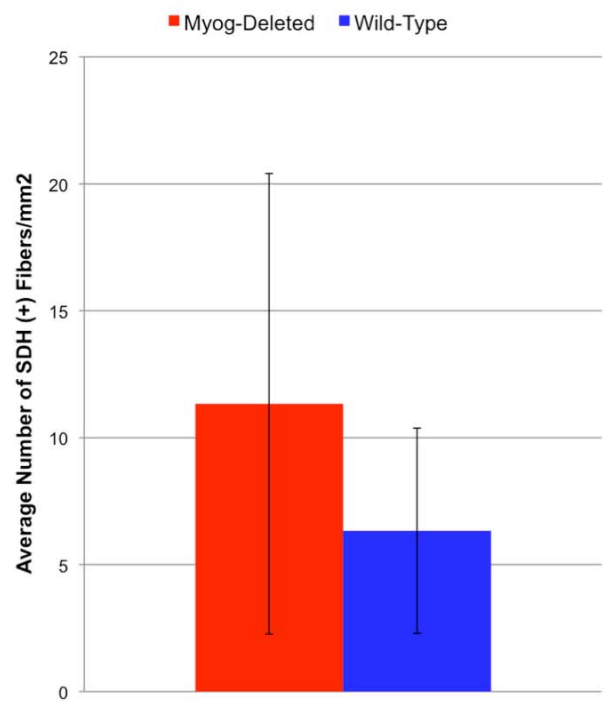
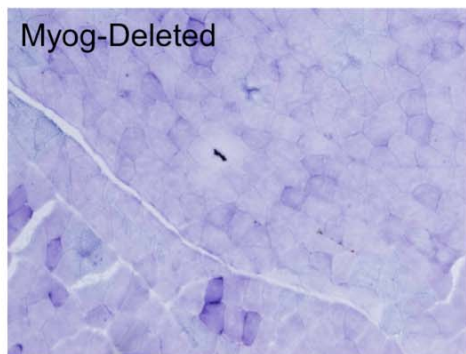
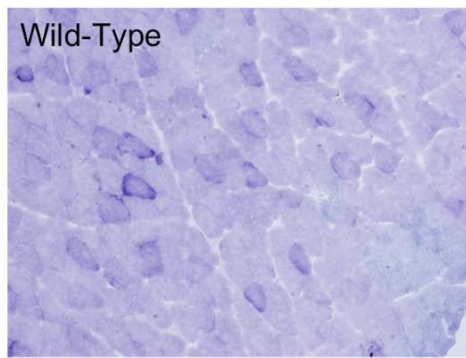


Figure 21 – *Myog*-deleted mice exhibit normal expression of fatty-acid metabolism genes in gastrocnemius muscle. Taqman RT-qPCR of selected genes that play a role in fatty-acid metabolism. No significant changes in gene expression were detected in gastrocnemius muscle of *Myog*-deleted mice. These genes include: *Acc2* (Acetyl-Coenzyme A carboxylase beta, Involved in the biosynthesis of fatty acids), *CD36* (Cluster of Differentiation 36, Involved in fatty acid and glucose metabolism), *Cox8b* (Cytochrome C oxidase subunit 8b, Mitochondrial electron transport chain, oxidative ATP production), *Cpt-1* (Carnitine Palmitoyltransferase I, Involved in transport of long chain fatty acids across mitochondrial membrane), *Glut4* (Glucose Transporter Type 4, Glucose uptake), *Ppar-a* (Peroxisome Proliferator-Activated Receptor Alpha, Nuclear receptor, Regulates fatty acid storage and glucose metabolism), *Ppar-g* (Peroxisome Proliferator-Activated Receptor Gamma, Nuclear receptor, Regulates fatty acid storage and glucose metabolism), *UCP2* (Mitochondrial Uncoupling Protein 2, Involved in oxidative phosphorylation) and *UCP3* (Mitochondrial Uncoupling Protein 3, Involved in oxidative phosphorylation). Blue bars indicate wild-type control values; red bars indicate *Myog*-deleted values. Error bars represent one standard deviation.

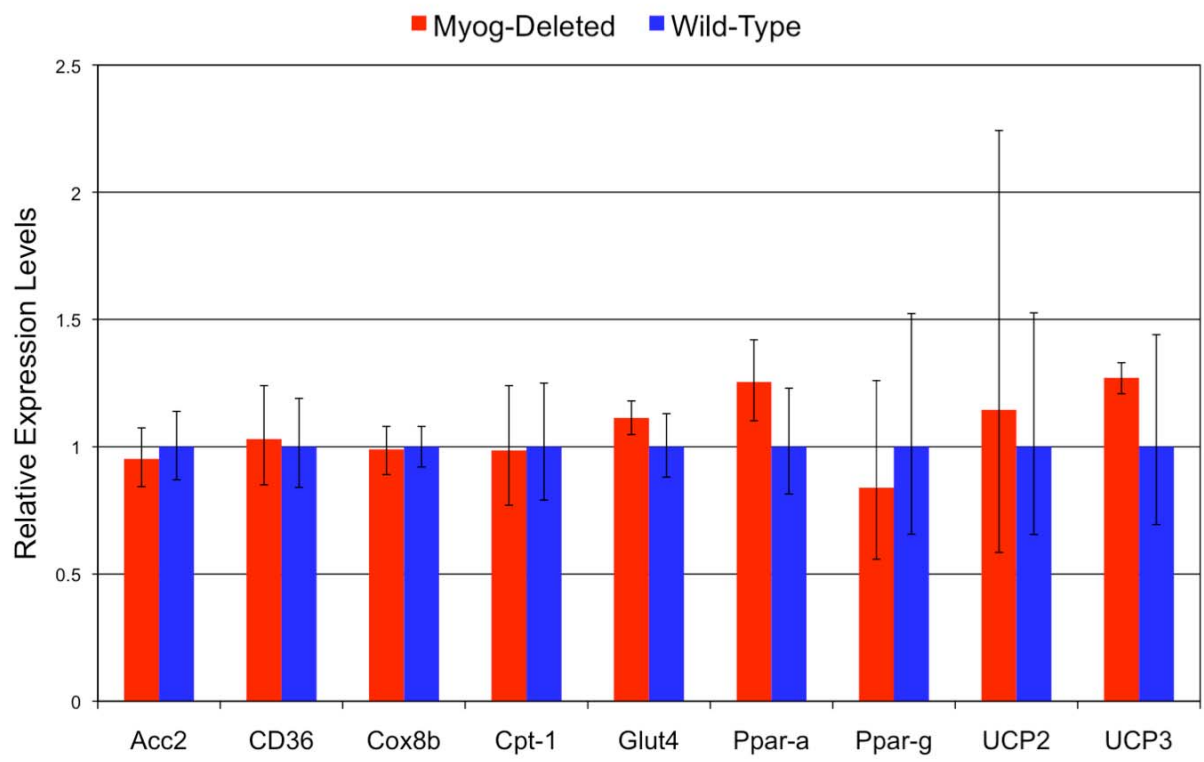
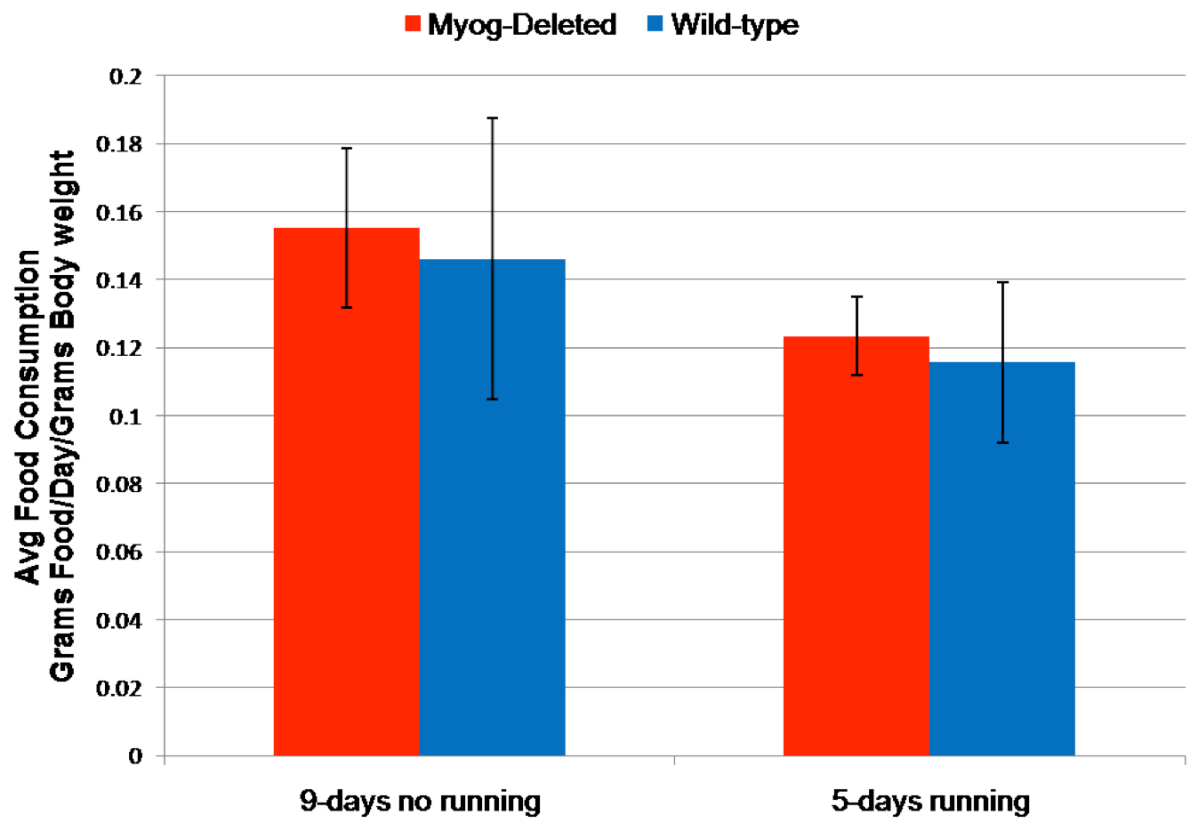


Figure 22 – *Myog* deleted mice do not consume more food

During a 9-day period of inactivity and a 5-day period of treadmill running, *Myog*-deleted mice consumed similar amounts of food compared to wild-type control mice. Food consumption reported as average amount consumed per day, normalized to body weight. Blue bars indicate wild-type control values; red bars indicate *Myog*-deleted values. Error bars represent one standard deviation.



Myog-deleted mice were subjected to a 96-hour fast and exercised daily with the high-intensity protocol to exhaustion. As expected in the fed state, *Myog*-deleted mice initially ran 1.6-fold farther than wild-type control mice. After 24 hours of fasting, *Myog*-deleted mice continued to outperform wild-type control mice by 2.2-fold. By 48, 72, and 96 hours, *Myog*-deleted mice no longer significantly outperformed wild-type mice, running 1.4-fold, 1.4-fold, and 0.9-fold of controls, respectively. Ten days after the mice were returned to their normal diet, *Myog*-deleted mice again significantly outperformed wild-type control mice by 1.5-fold (Figure 23). *Myog*-deleted mice exhibited similar weights to wild-type control mice throughout the experiment (data not shown).

Blood lactate and glucose values were measured daily before and after exhaustion during 48, 72, and 96 hours of fasting. At 96 hours, blood lactate levels at exhaustion in *Myog*-deleted mice were nearly identical to wild-type (6.1 mM and 6.12 mM, respectively) (Figure 24). Similarly, blood glucose levels at 96 hours were not significantly different before (*Myog*-deleted 75 mg/dL, Wild-type 73 mg/dL) or after exercise exhaustion (*Myog*-deleted 88 mg/dL, Wild-type 72 mg/dL) (Figure 25). Similar blood lactate and blood glucose values before and after exhaustion after 96 hours of fasting, along with similar exercise capacity, support the idea that enhanced glycolytic flux is associated with enhanced exercise capacity. These results demonstrate that *Myog*-deleted mice require fed-state blood glucose levels in order to exhibit enhanced exercise capacity.

Section 2.7 - Mice lacking myogenin do not voluntarily run more than wild-type during running-wheel exercise

Figure 23 – *Myog*-deleted mice do not run more than wild-type mice during high-intensity running in the fasted state. Mice were subjected to high-intensity exercise before, during, and after a 96-hour fast. Under normal dietary conditions, *Myog*-deleted mice ran approximately 1.5-fold more than wild-type control mice. After 24-hours of fasting, *Myog*-deleted animals ran 2-fold more than wild-type control mice. By 96-hours of fasting, *Myog*-deleted mice completely lost their enhanced exercise endurance. Restoration of normal diet restores the enhanced exercise endurance of *Myog*-deleted mice within 10 days. The daily increase in running distance between 24- and 72-hours is concomitant with a daily loss of 10% body mass (data not shown). Blue line indicates wild-type control values; red line indicates *Myog*-deleted values; green line indicates fold change of *Myog*-deleted values relative to wild-type values. Error bars represent one standard deviation. * $p < 0.05$

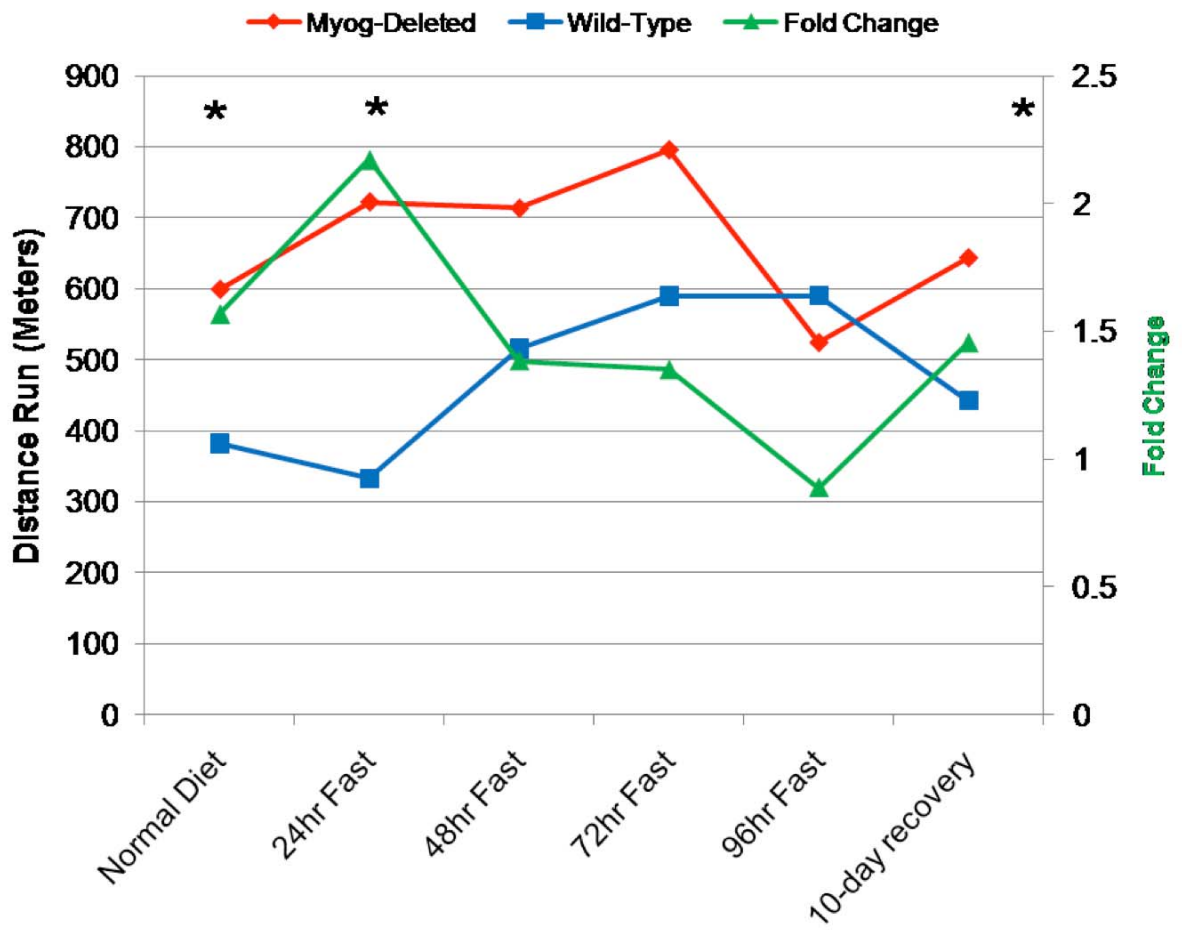


Figure 24 – *Myog*-deleted mice have normal blood lactate levels after high-intensity running in the fasted state. After a 96-hour fast, *Myog*-deleted mice and wild-type mice have similar blood lactate levels after high-intensity exercise (6 mM). Blue bar indicates wild-type control values; red bar indicates *Myog*-deleted values. Error bars represent one standard deviation.

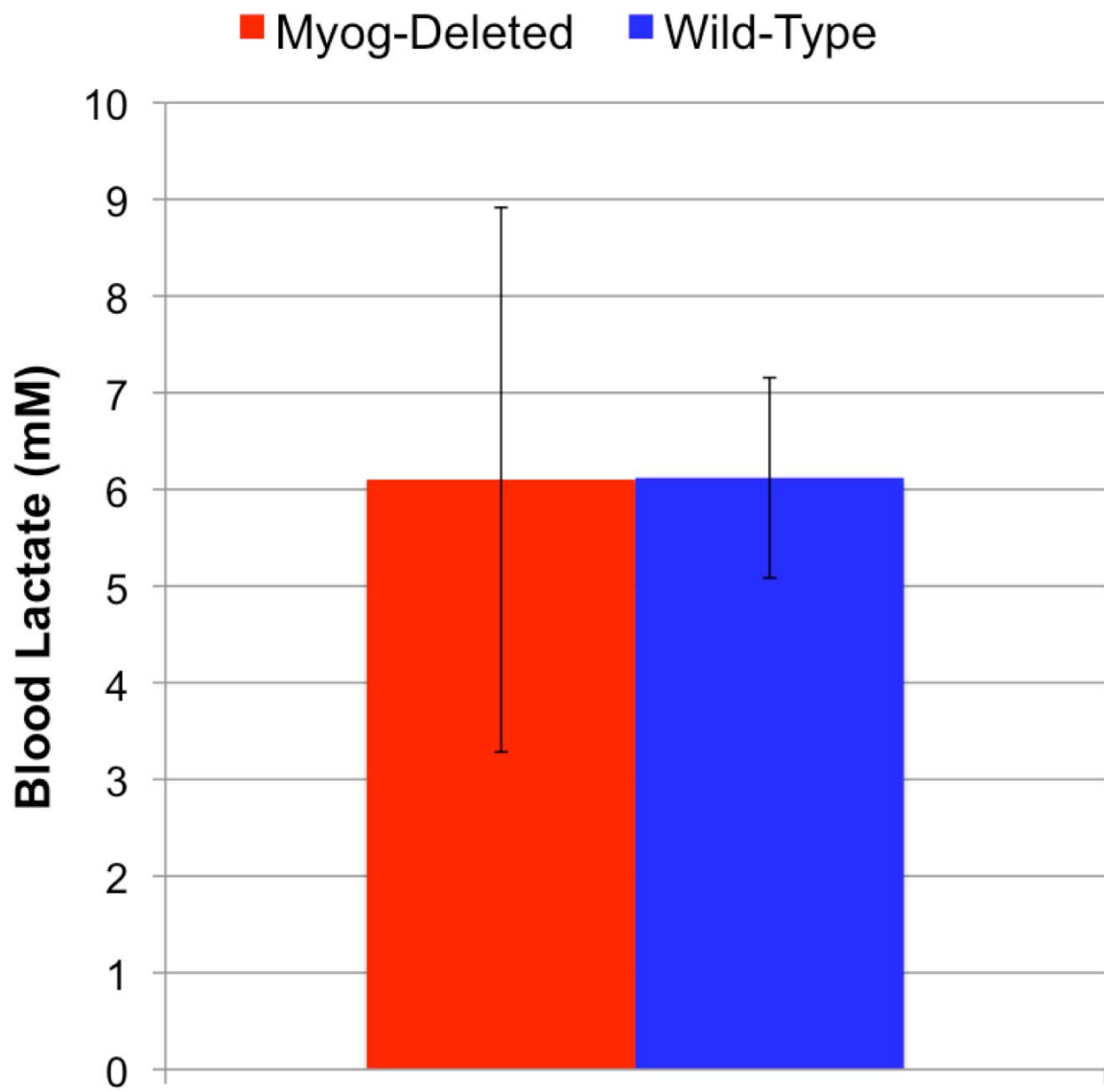
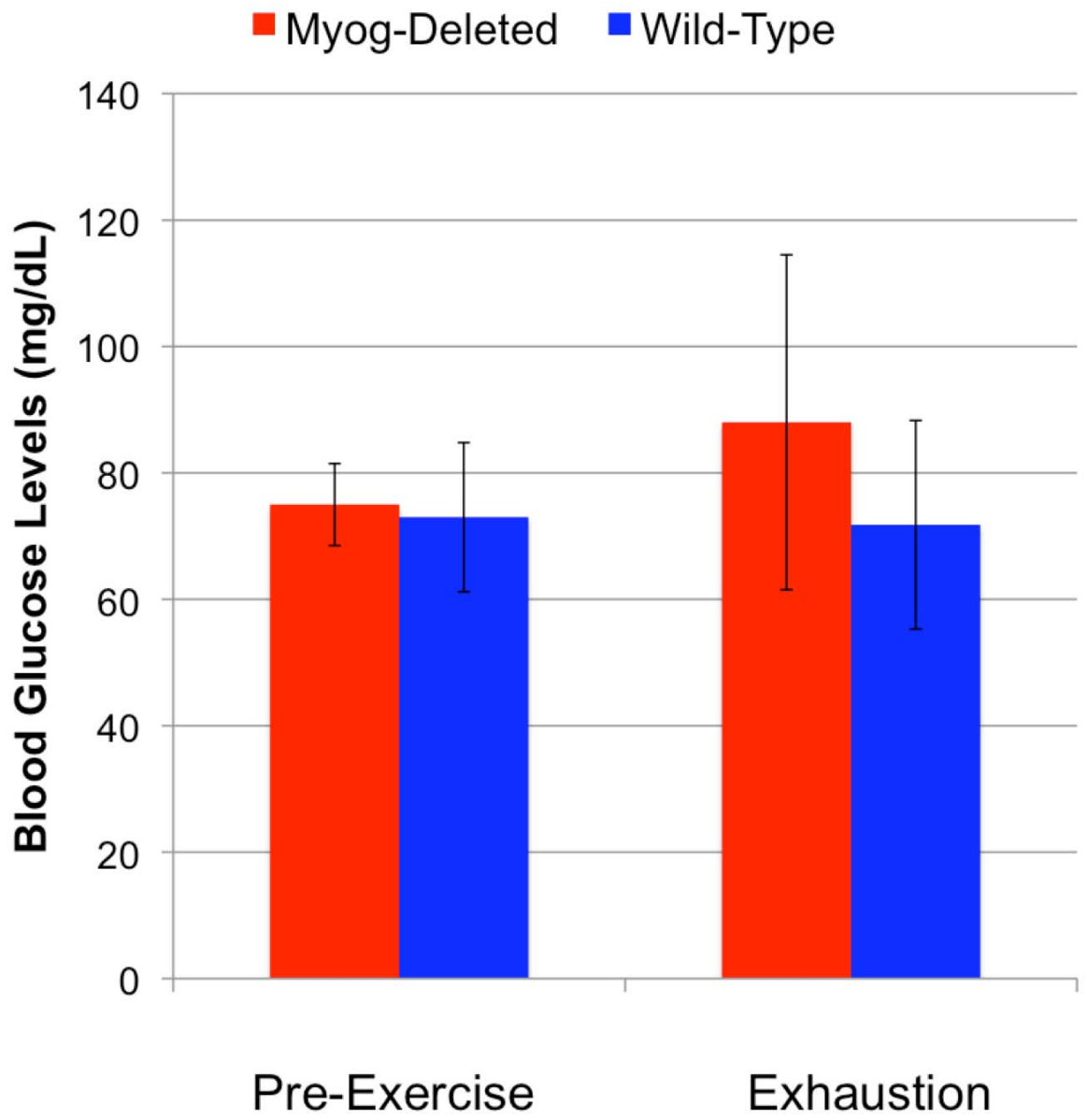


Figure 25 – *Myog*-deleted mice have normal blood glucose levels after high-intensity running in the fasted state. After a 96-hour fast, *Myog*-deleted mice and wild-type mice had similar, hypoglycemic, blood glucose levels prior to exercise (*Myog*-deleted 75 mg/dL, wild-type 73 mg/dL). After high-intensity exercise exhaustion, *Myog*-deleted and wild-type mice had similar blood glucose levels (*Myog*-deleted 88 mg/dL, wild-type 72 mg/dL). Blue bars indicate wild-type control values; red bars indicate *Myog*-deleted values. Error bars represent one standard deviation.



Enhanced involuntary exercise endurance may be due to increased fatigue resistance or the tendency for increased physical activity. To determine whether *Myog*-deleted mice exhibit the tendency for increased physical activity, voluntary running capacity was measured. *Myog*-deleted mice were allowed unrestricted access to running wheels (Figure 26). Over a period of 5 months, *Myog*-deleted mice did not run significantly farther than wild-type mice on running wheels allowed to rotate freely (*Myog*-deleted 7.4 km/day, Wild-type 8.2 km/day) (Figure 27A). *Myog*-deleted mice also ran similar average and maximum speeds compared to wild-type mice (Figure 27B, C). A 1 kg load was then applied to the axis of the running wheels to increase the turning resistance. Under a loaded state, *Myog*-deleted mice did not run significantly farther than wild-type mice (*Myog*-deleted 9.1 km/day, Wild-type 6.9 km/day) (Figure 27). *Myog*-deleted mice also ran similar average and maximum speeds compared to wild-type mice when the running wheel resistance was added (Figure 27B, C). The lack of significantly increased running capacity during voluntary exercise indicates that the lack of myogenin does not confer an increased tendency for exercise.

Section 2.8 - Superior adaptation to exercise training in mice lacking myogenin

To determine whether *Myog*-deleted mice are abnormally affected by exercise training, mice that were allowed unrestricted access to voluntary running wheels for 6 months (herein referred to as “trained mice”) were subjected to high-intensity involuntary exercise running. Wild-type mice exhibited a significant response to exercise training with a 1.8-fold increase in exercise capacity during high-intensity treadmill running (Untrained wild-type 382 meters/day, Trained wild-type 696 meters/day). *Myog*-deleted mice also exhibited a significant response to exercise training with a 2.2-fold increase in exercise capacity (Untrained *Myog*-deleted 599 meters/day, Trained *Myog*-deleted 1324 meters/day) (Figure 28). Comparative analysis of wild-

Figure 26 – The Klein Lab Voluntary Exercise Running Wheel

To facilitate long-term exercise training, we custom built a voluntary running wheel apparatus that allowed for measurements of average speed, maximum speed, distance, and time. See Methods Chapter for more information.

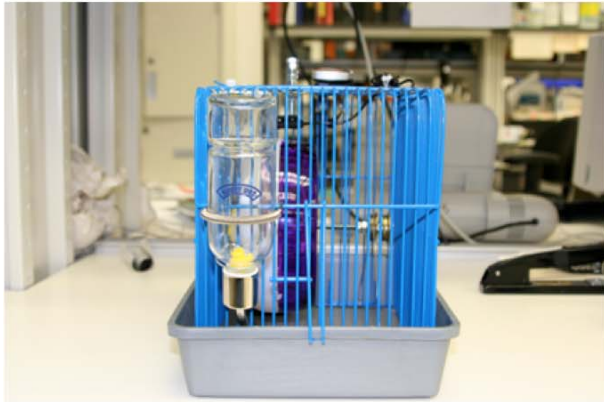
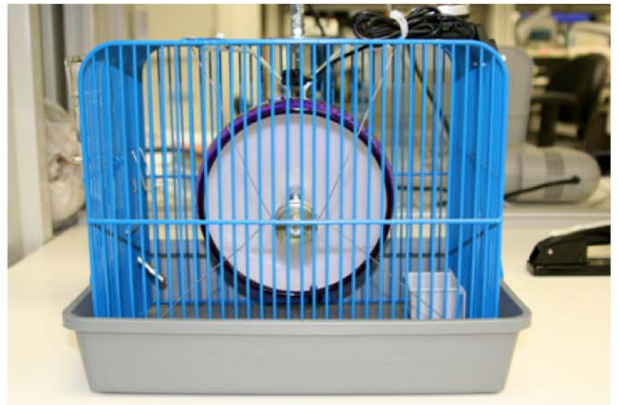
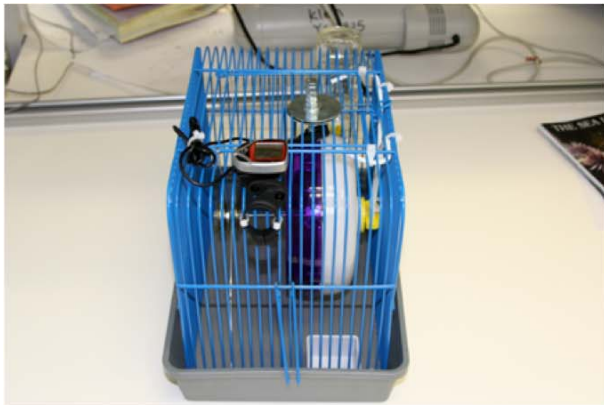


Figure 27 – Trained *Myog*-deleted mice do not voluntarily run farther or faster than trained wild-type mice. After the deletion of *Myog*, *Myog*-deleted and wild-type mice were allowed unrestricted access to voluntary running wheels for 6 months. At 4-5 months, trained *Myog*-deleted mice ran similar amounts as trained wild-type mice on running wheels were allowed to rotate freely (*Myog*-deleted 7.4 Km/day, wild-type 8.2 Km/day) (Figure 27A). At 6 months, trained *Myog*-deleted mice ran similar amounts as trained wild-type mice when a 1 kg load was added to the running wheel axis (*Myog*-deleted 9.1 Km/day, wild-type 6.9 Km/day) (Figure 27B). Additionally, no changes were observed in average speed (27B) or maximum speed (27C) during this time. Blue bars indicate wild-type control values; red bars indicate *Myog*-deleted values. Error bars represent one standard deviation.

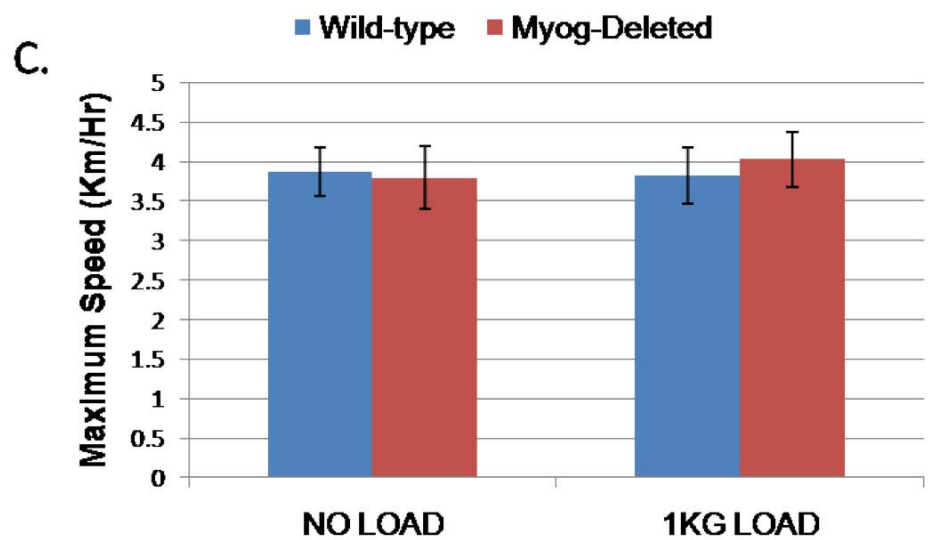
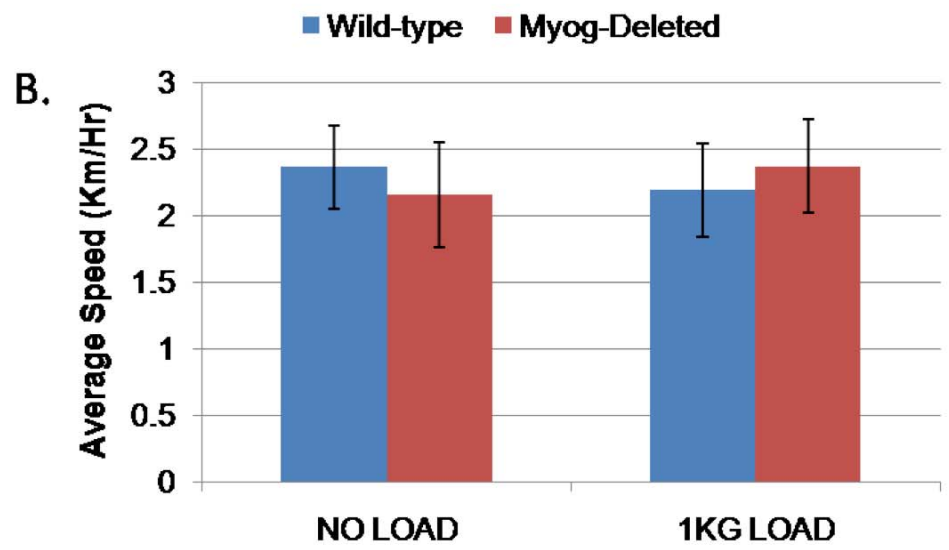
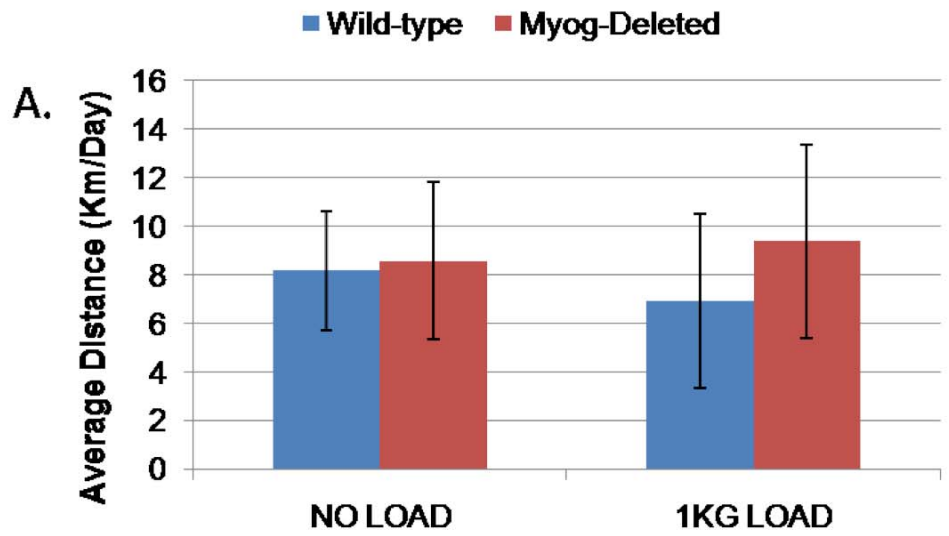
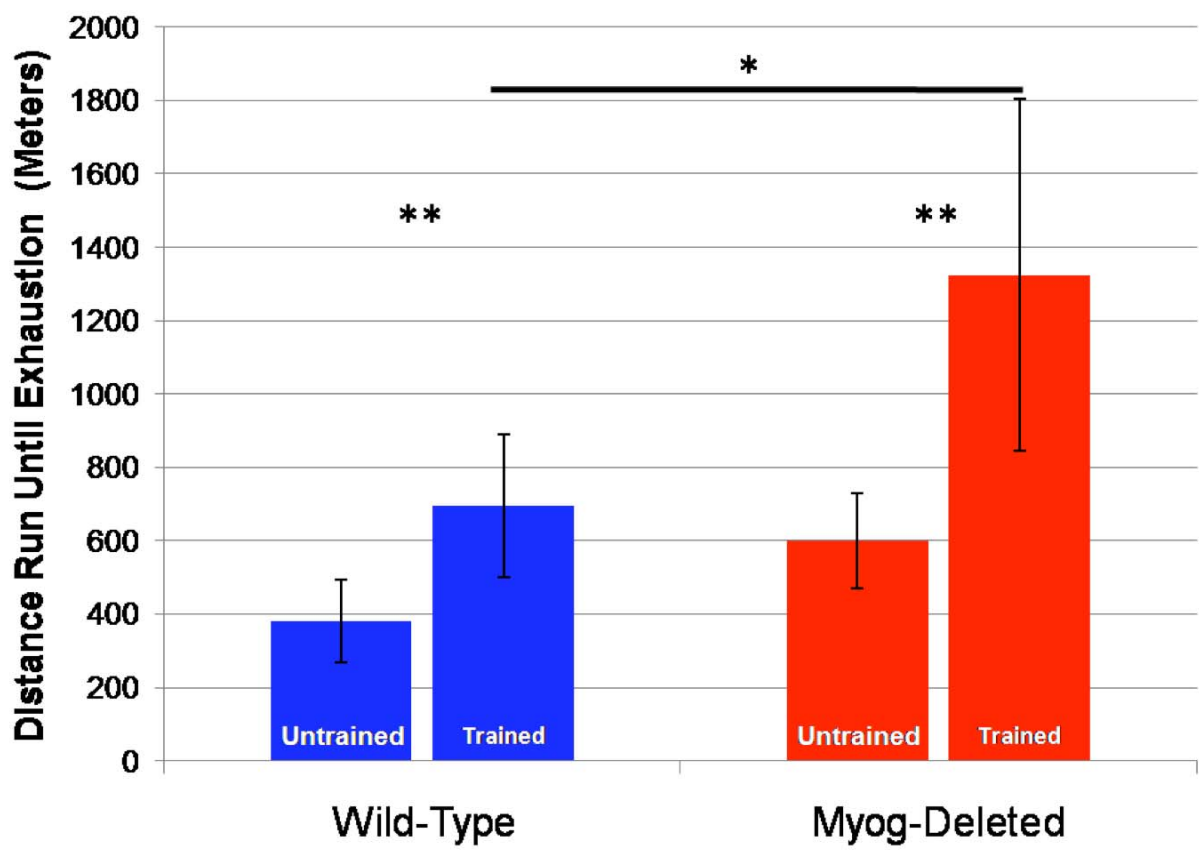


Figure 28 – Superior adaptation to exercise training in mice lacking myogenin.

After exercise training (trained) or during sedentary life (untrained), *Myog*-deleted and wild-type mice were subjected to >12 days of high-intensity treadmill running. Trained wild-type mice showed a typical adaptation to exercise training, running an average 1.8-fold more than untrained wild-type mice (untrained wild-type 382 meters, trained wild-type 696 meters). Trained *Myog*-deleted mice showed a superior adaptation to exercise training, running an average 2.2-fold more than untrained *Myog*-deleted mice (untrained *Myog*-deleted 599 meters, trained *Myog*-deleted 1324 meters). Trained *Myog*-deleted mice exhibit a 20% increase in their adaptive response to training relative to trained wild-type mice. Untrained wild-type n=7, untrained *Myog*-deleted n=8, trained wild-type n=10, trained *Myog*-deleted n=11. Blue bars indicate wild-type control values; red bars indicate *Myog*-deleted values. Error bars represent one standard deviation. *p<0.05, **p<0.01



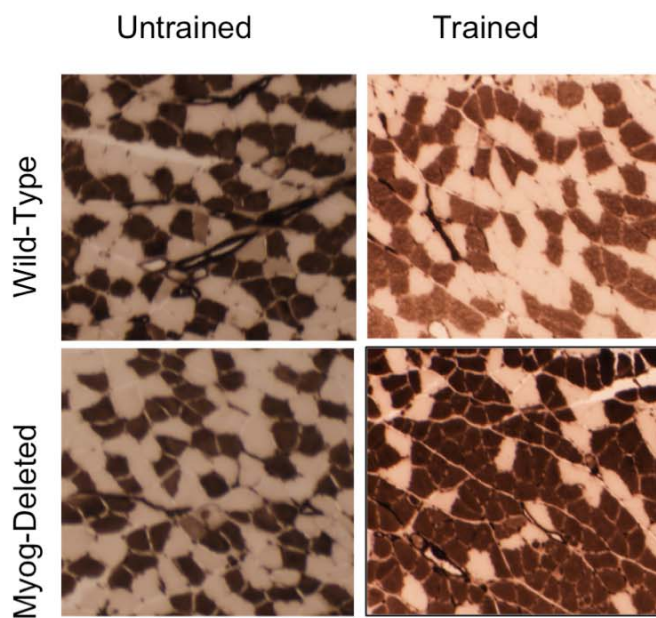
type and *Myog*-deleted groups reveals that *Myog*-deleted mice respond 20% better to exercise training than wild-type. These results indicate that *Myog*-deleted mice are more sensitive to long-term exercise-induced training adaptations.

Section 2.9 - Lack of myogenin during long-term exercise training increases slow-twitch fiber-type proportion and oxidative capacity of skeletal muscle

Histological sections from trained *Myog*-deleted and wild-type mice were analyzed with Myosin-ATPase and succinate dehydrogenase (SDH) assays. Myosin-ATPase staining revealed that training mildly increases the proportion of Type-I slow-oxidative fibers in the soleus muscle. Trained *Myog*-deleted mice showed a more robust 78% increase in the proportion of Type-I fibers. Gastrocnemius muscle showed similar changes (data not shown). Indeed, trained *Myog*-deleted mice show a 30% increase in the proportion of Type-I fibers when compared to trained wild-type mice (Figure 29).

SDH activity in gastrocnemius muscle revealed that exercise training dramatically increases SDH levels in wild-type mice from 6 SDH-fibers/mm² to 140 SDH-fibers/mm². Trained *Myog*-deleted mice also showed a dramatic increase in SDH enzymatic activity from 11 SDH-fibers/mm² to 234 SDH-fibers/mm². Comparison of trained *Myog*-deleted and trained wild-type SDH-fiber density revealed a 70% increase in SDH enzymatic activity in trained *Myog*-deleted mice (Figure 30). Myoglobin expression co-localized with SDH enzymatic activity, further verifying this result (data not shown). The increased proportion of Type-I fibers and SDH enzymatic activity indicates that *Myog*-deleted mice are more prone to histologic changes associated with exercise training.

Figure 29 – Trained *Myog*-deleted mice exhibit an increase in Type-I slow-twitch fibers in soleus muscle. Myosin ATPase staining was used to identify Type-I and Type-II fibers in the soleus muscle of untrained and trained mice (images, left). Average quantitated values reveal a 22% increase in Type-I fibers in trained wild-type mice (untrained wild-type 50%, trained wild-type 61%); trained *Myog*-deleted mice exhibited a 93% increase in the proportion of Type-I fibers (untrained *Myog*-deleted 41%, trained *Myog*-deleted 79%) (graphs, right). Trained *Myog*-deleted mice exhibited a 30% increase in the proportion of Type-I fibers relative to trained wild-type mice. Blue bars indicate wild-type control values; red bars indicate *Myog*-deleted values. Error bars represent one standard deviation. * $p < 0.05$



- Dark Fibers: Type I - Slow Oxidative
- Light Fibers: Type II - Fast Glycolytic

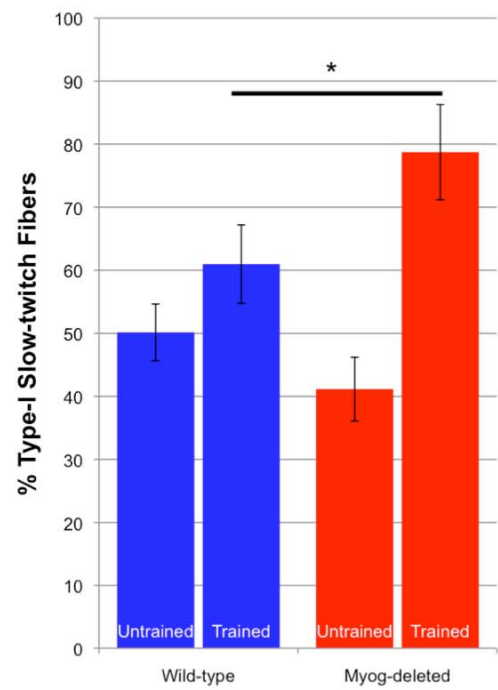
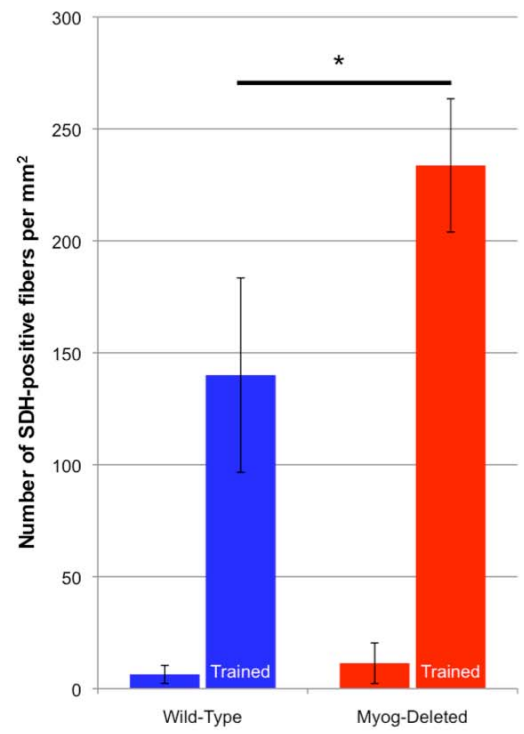
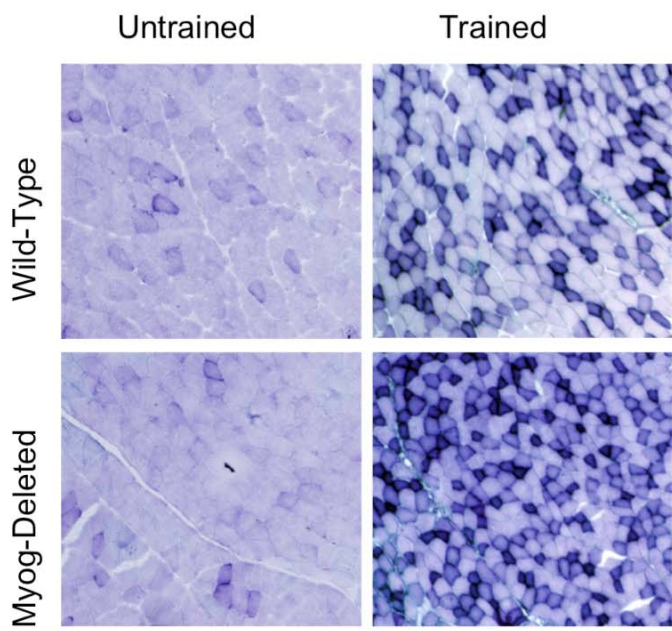


Figure 30 – Trained *Myog*-deleted mice exhibit an increase in Succinate Dehydrogenase enzyme activity in gastrocnemius muscle. Succinate Dehydrogenase (SDH) staining was used to identify oxidative fibers in the gastrocnemius of untrained and trained mice (images, left). Average quantitated values reveal a 23-fold increase in SDH-positive fibers in trained wild-type mice (untrained wild-type 6 SDH fibers/mm², trained wild-type 140 SDH fibers/mm²); trained *Myog*-deleted mice exhibited a similar 21-fold increase in SDH-positive fibers (untrained *Myog*-deleted 11 SDH fibers/mm², trained *Myog*-deleted 234 SDH fibers/mm²) (graphs, right). Trained *Myog*-deleted mice exhibited a 67% increase in SDH-positive fiber density relative to trained wild-type mice. Blue bars indicate wild-type control values; red bars indicate *Myog*-deleted values. Error bars represent one standard deviation. *p<0.05



Section 2.10 - Myogenin regulates the expression of genes involved in metabolism and signal transduction during adult life

A gene expression profiling study was next performed to identify changes in global gene expression due to *Myog* deletion during adult life. Total RNA from trained *Myog*-deleted and wild-type mice was extracted from gastrocnemius muscles and used for Affymetrix microarray analysis. The analysis revealed differential expression of 29 downregulated genes and 11 upregulated genes that significantly changed >1.4-fold. Changes in global gene expression patterns were enriched for genes involved in signal transduction and metabolism (Table 1). Thirteen genes were chosen for validation of gene expression changes by Taqman RT-qPCR analysis (Figure 31). These genes include: *RhoBTB1*, *Rhpn2*, *Htra1*, *Gpx3*, *Pcx*, *Nfatc2*, *Zscan21*, *Bmp5*, *Mpa2l*, *Bdh*, *Pfkfb3*, and *Dpyd*. Gene expression profiling indicates that while *Myog*-deleted mice appear normal, their enhanced exercise endurance is associated with global gene expression changes.

Section 2.11 - Myogenin is not essential for viability in adult mdx mice

To explore the role of myogenin in functionally compromised skeletal muscle, mice carrying the conditional alleles of *Myog* were bred with dystrophin-deficient (*mdx*) mice. The mice were then injected with tamoxifen to delete *Myog*. Control mice with functional dystrophin were also generated (Figure 32). Upon deletion of *Myog* from *mdx* mice between 3 and 5 months of age, no phenotypic differences were observed over a period of 6 months. Double knockout mice maintained healthy body weight and exhibited normal mobility relative to wild-type control mice. These results indicate that *Myog* is not essential for viability in young adult mice lacking dystrophin.

Figure 31 – Myogenin regulates genes involved in metabolism and signal-transduction during adult life. Taqman RT-qPCR validation was performed on selected differentially expressed genes in adult *Myog*-deleted gastrocnemius muscle. These genes include: RhoBTB1 (Rho-related BTB domain containing 1, a Rho GTPase), Rhpn2 (Rhopilin, a Rho GTPase binding protein), Htra1 (a serine peptidase), Gpx3 (glutathione peroxidase 3), Pcx (pyruvate carboxylase), Nfatc2 (Nuclear factor of activated T-cells 2), Zscan21 (zinc finger and SCAN domain containing 21), Bmp5 (bone morphogenetic protein 5), Mpa21 (macrophage activation 2 like), Bdh (3-hydroxybutyrate dehydrogenase), Pfkfb3 (phosphofructokinase/fructose-bisphosphatase 3), and Dpyd (dihydropyrimidine dehydrogenase). Blue bars indicate wild-type control values; red bars indicate *Myog*-deleted values. Error bars represent one standard deviation. * $p < 0.05$, ** $p < 0.01$

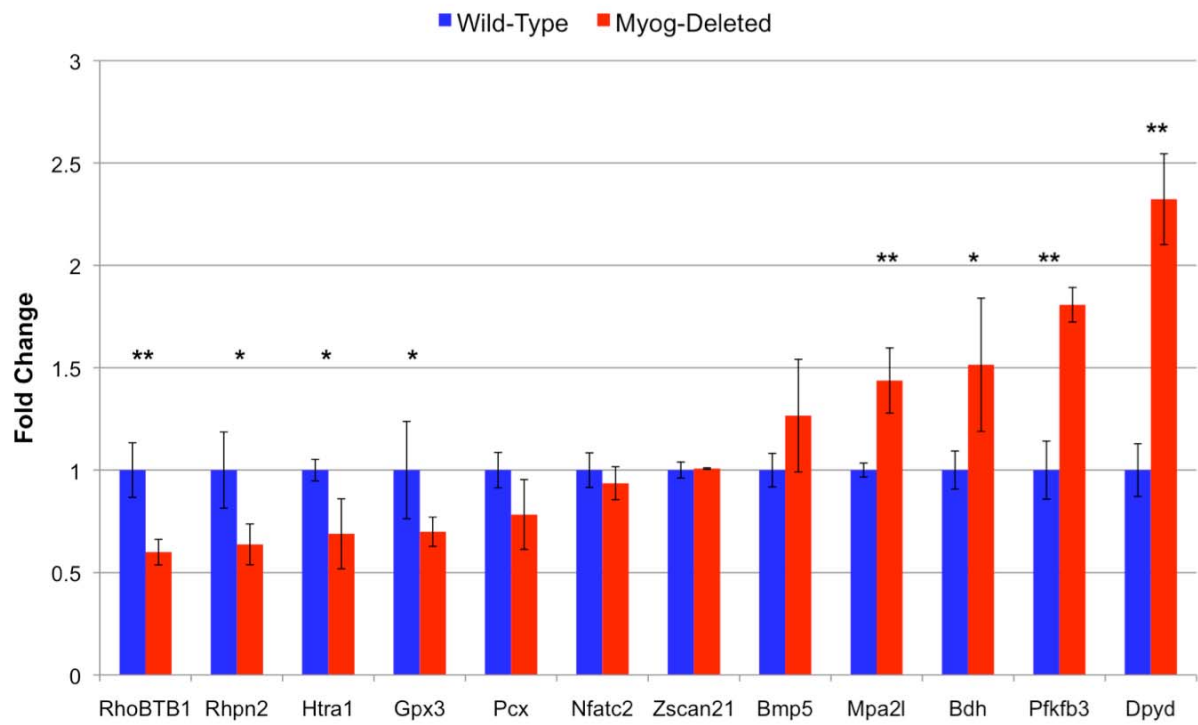


Figure 32 – Dystrophin genotype validation via sequencing

A sequencing plot reveals the nucleotide mutation resulting in dystrophin deficiency in mdx mice. Wild-type mice carry a cytosine (C) at the indicated nucleotide position. Dystrophin deficiency in mice is caused by a thymidine (T) substitution at this position, leading to a premature stop codon (AUA). Given that dystrophin is X-linked, only females may be heterozygous.

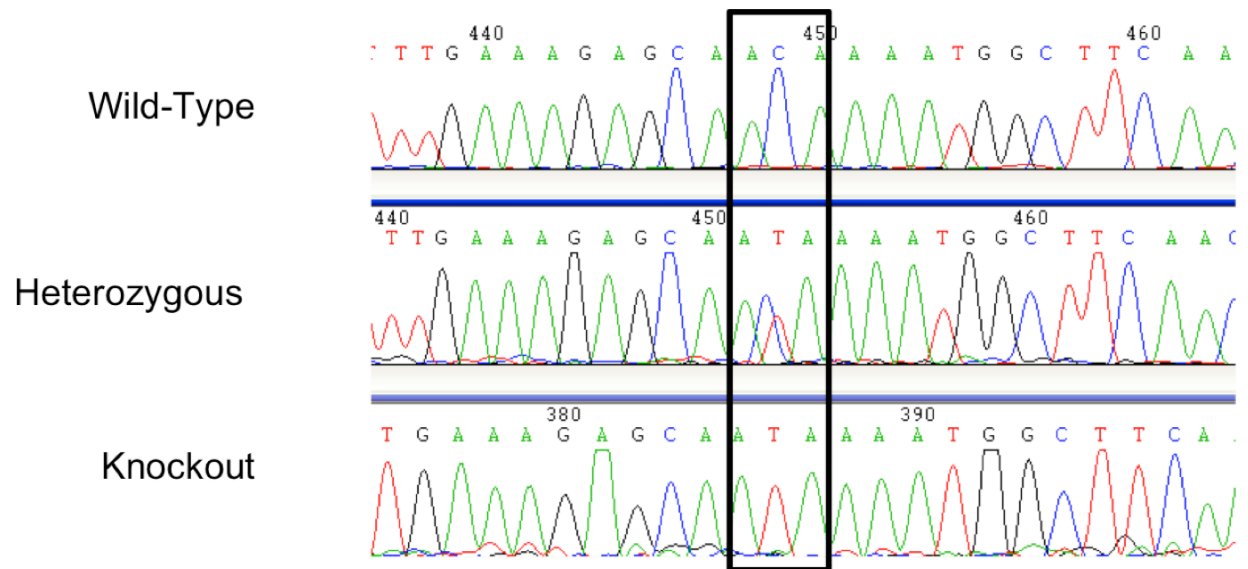


Table I – Description of selected and validated microarray genes

Fold change	Regulation	Gene Symbol	Gene Title	GO Biological Process Term
2.4	down	Rfx7	regulatory factor X, 7	regulation of transcription, DNA-dependent
1.8	down	Rhobtb1	Rho-related BTB domain containing 1	small GTPase mediated signal transduction
1.8	down	Rhpn2	rhopilin, Rho GTPase binding protein 2	signal transduction
1.7	down	<i>Myog</i>	myogenin	regulation of transcription, DNA-dependent
1.6	down	HtrA1	HtrA serine peptidase 1	regulation of cell growth /// proteolysis /// negative regulation of transforming growth factor beta receptor signaling pathway /// negative regulation of BMP signaling pathway
1.6	down	Gpx3	glutathione peroxidase 3	glutathione metabolic process /// response to oxidative stress /// hydrogen peroxide catabolic process /// protein homotetramerization /// protein homotetramerization /// oxidation reduction
1.6	down	Zscan21	zinc finger and SCAN domain containing 21	transcription /// regulation of transcription, DNA-dependent /// multicellular organismal development /// spermatogenesis /// cell differentiation /// positive regulation of transcription, DNA-dependent /// oogenesis
1.5	down	Pcx	pyruvate carboxylase	gluconeogenesis /// oxaloacetate metabolic process /// metabolic process /// lipid biosynthetic process
1.4	up	Bmp5	bone morphogenetic protein 5	skeletal system development /// ossification /// multicellular organismal development /// pattern specification process /// cell differentiation /// growth /// cartilage development
1.6	up	Pfkfb3	6-phosphofructo-2-kinase/fructose-2,6-biphosphatase 3	fructose metabolic process /// fructose 2,6-bisphosphate metabolic process /// metabolic process
1.8	up	Mpa2l	macrophage activation 2 like	immune response
1.9	up	Dpyd	dihydropyrimidine dehydrogenase	'de novo' pyrimidine base biosynthetic process /// pyrimidine base catabolic process /// uracil catabolic process /// thymidine catabolic process /// UMP biosynthetic process /// metabolic process /// oxidation reduction
2.0	up	Bdh1	3-hydroxybutyrate dehydrogenase, type 1	metabolic process /// oxidation reduction

Section 2.12 - *Mdx mice exhibit reduced exercise endurance*

Although dystrophin-deficient mice appear normal, a phenotypic difference may be uncovered during exercise. Young adult mdx mice were subjected to a modified high-intensity treadmill regime to determine whether they are capable of normal exercise duration and more prone to exercise-induced muscle fatigue relative to wild-type control mice. Over a period of 14 consecutive days, wild-type mice consistently outperformed mdx mice by approximately two-fold (Wild-type 527 meters/day, *Myog*-deleted 272 meters/day) (Figure 33). These results indicate that the lack of dystrophin in this mixed genetic background causes sufficient muscle trauma to mdx mice, thereby limiting their exercise endurance.

Section 2.13 - *Lack of myogenin in dystrophin-deficient adult mice attenuates reduced exercise endurance*

To determine whether myogenin is necessary in adult mdx mice during periods of exercise-induced stress, *Myog*-deleted; mdx double-knockout mice were subjected to the modified high-intensity exercise regime. Within one week of *Myog* deletion, double knockout mice initially exhibited a similar exercise capacity as mdx mice. Over a period of 14 consecutive days, *Myog*-deleted mice showed a marked improvement in exercise running performance relative to mdx mice. On average, double knockout mice ran approximately 2-fold farther than mdx mice, and similar distances as wild-type control mice (Figure 34). These results indicate that *Myog*-deletion from young adult mdx mice attenuates their inherently reduced capacity for exercise.

Figure 33 – Mdx mice exhibit a reduced exercise capacity

Wild-type and mdx mice were run using a modified high-intensity treadmill protocol for 14 consecutive days. On average, mdx mice ran only 52% of the distance of wild-type mice (Mdx 272 meters, wild-type 527 meters). Blue line and bar indicates wild-type control values; orange line and bar indicates Mdx values. Error bars represent one standard deviation. * $p < 0.005$

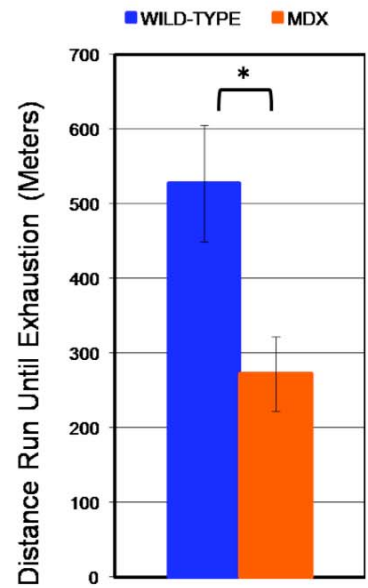
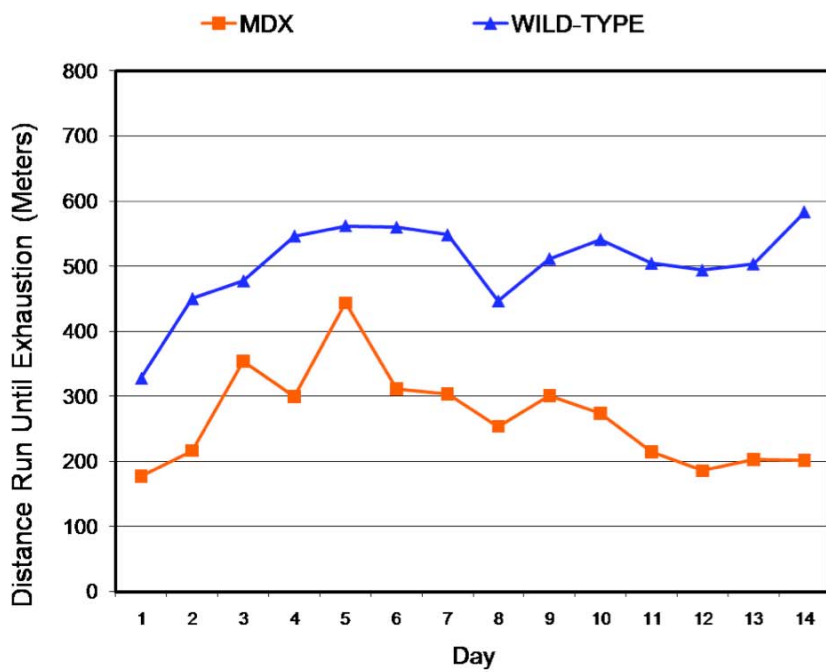
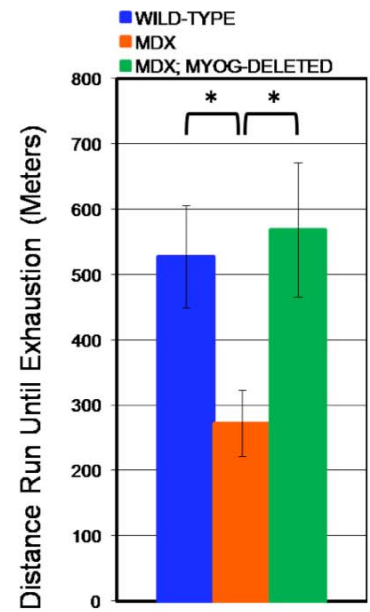
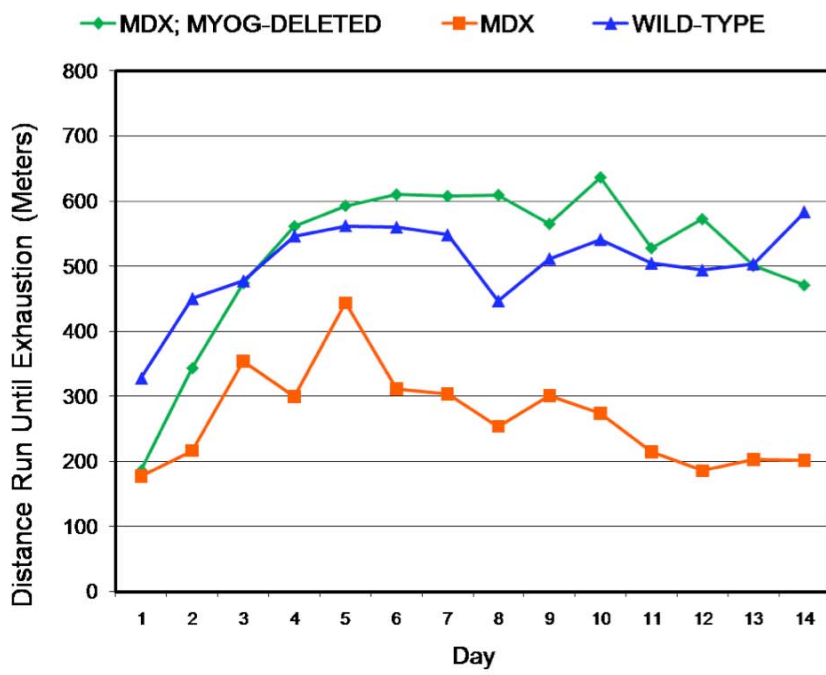


Figure 34 – *Myog* deletion from Mdx mice attenuates reduced exercise capacity

While mdx mice ran only 52% of the distance of wild-type mice, *Myog*-deleted; mdx mice ran similar distances to wild-type mice (*Myog*-deleted; mdx 569 meters, wild-type 527 meters).

Blue line and bar indicates wild-type control values; orange line and bar indicates mdx values; green line and bar indicates *Myog*-deleted; mdx values). Error bars represent one standard deviation. * $p < 0.005$



Chapter 3 - Discussion

Section 3.1 - Myogenin modulates exercise endurance by altering skeletal muscle metabolism

In order to avoid the effects of *Myog* deletion on postnatal body growth, *Myog* was deleted only after mice had reached their adult size. Deletion of *Myog* from adult mice demonstrates that *Myog* is not required for adult viability. Mice lacking *Myog* fed normally, maintained normal body weight, and exhibited normal mobility over a 2-year period of observation. The unremarkable phenotype of sedentary *Myog*-deleted mice suggests that myogenin may have redundant functions with other MRFs during adult life. Thus, it is possible that myogenin expression could be silenced during adult life in sedentary mice without fatal consequences.

Unexpectedly, mice lacking myogenin are remarkably better at exercise running than wild-type control mice within two weeks of *Myog* deletion. Under a low-intensity running regime, *Myog*-deleted mice out-performed their wild-type counterparts. While enhanced low-intensity exercise endurance indicated a potential enhancement in the aerobic metabolic pathways, we failed to find blood metabolite or histological evidence to support this conclusion. A seemingly enhanced aerobic endurance would typically be accompanied by measureable changes in fiber type properties, oxidative potential, and altered expression of fatty acid metabolism genes (Booth and Thomason, 1991). *Myog*-deleted mice appear to exhibit a better aerobic endurance without exhibiting the expected changes on the cellular level.

Myog-deleted mice were also better during high-intensity exercise. Subjecting the mice to uphill running at progressively faster speeds for 12 consecutive days revealed two phenomena: *Myog*-deleted mice are remarkably and consistently better than wild-type mice during high-intensity exercise, and the lack of myogenin does not cause a progressive decrease

in performance from day-to-day. The consistent exercise performance demonstrates that muscle maintenance and regeneration occur normally in exercising adult mice lacking myogenin and suggests that myogenin does not play a critical role during the maintenance of adult skeletal muscle.

Blood glucose and blood ketone measurements give some insight into why *Myog*-deleted mice have increased exercise endurance during exercise. Typical adaptations to endurance exercise involve a more efficient utilization of fatty acids while efficiently conserving muscle and liver glycogen stores (Booth and Thomason, 1991). Once muscle and liver glycogen stores are depleted, exercise performance sharply declines due to the inability of fatty acid metabolism to efficiently keep up with the ATP demands of the body (Fitts, 2004). In addition, the brain preferentially uses glucose for efficient function. Marathon runners who deplete their glycogen stores and experience this performance decline before finishing the race call this point “the wall” (Coyle, 2007). While the depletion of muscle and liver glycogen (as shown by blood glucose depletion) and the enhancement of exercise endurance could be independent of each other, *Myog*-deleted mice are nonetheless capable of exercise as blood glucose levels drop significantly below levels normally associated with exhaustion. Ketone bodies are typically produced in response to excess blood glucose depletion to provide an alternative source of fuel for the brain. Although *Myog*-deleted mice showed only a trend towards elevated blood ketone body production after low-intensity exercise, it further supports the conclusion that *Myog*-deleted mice are excessively using blood glucose. The ability to deplete muscle and liver glycogen stores while continuing to exercise suggests that *Myog*-deleted mice have a higher exhaustion threshold and can push beyond “the wall”. The reduction of blood glucose during low- and high-intensity exercise suggests that the lack of myogenin allows trained *Myog*-deleted mice to preferentially use muscle and liver glycogen stores as a source of energy for longer periods and indicates an enhanced glycolytic flux.

Blood lactate gives further insight into the increased exercise endurance and fatigue resistance of *Myog*-deleted mice. Blood lactate levels traditionally build as exercise intensity increases (Gladden, 1996). The concentration of lactate in the blood is directly associated with exercise fatigue and has been long argued to be a contributing factor. During high-intensity exercise, blood lactate levels in *Myog*-deleted mice are dramatically increased beyond their baseline values after wild-type mice reach exhaustion. The excessive production of blood lactate during the later stages of exercise indicates that *Myog*-deleted mice heavily rely on the glycolytic pathway for energy demand and that blood lactate does not limit their exercise endurance. Indeed, as others have shown, lactate may actually enhance exercise performance and contribute to the enhanced exercise performance of *Myog*-deleted mice (Allen and Westerblad, 2004; Allen et al., 2008; Pedersen et al., 2004). *Myog*-deleted mice may ultimately reach exhaustion under high-intensity exercise due to the acidosis associated with extreme lactic acid production. Acidosis likely limits exercise performance during high-intensity exercise before blood glucose is excessively depleted as it is during low-intensity exercise. Indeed, blood lactate levels are unchanged following low-intensity exercise, suggesting the efficient metabolism of lactate through the Cori Cycle. These results suggest that the extreme exercise performance of *Myog*-deleted mice is ultimately governed by the availability of liver- and muscle-glycogen stores and by the performance-enhancing effects of lactate. A decreased sensitivity to the depletion of glycogen reserves and the ability to withstand extreme muscle acidosis may ultimately enhance exercise endurance.

An increased glycolytic flux in *Myog*-deleted mice suggests that carbohydrate depletion may adversely affect their exercise endurance. Indeed, when *Myog*-deleted mice were fasted for a period of 96 hours, they completely lost their enhanced exercise endurance compared to wild-type mice. Blood glucose measurements indicate that both wild-type and *Myog*-deleted mice were hypoglycemic prior to exercise at 96 hours, and measurements at exhaustion remained

similar to pre-exercise levels in both groups. These data suggest that the reduction in pre-exercise blood glucose dramatically decreased the glycolytic flux in *Myog*-deleted mice during exercise. Likewise, exhausted *Myog*-deleted mice displayed similar blood lactate levels as exhausted wild-type mice after the 96-hour fast. Upon returning the mice to their normal diets, *Myog*-deleted mice recovered their enhanced exercise endurance within 10 days. These results suggest that the enhanced exercise endurance of *Myog*-deleted mice is due to an increased dependence on muscle and liver glycogen as a source of energy.

In addition to myogenin, other investigators have discovered factors that influence exercise capacity. The over-expression of phosphoenolpyruvate carboxykinase (PEPCK) in skeletal muscle increases cage activity and treadmill exercise capacity in mice by repatterning energy metabolism (Hakimi et al., 2007). These mice also exhibited a higher oxygen consumption, increased food intake, decreased body weight, and increased mitochondria in their muscle. Overall, PEPCK over-expression increases the citric acid cycle flux to generate more energy for muscle contraction during strenuous exercise. On the other hand, mice over-expressing PPAR-delta in skeletal muscle demonstrate enhanced exercise performance by an increase in slow-twitch fiber composition (Wang et al., 2004). PPAR-delta is a transcription factor involved in regulation of fat burning in adipose tissue and muscle fiber specification. The transcriptional co-activator PGC-1 alpha also drives slow-twitch fiber formation. PGC1-alpha is expressed in brown fat and skeletal muscle and activates mitochondrial biogenesis (Wu et al., 1999). Furthermore, oxidative metabolism genes are activated when PGC1-alpha is expressed in fast-twitch muscle fibers (Lin et al., 2002). The transformation of fiber type characteristics involves cooperation with Mef2 proteins and calcineurin signaling (Olson and Williams, 2000). Acting through calcineurin signaling, Calsarcin-2, a muscle-specific protein of the sarcomeric Z-disk, modulates exercise performance and alters skeletal muscle fiber type composition (Frey et al., 2008). Together, enhanced exercise performance is associated with alterations in

mitochondrial activity, muscle fiber specification, and calcium signaling. The enhanced exercise endurance of *Myog*-deleted mice may involve pathways that are independent of the pathways described above.

As the innervation of muscle largely determines its fiber type composition, the denervation of *Myog*-deleted mice gives some insight into which pathways myogenin is involved. *Myog* expression is induced upon muscle denervation and this induction requires HDAC4 activity (Tang and Goldman, 2006). After denervation, *Myog* and HDAC4 differentially regulate genes involved in muscle fiber type specification, positively regulating oxidative gene expression while suppressing glycolytic gene expression (Tang et al., 2009). In addition to gene expression changes induced by denervation, denervation also induces muscle atrophy (Jackman and Kandarian, 2004). Myogenin plays an unexpected role as an essential activator of muscle atrophy, and its deletion during adult life suppresses muscle atrophy after denervation (Moresi V., 2010). After denervation, myogenin activates skeletal muscle E3 ubiquitin ligases (MuRF1 and atrogin-1), which mediate muscle proteolysis and atrophy. These results indicate that the expression of *Myog* and glycolytic genes is mutually exclusive and that the deletion of *Myog* during adult life may relieve the HDAC4-mediated suppression of glycolytic genes, thus enhancing glycolytic flux in *Myog*-deleted mice (Figure 36). Furthermore, the ability of *Myog*-deleted mice to resist muscle atrophy after denervation suggests that *Myog*-deleted mice may be resistant to muscle damage after exercise-induced injury.

To summarize, adult mice lacking myogenin exhibit an enhanced exercise capacity associated with increased blood glucose utilization and excessive lactate production. These changes are completely abolished when mice reach a hypoglycemic state during a 96-hour fast. This enhanced exercise endurance is not associated with a change in myosin ATPase fiber type, myosin isoform expression, myofiber oxidative potential, the metabolism of fatty acids, or

increased dietary consumption. The ability to shift the metabolic activity of skeletal muscle fibers without a change in myosin heavy chain expression is well documented (Hughes et al., 1999; Kiens et al., 1993; Schluter and Fitts, 1994). As fiber-type switching is more of a long-term adaptation, changes in metabolic activity in *Myog*-deleted mice are likely responsible for the enhanced exercise capacity observed within 2-weeks of *Myog* deletion. Notably, the over-expression of myogenin shifts the muscle enzymatic activity from glycolytic towards oxidative metabolism, independent of a change in fiber type (Hughes et al., 1999). While the presence of myogenin leads to increased oxidative enzyme activity and mediates the effect of innervation on slow-twitch muscle fibers (Hughes et al., 1993), the absence of myogenin may provide a less oxidative (more glycolytic) environment. Together, these results suggest that the enhanced exercise capacity of *Myog*-deleted mice is not due to changes traditionally associated with enhanced exercise capacity but the result of enhanced glycolytic flux.

This study is the first to demonstrate both a positive effect of removing a MRF during adult life and a phenomenon involving a shift from oxidative towards glycolytic metabolism. The ability of mice lacking myogenin to outperform wild-type mice during exercise running raises a seemingly paradoxical question: Why does myogenin expression persist in adult skeletal muscle? These results suggest that myogenin is not required and that the deletion of *Myog* is actually advantageous to exercise endurance. Two potential explanations for myogenin expression during adult life are offered:

- 1.) Myogenin may be more highly expressed in populations of mice that are dependent on environmental adaptations. Over many years and generations away from natural predators, laboratory mice may experience less selective pressure towards the adulthood silencing of myogenin, thus leading to the increased development of slow-oxidative fibers. Myogenin may exhibit lower levels of expression in some wild populations of

mice that evolved in heavily wooded areas, where sprinting to avoid predators may be an evolutionary advantage. The ability to sprint would be enhanced by the increased glycolytic enzyme activity due to the loss of myogenin.

- 2.) Myogenin is essential throughout adult life. While the deletion of *Myog* confers enhanced exercise endurance, this phenotype is not without an excessive depletion of blood glucose. The body's natural ability to sense hypoglycemia and react by ceasing exercise activity would likely prove more beneficial in most environments, given that long-term effects of hypoglycemia increase overall morbidity and mortality (Fischer et al., 1986; Service, 1995). While we did not detect an increased morbidity and mortality associated with *Myog*-deleted mice after exercise exhaustion, environmental pressure may be required to witness this selection. The presence of myogenin during adult life may contribute to feedback mechanisms ultimately allowing the body to cease excessive skeletal muscle activity in favor of blood glucose conservation.

Section 3.2 – The lack of myogenin enhances adaptation to exercise training

While determining that *Myog*-deleted mice have enhanced exercise endurance during involuntary treadmill running, we also tested their voluntary exercise capacity. Although we were not able to detect that mice lacking myogenin voluntarily run more, the mice used in this experiment gave additional insight into this phenotype. Given that *Myog*-deleted mice run similar distances and speeds as wild-type mice during voluntary exercise, their will and capacity to perform under voluntary exercise is unaffected by the loss of myogenin. Indeed, low-intensity, voluntary exercise would most certainly not stress glycolytic pathways or blood glucose levels (Allen et al., 2001).

Over a 6-month period, wild-type and *Myog*-deleted mice were allowed unrestricted access to voluntary exercise. During this training period, wild-type mice are expected to exhibit long-term adaptations to exercise, such as fiber-type changes, increased mitochondria density and activity, and enhanced vasculature. Fast- to slow-twitch fiber-type transition and increased oxidative capacity are well-documented, long-term adaptive responses to exercise training (Baldwin et al., 1977; Baldwin et al., 1972; Dudley et al., 1982; Holloszy et al., 1970; Ishihara et al., 1991; Rodnick et al., 1989; Sexton, 1995). Indeed, these changes were quite apparent in trained wild-type mice, which exhibited enhanced exercise endurance when they were retested with involuntary high-intensity exercise. Surprisingly, trained *Myog*-deleted mice exhibited a superior adaptive response to exercise training under similar conditions. In addition, untrained (sedentary) *Myog*-deleted mice had similar exercise endurance as trained wild-type mice. This suggests that merely silencing myogenin expression during adult life confers the same exercise endurance obtained after long-term exercise training. The effect of exercise training and deletion of myogenin on exercise performance appears to be a synergistic effect as trained *Myog*-deleted mice have a nearly 4-fold enhanced exercise capacity over untrained wild-type mice.

The enhanced exercise endurance of trained wild-type mice is associated with a mild increase in slow-twitch fiber-type proportion and a dramatic increase in succinate dehydrogenase (SDH)-positive fibers. The superior exercise endurance of trained *Myog*-deleted mice is associated with a comparatively higher proportion of both slow-twitch fibers and SDH-positive fibers than trained wild-type control mice. These changes indicate a typical response to training in trained wild-type mice and an enhanced response to training in trained *Myog*-deleted mice. The increased proportion of the slow-twitch fibers and oxidative capacity allow trained *Myog*-deleted mice the ability to efficiently conserve muscle and liver glycogen stores by more efficiently utilizing fatty acids during low-intensity exercise. As exercise intensity progresses,

the more efficient glycolytic flux of *Myog*-deleted mice may better support the energy demands of high-intensity exercise. It is also likely that the ability of *Myog*-deleted mice to excessively deplete their glucose reserves supports the high-energy demands of high-intensity exercise. The dramatic changes in fiber type and SDH enzyme activity support the conclusion that *Myog*-deleted mice respond better to training than wild-type mice.

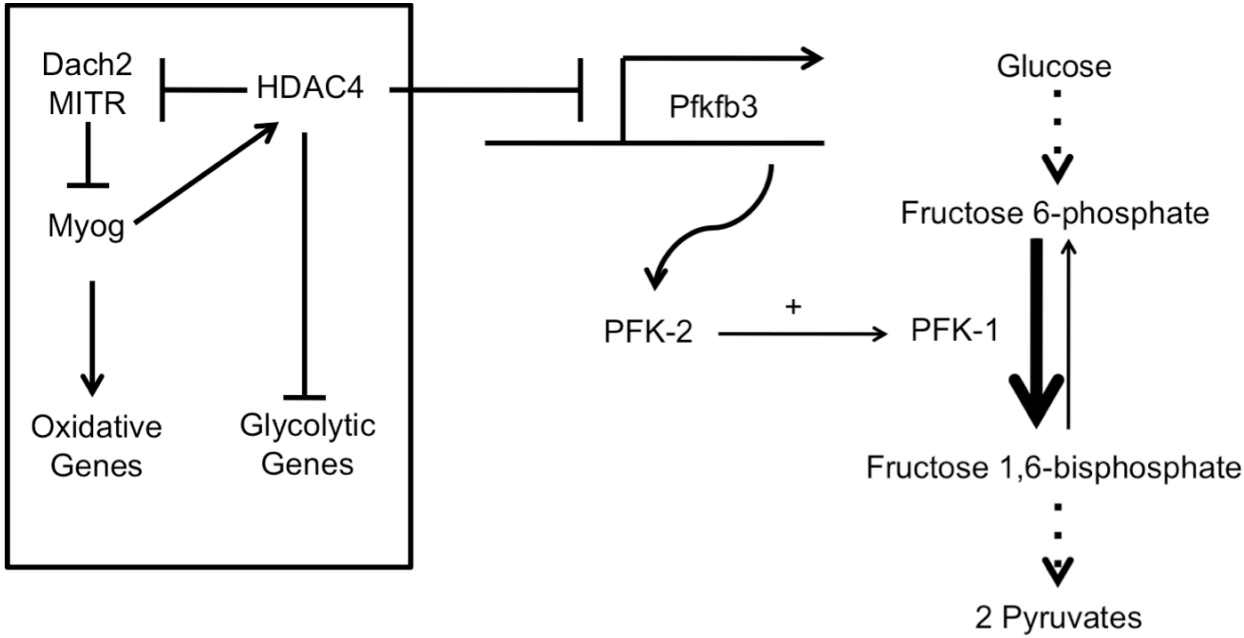
Because myogenin functions as a transcription factor, changes in gene expression would be expected following its deletion. Indeed, genes involved in signal transduction and metabolism were altered in trained *Myog*-deleted mice when compared to trained wild-type mice. Gene expression changes of particular interest include: *Gpx3*, *Pcx*, *Bdh*, and *Pfkfb3*. *Gpx3* (Glutathione peroxidase 3) is a primary antioxidant enzyme, which has been suggested to potentially improve exercise performance and delay muscle fatigue (Powers et al., 1999). Given that *Gpx3* is downregulated 30% in mice lacking myogenin, *Myog*-deleted mice may be more prone to long-term oxidative stress while exhibiting enhanced exercise performance. *Pcx* (Pyruvate Carboxylase) is involved in the first step of gluconeogenesis and plays a major role in both carbohydrate and lipid metabolism (Jitrapakdee et al., 2008). The 20% downregulation of *Pcx* in mice lacking myogenin may offer insight into why *Myog*-deleted mice have increased glycolytic activity. *Pcx* catalyzes an anaplerotic reaction, replenishing oxaloacetate within the citric acid cycle to maintain efficient oxidative metabolism. A reduction in *Pcx* activity may enhance glycolytic metabolism by partially shunting pyruvate away from the citric acid cycle, thus contributing to the increase in blood lactate levels. Currently, there are no known references to such a phenomenon, and *Pcx* deficiency is typically detrimental (Jitrapakdee et al., 2008). *Bdh* (3-hydroxybutyrate-dehydrogenase) is involved in the process of ketone body production (Owen et al., 1967). The 50% increase in *Bdh* expression in mice lacking myogenin may be a result of decreased blood glucose availability to the brain. Given that the brain switches to ketone bodies for energy when blood glucose is low, this could be a compensatory

effect. *Pfkfb3* (Phosphofructokinase / Fructose-bisphosphatase) is a gene involved in a rate-limiting, reversible step of the glycolytic pathway (Minchenko et al., 2003; Yalcin et al., 2009). *Pfkfb3* encodes a muscle-specific protein called Pfk2, which regulates the activity of Pfk1, and ultimately regulates glycolytic flux. Although Pfk2 is a dual activity enzyme, promoting both glycolysis and gluconeogenesis, this particular isoform has a 400:1 tendency to enhance glycolytic flux in skeletal muscle (Yalcin et al., 2009). The 80% increase in *Pfkfb3* expression in mice lacking myogenin may be involved in the mechanisms conferring enhanced exercise capacity. Indeed, myogenin has been previously shown to indirectly inhibit genes involved in the glycolytic pathway (Tang et al., 2009). Together, these results suggest that glycolytic metabolism may be partially enhanced by *Myog* deletion, mediated through a release of *Pfkfb3* inhibition (Figure 35).

While some of these changes in gene expression may require exercise training, they are nonetheless changed due to myogenin's absence. Mild changes in gene expression for any one or more of these genes may sufficiently alter the metabolic properties of skeletal muscle to confer enhanced exercise endurance. It is unclear how an enhanced glycolytic metabolism (i.e. the ability to preferentially use glycogen stores during exercise training) leads to increased proportion of slow-twitch fibers and oxidative capacity in trained *Myog*-deleted mice. Although the over-expression of myogenin in fast-twitch muscle increases oxidative enzyme activity (Hughes et al., 1999), the absence of myogenin does not appear to leave mice with an inferior oxidative capacity. While myogenin has been shown to mediate the effects of innervation on slow-twitch muscle fiber formation (Hughes et al., 1993), other factors clearly play similar roles during the exercise training of mice lacking myogenin. The absence of myogenin during periods of long-term exercise training may provoke compensatory pathways that also mediate the effects of slow-twitch fiber formation and increased oxidative metabolism.

Figure 35 – Potential Mechanism

Myogenin positively regulates the expression of oxidative metabolism genes (Hughes et al., 1999; Hughes et al., 1993; Tang et al., 2009) and represses glycolytic metabolism genes through HDAC4 activity. Pfkfb3, a glycolytic gene involved in a rate-limiting step of glycolysis, converts F6P to F2,6BP, which positively regulates the activity of PFK-1. PFK-1 is a dual-activity enzyme that interconverts F6P and F1,6BP, directly regulating glycolytic flux. Pfkfb3 expression may be upregulated in the absence of myogenin, thereby increasing PFK-1 activity and enhancing glycolytic flux.



Overcompensation by one or more deregulated genes in this pathway could explain how exercise training not only induces the formation of slow-oxidative fibers but also enhances this adaptive response.

In summary, trained *Myog*-deleted mice exhibit a better adaptive response to exercise training because of their ability to selectively use, and excessively deplete, liver and muscle glycogen stores during exercise. Changes in global gene expression due to myogenin's absence may play a role in mediating the innervation-dependent formation of slow-oxidative fibers during exercise training. These traits allow trained *Myog*-deleted mice to reach exercise intensities beyond normal physical limitations. The identification of *Myog*-dependent genes and pathways during adult life is an aim of Project II.

Section 3.3 – The lack of myogenin attenuates muscle fatigue associated with muscular dystrophy

Muscular dystrophy is a condition characterized by progressive muscle weakness and muscle wasting, ultimately resulting in early mortality (Blake et al., 2002). The progressive muscle weakness in mice lacking dystrophin makes them ideal to test whether myogenin is required during adult life. Mdx mice exhibited no phenotypic difference during sedentary life and were seemingly normal. Although dystrophin-deficiency results in a varying degree of strain-dependent mouse phenotypes, increased muscle fatigue was successfully demonstrated in mdx mice during treadmill running. Mdx mice were capable of exercise for only 50% of total exercise time compared with wild-type control mice. Overall, dystrophin was not essential for a sedentary lifestyle in mdx mice yet was necessary for normal exercise endurance.

Deleting myogenin from mdx mice allowed us to test the necessity of myogenin in structurally weakened and dysfunctional skeletal muscle. Given that muscle function is

compromised at the cytoskeletal level in mdx mice, myogenin was hypothesized to be essential for the maintenance of many other critical skeletal muscle structural proteins. However, the deletion of *Myog* from young adult mdx mice did not affect their mobility or ability to feed. This result indicates that myogenin is not required for sedentary muscle function or viability in mdx mice. When mdx mice lacking myogenin were initially subjected to treadmill running, these double-knockout mice had similar exercise endurance as mdx mice. Unexpectedly, over a 14-day period we observed an attenuation of the reduced exercise endurance associated with dystrophin deficiency. The deletion of myogenin not only had immediate positive effects on muscle fatigue, but also consistently maintained this trend during two weeks of exhaustive exercise.

Interestingly, fast glycolytic muscle fibers have a 50% reduction in phosphofructokinase activity in human patients with muscular dystrophy (Chi et al., 1987). Similarly, loss of phosphofructokinase activity contributes to defects in glycolysis and increased fatigability in mice with muscular dystrophy (Wehling-Henricks et al., 2009). When phosphofructokinase activity is artificially increased in the skeletal muscle of mdx mice, glycogen metabolism is enhanced concomitantly with increased exercise endurance. Deletion of *Myog* from our mdx mice may offset their inherent glycolytic dysfunction. This effect may be partly mediated through an upregulation of phosphofructokinase expression as a consequence of *Myog* deletion. Thus, the loss of myogenin may ultimately result in a partial rescue of fatigability and exercise endurance in mice with muscular dystrophy. These data suggest that the modulation of myogenin expression during young adult life in humans may provide another avenue for muscular dystrophy therapy development.

PROJECT II

Myogenin target gene activation in adult muscle stem cells

Chapter 4 - Introduction

Myogenesis coordinates skeletal muscle formation and accretion, which begins during embryonic life and ends postnatally after an animal reaches adulthood. The maintenance and repair of skeletal muscle during adult life recapitulates the process of embryonic skeletal muscle development, and is coordinated by adult satellite stem cells (Charge and Rudnicki, 2004; Cossu and Molinaro, 1987; Gibson and Schultz, 1983; Schultz et al., 1985). Satellite stem cells reside along myofibers and are activated by signals during postnatal growth, muscle repair, and muscle maintenance. Muscle stem cell differentiation is a process that is tightly controlled primarily by MRFs (Figure 1). MRFs dimerize with the ubiquitous E12/E47 proteins and bind to E-box motifs present within the transcriptional control regions (TCR) of skeletal muscle-expressed genes. These genes must be activated for the proper development of skeletal muscle. MRF proteins cooperate with MEF2 proteins to efficiently activate the expression of skeletal muscle-expressed genes (Black and Olson, 1998).

Significant progress has been made towards distinguishing the individual MRF family members. While many functions of individual MRFs are functionally redundant, each MRF is efficiently expressed during muscle stem cell proliferation and differentiation and is conserved among vertebrate animals (Sabourin and Rudnicki, 2000). Quiescent muscle stem cell activation and proliferation primarily involves the activity of MyoD, Myf5, and Mrf4. Myoblast differentiation into myofibers involves the activity of MyoD, myogenin, and Mrf4 (Berkes and Tapscott, 2005; Charge and Rudnicki, 2004) (Figure 1). Mild phenotypes are observed with the single knockouts of *MyoD*, *Myf5*, and *Mrf4*, but the knockout of *Myog* severely disrupts myoblast differentiation and the subsequent formation of skeletal muscle during embryonic myogenesis (Hasty et al., 1993; Kablar et al., 1998; Kassam-Duchossoy et al., 2004; Nabeshima et al., 1993; Rudnicki et al., 1993). Although myogenin activates many genes required for skeletal muscle development, it is not required for the activation of all skeletal muscle genes

(Venuti et al., 1995). Furthermore, other MRF family members do not compensate for myogenin's loss (Rawls et al., 1995). These results suggest that myogenin efficiently activates target genes required for differentiation, and these target genes are not efficiently activated by compensatory mechanisms of other MRF family members.

To simplify the analysis of myogenin-dependent gene activation, the function of myogenin is often compared with another MRF with broad functions throughout myogenesis, MyoD. Recently, embryonic myogenin target genes were discovered using gene expression profiling. Data analysis revealed that many of the differentially expressed genes were Z-line structural components (Figure 36). The Z-line functions as an anchor for contractile proteins. ChIP analysis of selected genes showed preferential binding of myogenin rather than MyoD at many of the transcriptional control regions upstream of these target genes (Davie et al., 2007) (Figure 37).

Other investigators have published results that help elucidate the roles of myogenin and MyoD during skeletal muscle development. These studies show MyoD may bind the TCRs of many muscle-expressed genes at relatively earlier times than myogenin (Cao et al., 2006; Ohkawa et al., 2006). MyoD contains an alpha-helix domain, not functionally conserved in myogenin, which allows it to interact with cofactors such as the Pbx/Meis complex to mediate the early stages of chromatin remodeling (Berkes et al., 2004). Pbx/Meis is constitutively bound to many promoters of muscle specific genes and this may help recruit MyoD to nearby E-box sites to promote the activation of these genes. This activity is thought to loosen the chromatin

Figure 36 – Differentially expressed genes in embryonic muscle lacking myogenin. RT-qPCR validation of selected differentially expressed genes in *Myog*-null E15.5 tongue muscle. These genes are generally involved in muscle contraction, structural components, and found within the sarcomeric Z-disk of the myofiber. Blue bars indicate wild-type control values; red bars indicate *Myog*-null values. Error bars represent one standard deviation. Figure borrowed from (Davie et al., 2007).

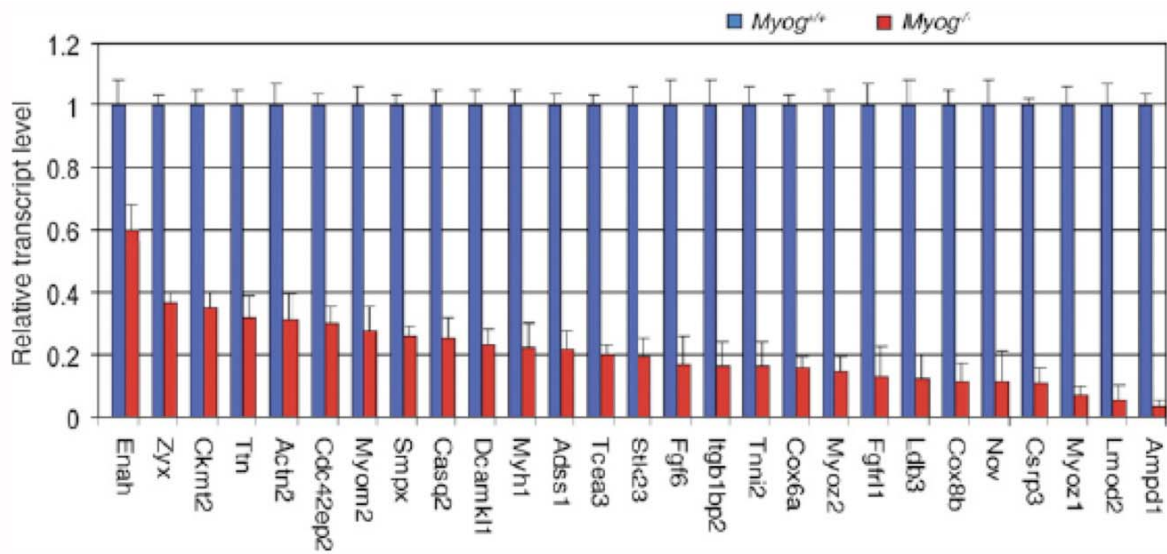
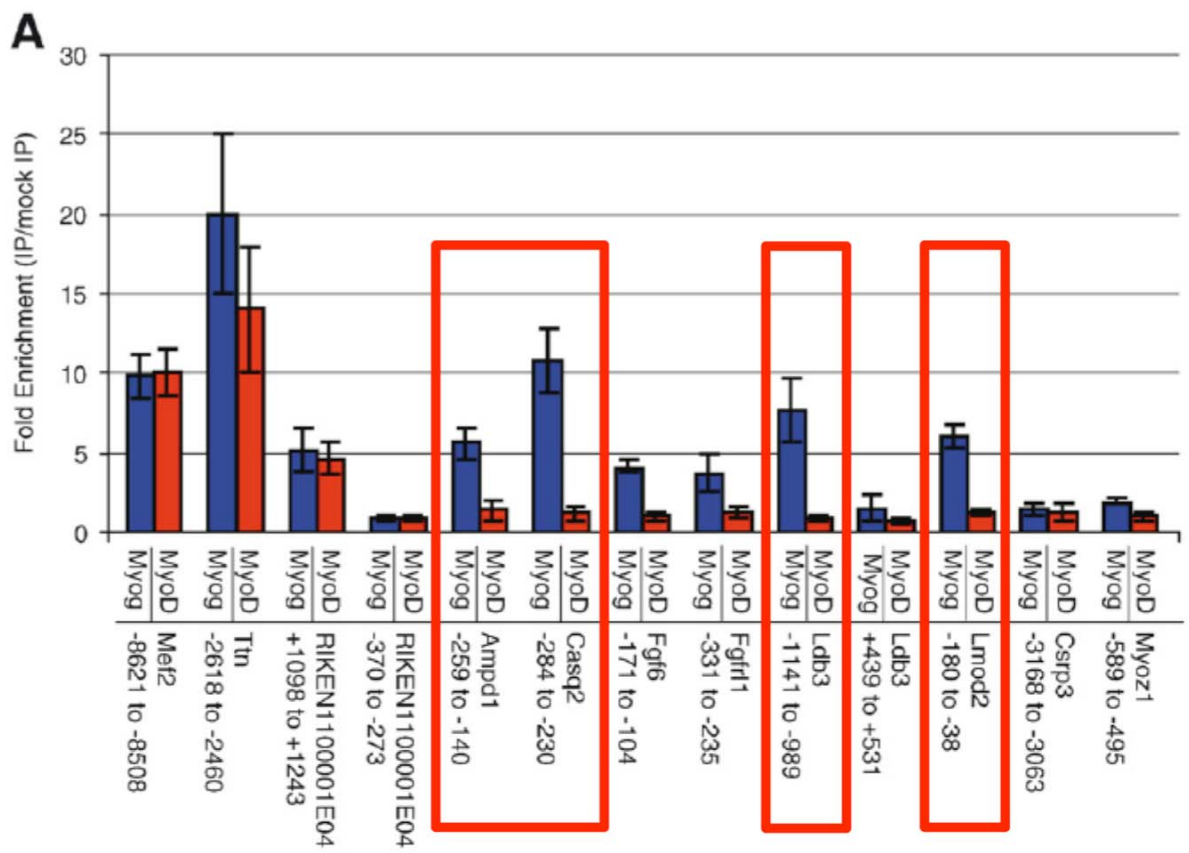


Figure 37 – Embryonic *Myog*-dependent target genes

ChIP analysis revealed that many differentially expressed genes in *Myog*-null embryonic tongue muscle were also preferentially bound by *Myog* within their TCRs. Data is presented as fold enrichment of the immunoprecipitation (IP) over mock IP. Red boxes indicate gene TCRs where myogenin association is highly enriched. Blue bars indicate wild-type control values; red bars indicate *Myog*-null values. Error bars represent one standard deviation. Figure borrowed from (Davie et al., 2007).



structure at some muscle-expressed genes later in development where myogenin can subsequently bind the TCRs for efficient gene activation. While this is a promising result and contributes to the mechanistic differences between myogenin and MyoD, it does not explain why MyoD cannot compensate in myogenin germline-knockout mice. It also does not explain why MyoD germline-knockout mice are apparently normal if myogenin would not have complete access to its target genes.

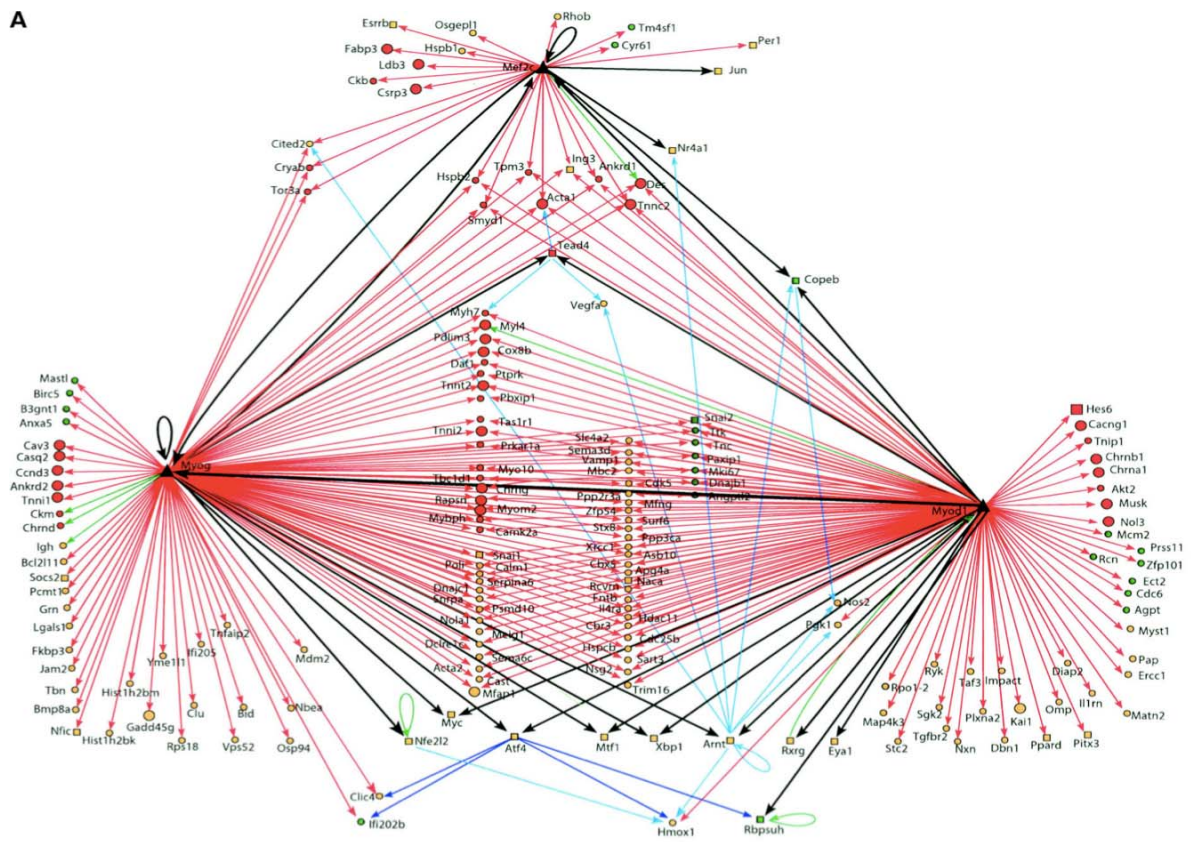
Blais et al. analyzed the genome-wide binding of myogenin, MyoD, and Mef2 using ChIP-chip technology (Blais et al., 2005). The authors discovered many distinct and overlapping target-genes of myogenin and MyoD (Figure 38). An enriched list of myogenin-specific target genes will contribute to the future understanding of why MyoD is not associated with the TCRs of myogenin-specific genes.

The embryonic lethality observed in myogenin knockout mice precludes postnatal and adult studies of skeletal muscle lacking this transcription factor. To circumvent this, a conditional knockout was created where exon I of *Myog*, which contains the bHLH domain, was flanked with *loxP* sites and deleted upon activation of the Cre-ER transgene via tamoxifen injection (Hayashi and McMahon, 2002; Knapp et al., 2006) (Figure 2). When *Myog* was deleted between E16.5 and birth, *Myog*-deleted mice died at birth due to asphyxiation. While it was previously believed that most skeletal muscle has developed by E15.5 (Venuti et al., 1995), closer inspection of *Myog* conditional knockout mice revealed that myogenin was required for proper skeletal muscle formation until birth (Meadows et al., 2008).

To summarize, myogenin is a transcription factor that cannot be compensated for by the other MRFs, and cannot activate all muscle-expressed genes. A detailed understanding of how myogenin achieves this specificity to regulate skeletal muscle development is essential. Identifying mechanisms involved in conferring myogenin target-gene specificity will allow for a

Figure 38 – A global comparison of genes bound by *Myog* and MyoD reveals many distinct and overlapping target genes. ChIP on chip and RT-qPCR analyses reveal *Myog*-dependent and MyoD-dependent target genes. Borrowed from (Blais et al., 2005).

A



broader understanding of target gene regulation by transcription factor families. To help facilitate this goal, a Tet-On-*Myog* cell culture system was engineered and employed. The ability to conditionally express myogenin in *Myog*-deleted adult muscle stem cells allowed for the analysis of myogenin-dependent target gene specificity. Tet-On-*Myog* adult muscle stem cells were analyzed throughout the process of differentiation to identify the TCRs where myogenin is binding and activating target gene transcription.

Hypothesis

Mechanisms exist that allow myogenin, but not the three other MRFs, to bind more efficiently to distinct E-box motifs present within the transcriptional control regions of many genes expressed in skeletal muscle. These mechanisms are involved in conferring target gene dependence on myogenin (Figure 39).

Specific Aims

- 1.) **Engineer a cell culture system where myogenin is conditionally expressed to study the process of myogenin-dependent gene regulation.** *Myog*-deleted adult muscle stem cells will be used for the stable viral integration of a Tet-On-*Myog*-GFP construct. These cells will be characterized for myogenin expression, GFP expression, and a doxycycline-dose dependent response of *Myog* induction.
- 2.) **Identify a set of muscle-expressed genes that is strictly dependent on myogenin for normal expression.** Differentially expressed genes identified in previous studies serve as potential *Myog*-dependent genes (Davie et al., 2007; Meadows et al., 2008) (Figures 36, 40). Genes from these studies will be used to determine whether they are strictly dependent on myogenin in the context of adult muscle stem cells.
- 3.) **Identify the regulatory elements and cofactors that confer target gene dependence on myogenin for normal expression.** ChIP analysis will be employed, along with sequence analysis of myogenin-dependent gene TCRs, to identify potential mechanisms that confer myogenin dependence in adult muscle stem cells.

Figure 39 – Hypothesized model of myogenin target gene dependence.

At the TCR of myogenin-dependent genes, the following sequence of events would be required for myogenin-dependent gene activation: 1.) Once canonical E-box motifs are exposed, *Myog* will bind to E-box motifs and associate with unknown cofactor(s). The cofactor(s) will help stabilize myogenin-promoter binding. 2.) Myogenin and the unidentified cofactor(s) will cooperate to initiate gene transcription. The cofactor may have a consensus-binding motif. MyoD will not interact with the cofactor(s) in the context of a myogenin-dependent TCR, and will not efficiently initiate gene transcription.

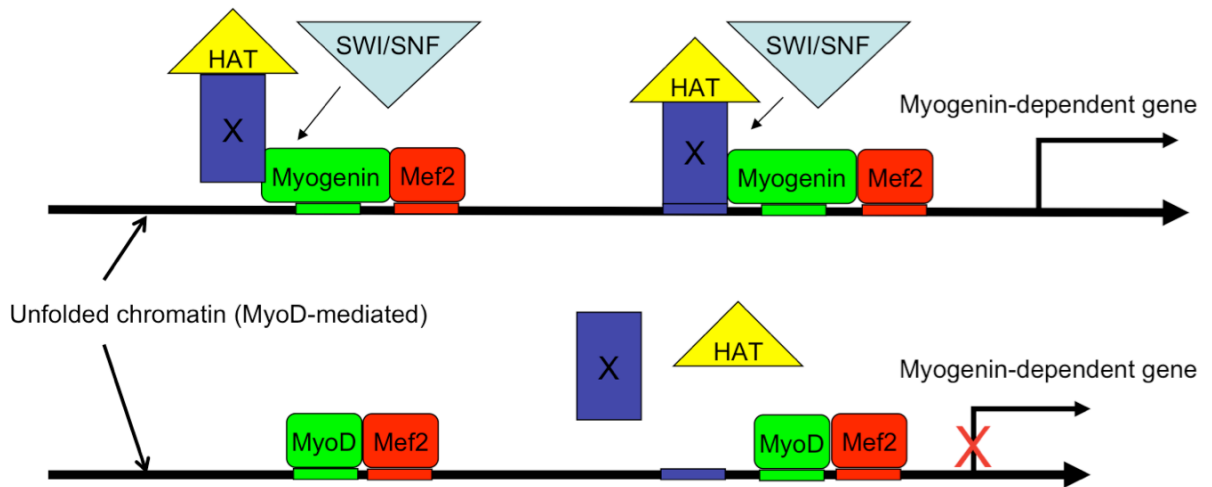
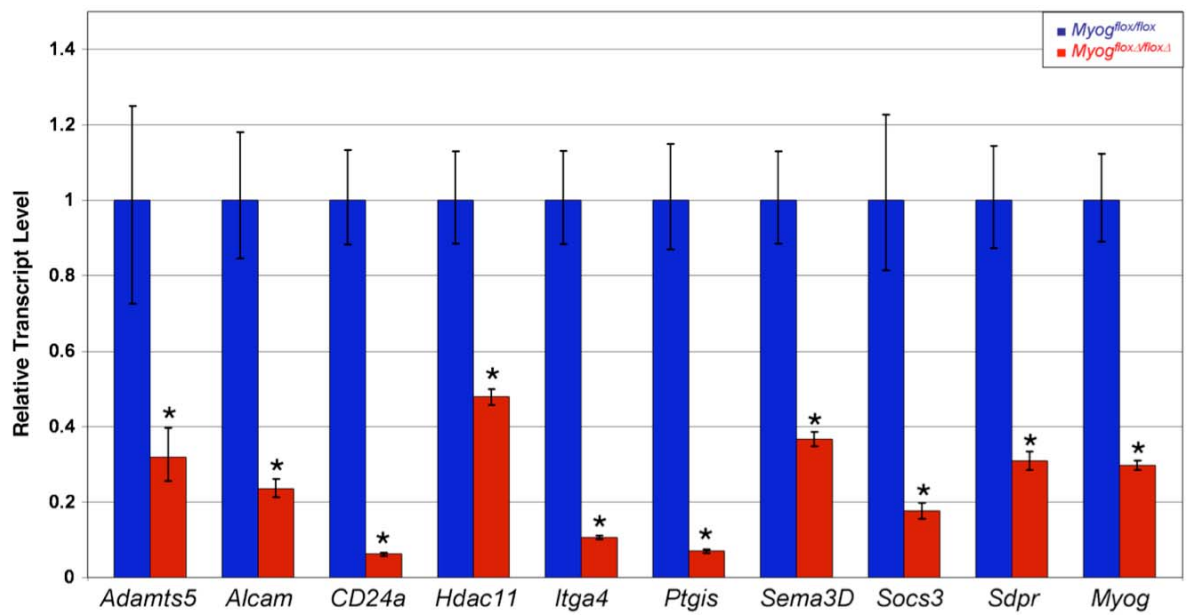


Figure 40 – Differentially expressed genes in muscle stem cells lacking myogenin. RT-qPCR validation of selected differentially expressed genes in *Myog*-deleted muscle stem cells. These genes are generally involved in cell fusion, adhesion, and signaling. Blue bars indicate wild-type control values; red bars indicate *Myog*-null values. Error bars represent one standard deviation. Figure borrowed from (Meadows et al., 2008).



Chapter 5 - Results

Section 5.1 - Inducible myogenin expression in Tet-On-Myog-GFP adult muscle stem cells

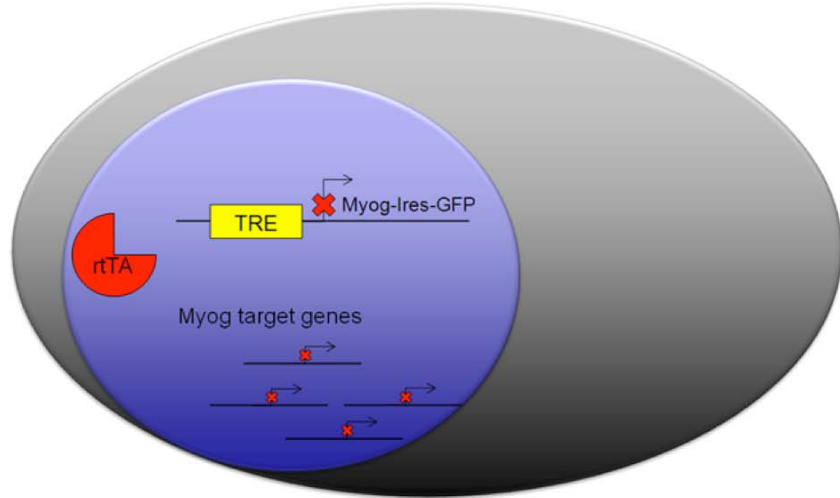
Myog-deleted adult muscle stem cells [and embryonic myoblasts] were used to genetically engineer a cell culture-based system where *Myog* is conditionally activated with a Tet-On approach and easily visualized with a GFP reporter gene (Figure 41). The Clontech pRetroX-Advanced System was used to facilitate this experiment (Figure 42). Initial screening, selection, and characterization of the cells involved multiple methods. Clonal selections were based on a 500 ng/ml concentration of doxycycline to efficiently identify clones with a low basal expression of the Tet-On-*Myog*-GFP and a strong expression upon induction. Our selected primary clones exhibited a combination of strong cytoplasmic GFP expression in the +Dox state and extremely weak GFP expression in the –Dox state (Figure 43A). These clones also exhibited strong nuclear expression of myogenin in the +Dox state and weak myogenin expression in the –Dox state. RT-qPCR analysis revealed that the basal expression of *Myog* in proliferating, non-Dox-induced Tet-On-*Myog*-GFP cells was only 15% of normal expression found in wild-type control cells (Figure 43B). When these cells were treated with 500 ng/ml of doxycycline, a strong ten-fold increase in *Myog* was observed relative to wild-type control cells (Figure 43B). *Myog*-deleted adult muscle stem cells (negative control cells) expressed myogenin at 5% of normal levels. These results demonstrate that we have successfully created adult muscle stem cells [and embryonic myoblasts] where myogenin can be conditionally activated, or completely removed, dependent on the presence of doxycycline.

Section 5.2 - Myogenin expression is doxycycline dose-dependent

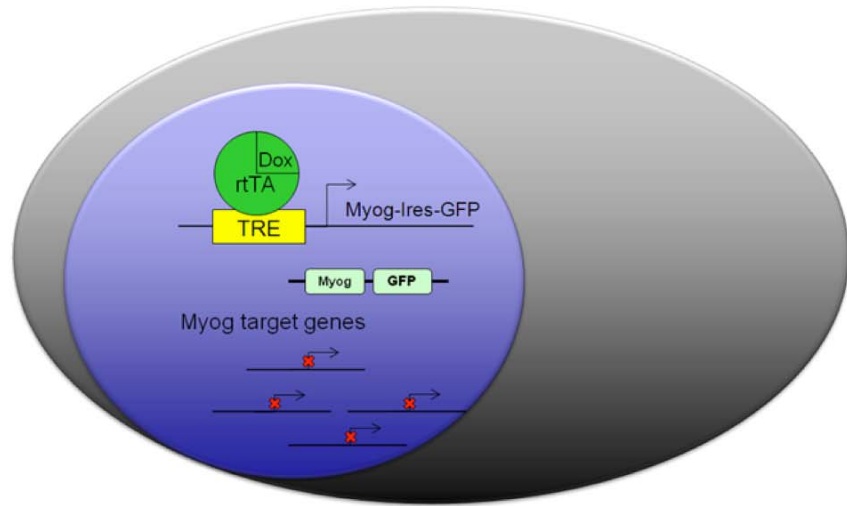
Figure 41 – Tet-On inducible myogenin system

Myog-deleted adult muscle stem cells express both a *Myog*-IRES-GFP driven by a Tetracycline Response Element (TRE) and a reverse Tetracycline-controlled Transactivator (rtTA) protein (A). Upon addition of doxycycline, the doxycycline will dock with the rtTA protein, allowing the rtTA to bind with the TRE and to activate *Myog*-Ires-GFP gene expression (B). The activation of *Myog*-Ires-GFP will lead to a cytoplasmic expression of GFP concomitant with a nuclear expression of myogenin. Myogenin will proceed to activate myogenin-dependent target gene expression.

A.



B.



C.

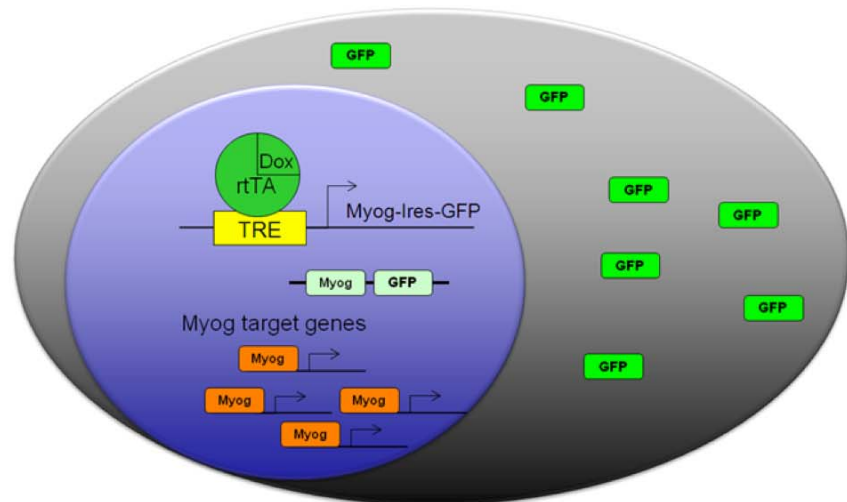


Figure 42 – Clontech’s pRetroX-Advanced System

The pRetroX-Tet-On-Advanced vector is designed to express the reverse Tetracycline-controlled Transactivator protein (rtTA) (A). The pRetroX-Tight-Pur vector is designed to express a gene of interest (i.e. *Myog-Ires-GFP*) (A). The addition of doxycycline to cells stably expressing both of these genes will allow the rtTA protein to bind the Tetracycline Response Element (TRE) and activate gene expression (B). After each of these vectors is transfected into packaging cells, virus may be harvested from the supernatant. Serial infection and selection for Tet-On-Adv and then *Myog-Ires-GFP* results in a double-stable Tet-On Advanced cell line (C). In the absence of doxycycline, the *Myog*-deleted adult muscle stem cells will not express *Myog*, while the presence of doxycycline will conditionally activate *Myog* expression. (www.Clontech.com)

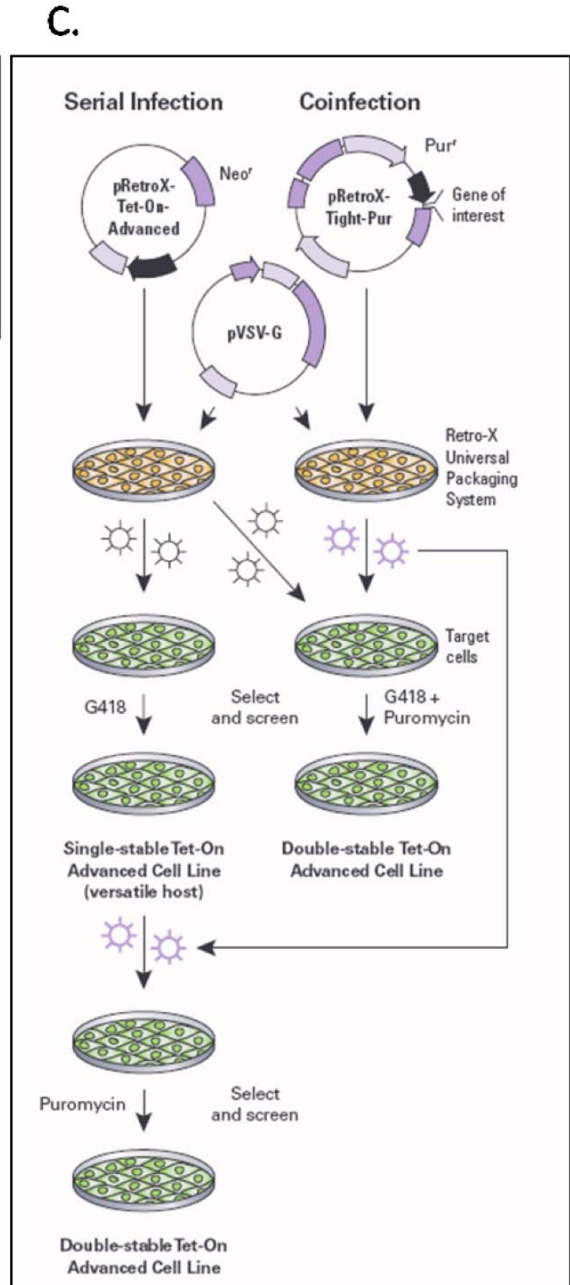
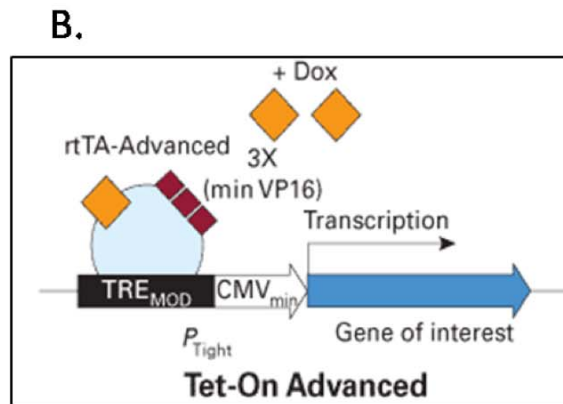
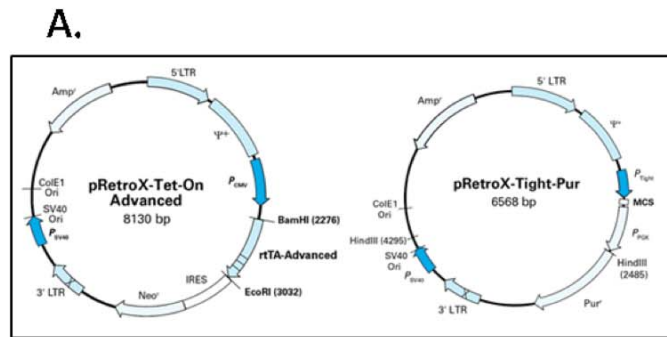
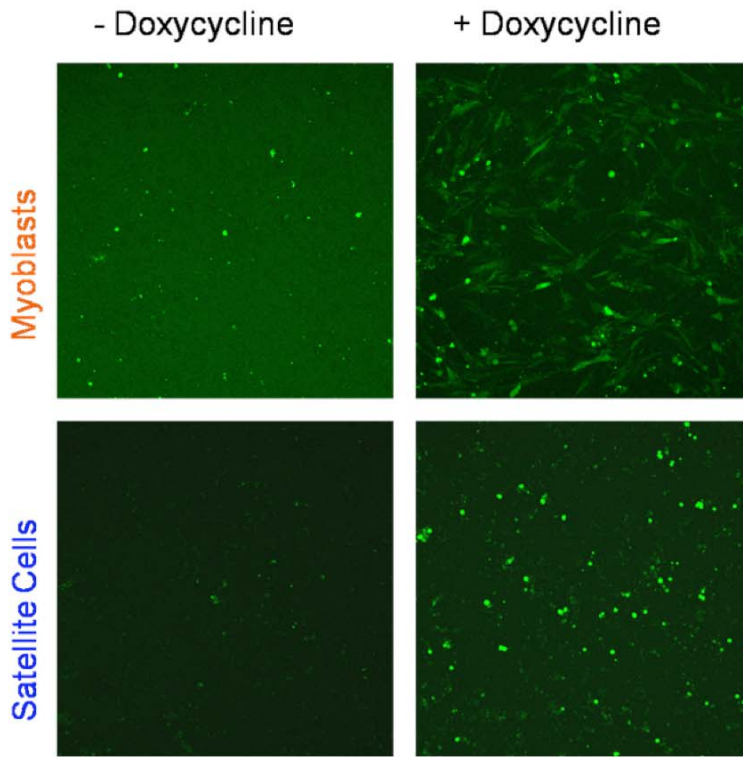


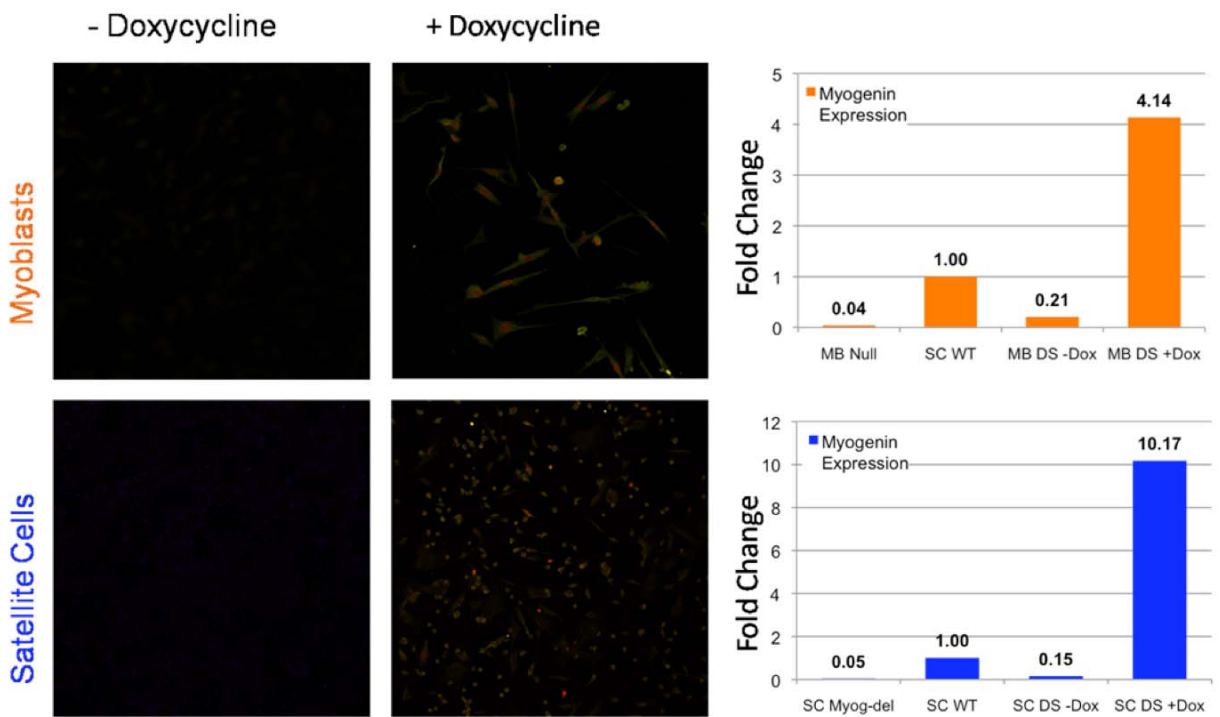
Figure 43 – Inducible myogenin expression in adult muscle stem cells.

Myog-deleted adult muscle stem cells [and *Myog*-null embryonic myoblasts] were stably integrated with the Tet-On *Myog*-Ires-GFP system. Cells exhibited very weak GFP expression in the absence of doxycycline and strong cytoplasmic GFP expression after the addition of 500 ng/mL doxycycline (A). Antibody staining for both myogenin and GFP revealed nuclear localization of myogenin and cytoplasmic localization of GFP after the addition of 500 ng/mL doxycycline (B, pictures). RT-qPCR revealed that double-stable *Myog*-deleted satellite cells, in the absence of doxycycline, express 15% of the *Myog* levels found in wild-type satellite cells. After addition of 500 ng/mL doxycycline, *Myog* expression is upregulated 10-fold. *Myog*-deleted satellite cell controls expressed only 5% of wild-type *Myog* (B, graphs). Blue text and bars represents data from satellite cells, orange text and bars represent data from embryonic myoblasts.

A.



B.



In order to study *Myog*-dependent gene activation, we determined the proper dosage of doxycycline to simulate physiological levels of *Myog* during cell differentiation. Tet-On-*Myog*-deleted cells demonstrated a dose-dependent response to the addition of varying concentrations of doxycycline (Figure 44). After 48-hours of differentiation, -Dox cells showed a 27% expression of *Myog* relative to wild-type control cells. The addition of 50 ng/mL of doxycycline stimulated the expression of *Myog* at levels near 80% of control cells. Notably, for every additional 50 ng/mL added beyond 50 ng/mL, an approximate two-fold increase in *Myog* expression was observed. The addition of 100 ng/mL doxycycline stimulated myogenin to 2.3-fold higher than control cells, 150 ng/mL yielded 4.7-fold *Myog*, 200 ng/mL yielded 9.3-fold *Myog*, and 250 ng/mL yielded 16.6-fold *Myog*. These results demonstrate that Tet-On-*Myog*-GFP cells can be manipulated to express a wide range of *Myog* expression levels in a dose-dependent manner, and that wild-type levels of *Myog* may be obtained by treating the cells with approximately 70 ng/mL doxycycline.

Section 5.3 - Adult myogenin-target gene activation in myogenin-induced adult muscle stem cells

To identify a set of genes that exhibit a dependence on myogenin for expression, previously identified differentially expressed genes in *Myog*-deleted adult muscle stem cells were selected as candidate target genes. We also included previously identified and confirmed embryonic myogenin-dependent target genes. Despite multiple RT-qPCR attempts to determine the dependence of the selected genes on myogenin for normal expression, we were unsuccessful at obtaining unambiguous data (Figures 45, 46). These data indicate that further optimization of the Tet-On-*Myog*-GFP expression system is required in order to take full advantage of its applicability.

Figure 44 – *Myog* Expression is doxycycline dose-dependent

Double-stable *Myog*-deleted adult muscle stem cells were treated with a range of doxycycline concentrations (50 ng/mL, 100 ng/mL, 150 ng/mL, 200 ng/mL, 250 ng/mL) and *Myog* expression measured with RT-qPCR. For every additional 50 ng/mL increase in doxycycline, the associated *Myog* expression increases approximately 2-fold. Approximately 70 ng/mL of doxycycline appears to simulate wild-type expression levels of *Myog*. Error bars represent one standard deviation.

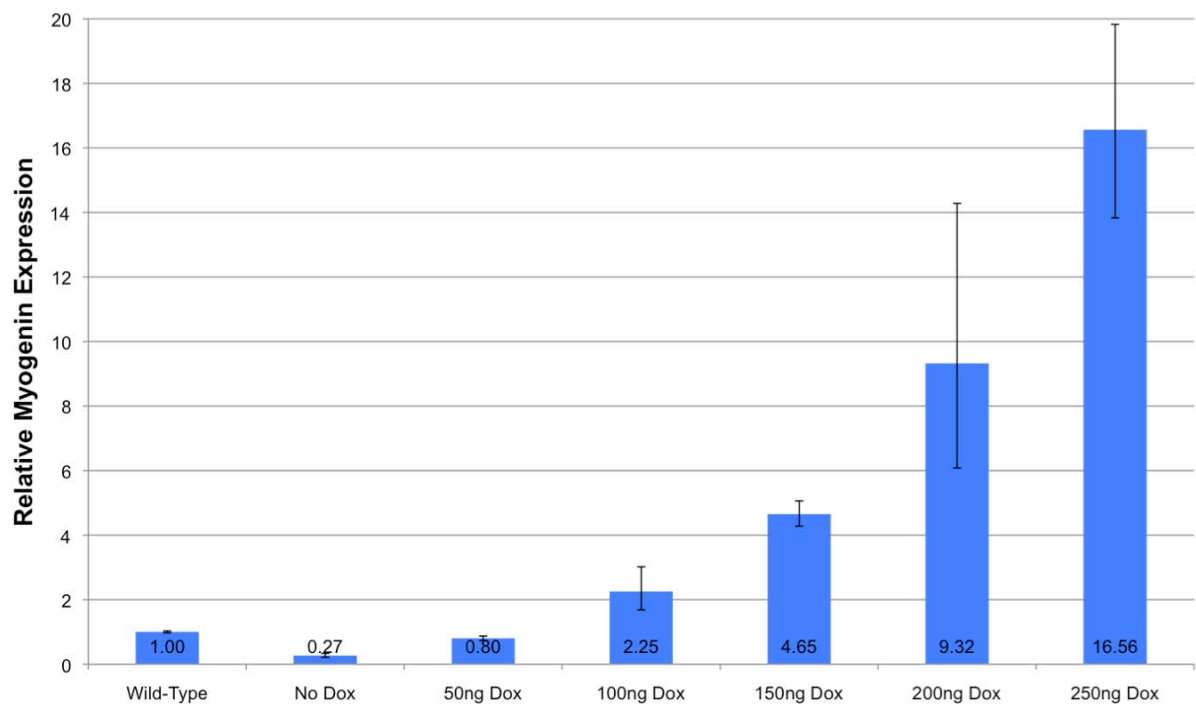


Figure 45 – Example experiment #1

RT-qPCR of selected genes expressed in double-stable *Myog*-deleted muscle stem cells after the addition of 500 ng/mL doxycycline. *Myog* expression is increased 140-fold, while *MyoD*, *Myf5*, and *Mrf4* expression is unchanged. Selected potential adult target genes of myogenin show a 2-fold or greater upregulation while selected and confirmed embryonic target genes of myogenin remain unchanged in double-stable *Myog*-deleted adult muscle stem cells. Blue bars represent baseline gene expression in the absence of doxycycline, green bars represent result gene expression after the addition of doxycycline. Error bars not shown due to irreproducibility.

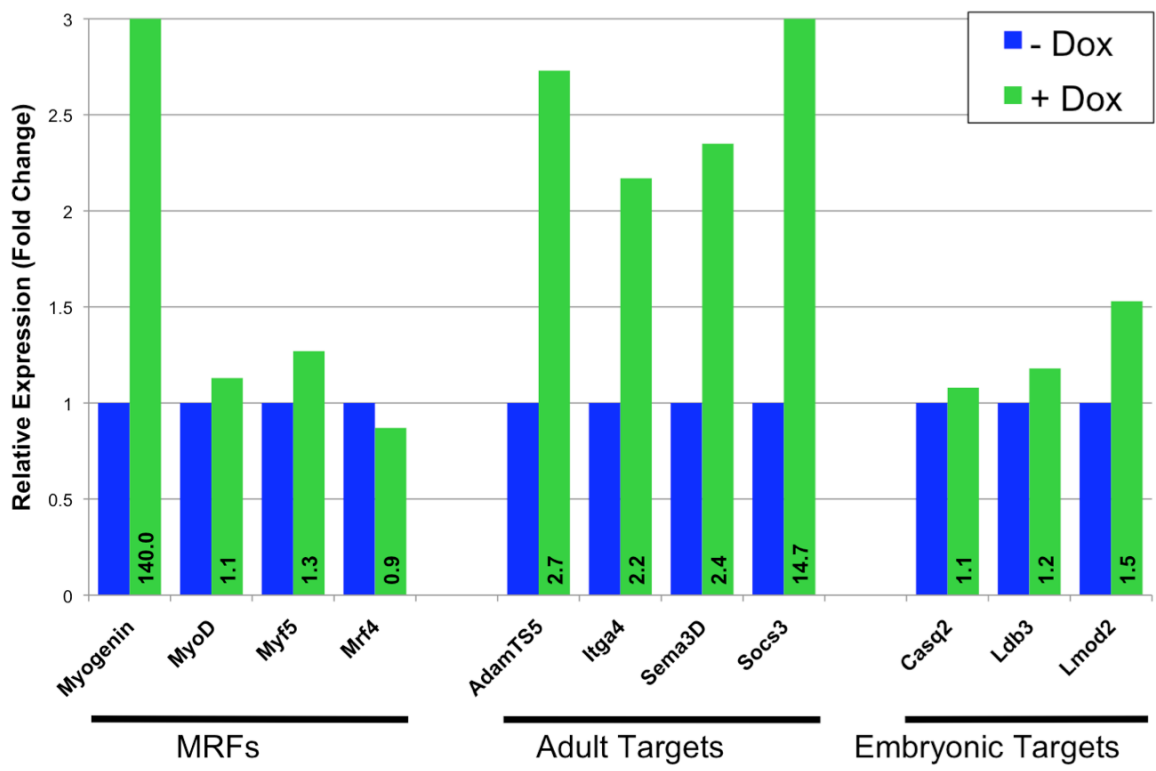
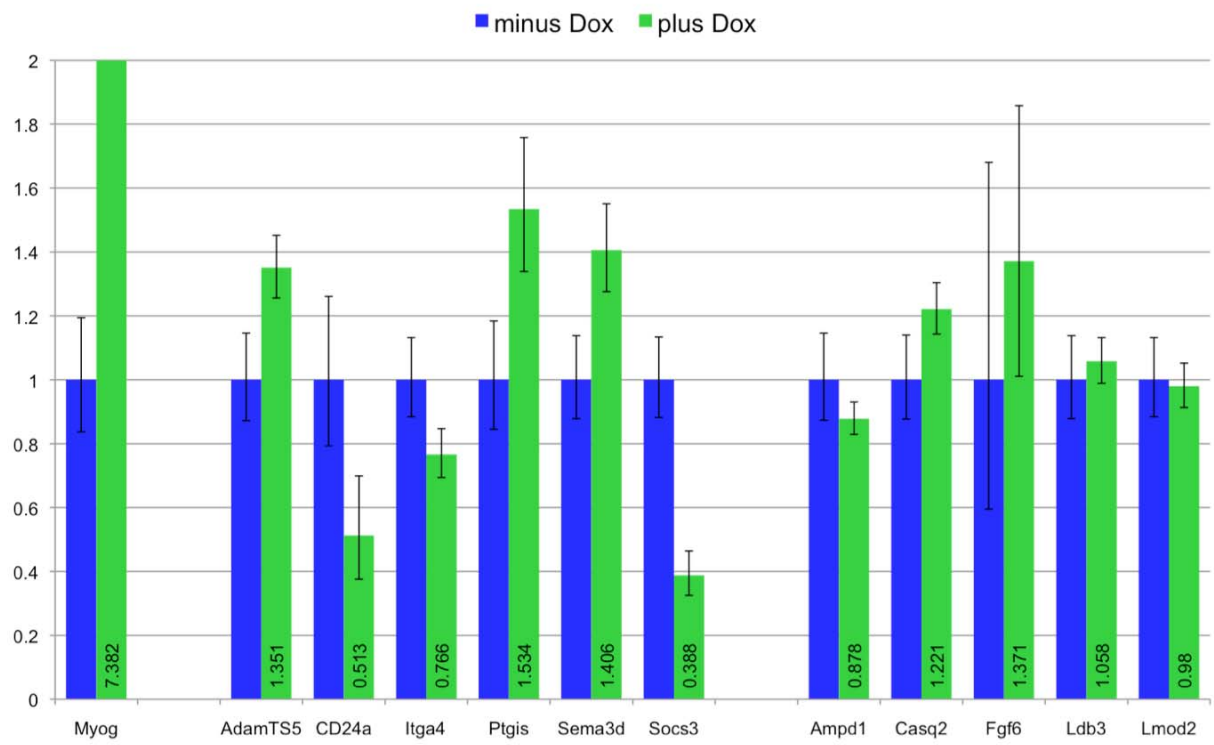


Figure 46 – Example experiment #2

RT-qPCR of selected genes expressed in double-stable *Myog*-deleted muscle stem cells after the addition of 70 ng/mL doxycycline. *Myog* expression is increased 7-fold, while *MyoD*, *Myf5*, and *Mrf4* expression is unchanged. Selected potential adult target genes of myogenin show aberrant gene expression changes while selected and confirmed embryonic target genes of myogenin remain unchanged in double-stable *Myog*-deleted muscle stem cells. Blue bars represent baseline gene expression in the absence of doxycycline, green bars represent result gene expression after the addition of doxycycline. Average of 3 independent experiments. Error bars represent one standard deviation.



Chapter 6 - Discussion

The mechanisms conferring target gene specificity upon individual members of transcription factor families are poorly understood. An excellent example of this specificity is found when comparing gene expression profiles between embryonic and adult muscle lacking myogenin. Myogenin regulates the expression of contractile and structural components of skeletal muscle in embryonic myogenesis, while it regulates a distinctly different set of target genes in adult life. During adult life, myogenin appears to regulate the expression of genes involved in signal transduction and metabolism. Furthermore, microarray analysis of adult muscle stem cells lacking myogenin demonstrates that myogenin regulates genes involved in cell adhesion, cell fusion, and cell signaling. Using a cell culture-based system where myogenin may be conditionally expressed, we can gain insight into how muscle-expressed genes become dependent on myogenin and why these genes lose their dependence on myogenin at different times during life.

High levels of *Myog* expression may prevent or mitigate its selectivity because high levels of myogenin may bind promiscuously to MRF E-box consensus sites. Using previously isolated adult muscle stem cells that have been deleted of *Myog* in cell culture, we developed a system that allowed us to tightly control the expression of myogenin. We successfully obtained multiple cell lines that exhibited very low basal expression of *Myog* transcripts, myogenin protein expression, and GFP reporter gene expression in the absence of doxycycline. Upon addition of doxycycline, the selected cell lines exhibited efficient and robust up-regulation of *Myog* transcripts, myogenin protein expression, and GFP reporter gene expression. Furthermore, myogenin protein expression was successfully detected in the nucleus while GFP expression was detected in the cytoplasm. *Myog* transcript expression was also dose-dependent on doxycycline.

After 48-hours of serum withdrawal, Tet-On-*Myog*-GFP cells efficiently expressed wild-type levels of *Myog* transcripts at low doses of doxycycline, demonstrating the ability to obtain physiologically relevant levels of myogenin expression. Cells without doxycycline treatment maintained less than heterozygous expression levels of *Myog* to maintain gene expression patterns associated with myogenin's absence. Certainly, Tet-On-*Myog*-GFP cells serve as an excellent system to identify *Myog*-dependent genes.

Given that *Myog*-dependent target gene expression should be strictly dependent on the presence of myogenin, RT-qPCR assays were used to determine whether genes were dependent on myogenin. Despite the successful development of this cell line, technical problems impeded progress on this project. After optimizing a number of issues, including FBS tetracycline-analogs contaminating cell culture media, RT-qPCR conditions, and primer design, we were still unsuccessful at detecting *Myog*-dependent target genes. Regardless of whether doxycycline was added to the cells, gene expression was not consistently dependent on myogenin. Potential reasons and solutions to this problem include:

- 1.) The clones expressing Tet-On-*Myog*-GFP were selected using excessive amounts of doxycycline. As excessive amounts of doxycycline induce excessive *Myog* expression, clones may not have been selected under ideal conditions. It is possible that clonal selection using physiologically relevant levels of *Myog* may allow for the selection of cells that efficiently express myogenin-dependent genes.
- 2.) The *Myog*-deleted muscle stem cells have started to senesce. The cells may be particularly prone to high passage number, which could negatively influence myogenin-dependent target gene expression. This problem will be particularly difficult to overcome and may require a complete reengineering of the cell line.

3.) The dependence of predicted myogenin-dependent target genes is negatively influenced by the vast number of manipulations performed during the creation of the cell line. The stable integration of two viral vectors and overall passage number of the cells may confer a completely different set of *Myog*-dependent genes in the Tet-On-*Myog*-GFP cells. Myogenin could regulate a somewhat different set of target genes in the context of this manipulated primary cell line. Genome-wide expression profiling would be necessary to reveal genes that are newly dependent on myogenin.

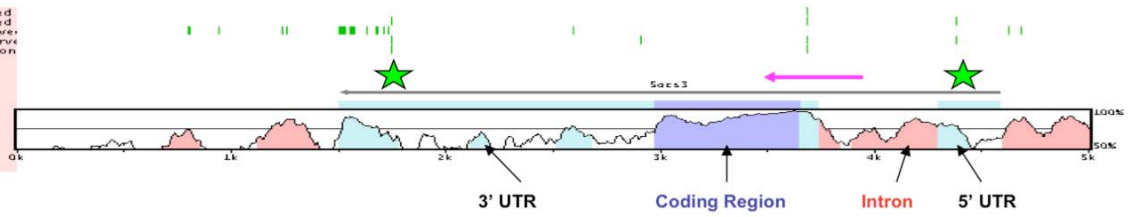
Nevertheless, once *Myog*-dependent genes are identified in the context of inducible *Myog* cells, a variety of critical issues can be addressed. The ability to coordinate the activation of myogenin expression in millions of cells in concert provides an invaluable system for studying *Myog*-dependent gene activation. TCRs responsible for conferring myogenin dependence can be identified using rVista analysis (Figure 47) and then used for ChIP assays. Myogenin-bound promoter elements can then be identified, and the expression of the associated genes at specific time-points during myoblast differentiation can be determined. The overall responsiveness of myogenin-dependent target genes towards myogenin can also be determined using RT-qPCR.

In summary, Tet-On-*Myog*-GFP adult muscle stem cells provide a valuable resource for monitoring and understanding the process of myogenin-dependent gene activation. The study of these cells will broadly impact other studies where the aim is to distinguish the function of an individual transcription factor from other members of its family.

Figure 47 – Conserved E-box motifs are present within the TCRs of adult myogenin target genes. Selected potential adult target genes of myogenin contain clusters of E-box and Mef2 binding motifs (indicated by green stars), as identified with rVista analysis.

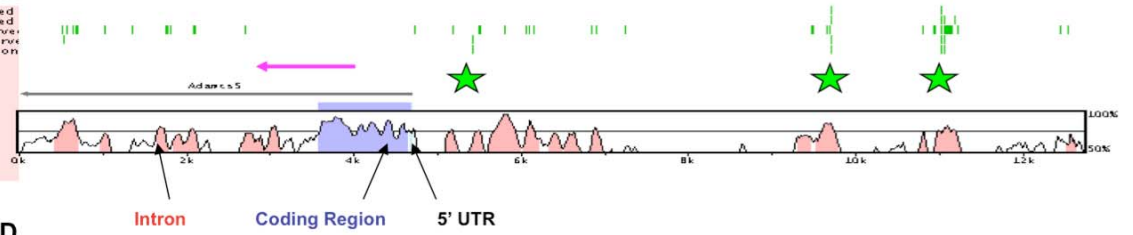
Socs3

E12_conserved
E47_conserved
MEF2_conserved
MYOD_conserved
MYOGENIN_con



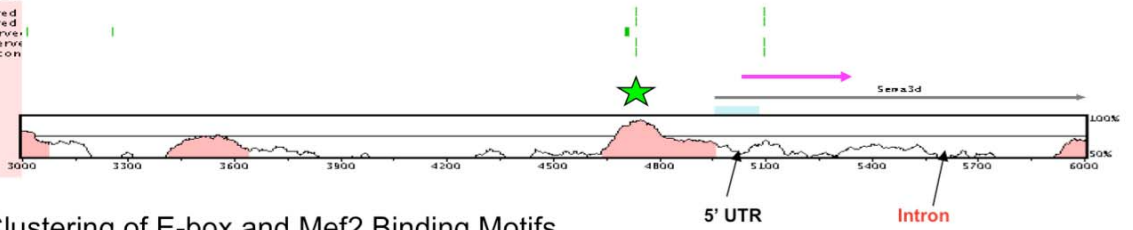
Adamts5

E12_conserved
E47_conserved
MEF2_conserved
MYOD_conserved
MYOGENIN_con



Sema3D

E12_conserved
E47_conserved
MEF2_conserved
MYOD_conserved
MYOGENIN_con



★ Clustering of E-box and Mef2 Binding Motifs

Materials and Methods

Section 7.1 – DNA isolation and genotyping

The mouse line used for the project was homozygous for the *Myog^{fllox}* allele and hemizygous for the CAGGCre-ER transgene (Hayashi and McMahon, 2002; Knapp et al., 2006). These mice were of mixed background, containing both 129 & C57BL/6 strains. Mouse-tail clippings were digested overnight at 65°C in tail lysis Buffer (10 mM Tris pH 8.0, 25 mM EDTA pH 8.0, 100 mM NaCl, 1% SDS) with 0.4µg/µl (final concentration) of proteinase K. The DNA was phenol-chloroform extracted and diluted in ddH₂O. PCR was performed using the Qiagen Hotstart kit. PCR genotyping was performed on a ABI Gene AMP PCR system model 9700 machine using the following conditions: denaturation 95°C 15 minutes, 35 cycles [denaturation 95°C for 15 seconds, annealing 58°C 30 seconds, extension 72°C 30 seconds], 5 minutes final extension. qPCR was performed using ABI SYBR mix on a ABI 7500 Fast Real Time PCR system using the following conditions: denaturation 95°C 10 minutes, 40 cycles [denaturation 95°C for 15 seconds, annealing/extension 58°C 30 seconds], 5 minutes final extension. Mdx genotyping consisted of PCR-amplifying the Mdx Exon 23 locus, gel-purifying the PCR fragment, and sequencing the fragment using the Mdx Rev primer.

DNA Primers used for Genotyping and cloning:

CAGGCre-ER Fwd	5'-TCCAATTTACTGACCGTACACCAA-3'
CAGGCre-ER Rev	5'-CCTGATCCTGGCAATTCGGCTA-3'
<i>Myog</i> Fwd	5'-GAGACATCCCCCTATTTCTACCA-3'
<i>Myog</i> Rev	5'-GCTCAGTCCGCTCATAGCC-3'
<i>Myog</i> -LoxP1 Fwd	5'-CCGGGTAGGAGTAATTGAAAGGA-3'

<i>Myog</i> -LoxP1 Rev	5'-GCCGTCGGCTGTAATTTGAT-3'
<i>MdxEx23</i> Fwd	5'-TGAAACTCATCAAATATGCGTGTTAG-3'
<i>MdxEx23</i> Rev	5'-TGTTTCCCATCACATTTTCCAA-3'
<i>Myog</i> cDNA Fwd	5'-TTCCGACCTGATGGAGCTGTAT-3'
<i>Myog</i> cDNA Rev	5'-GGTAACCTCAGTTGGGCATGGTTTCGT-3'

Section 7.2 – Deleting Myog during adult life

After approximately 12 weeks of age, adult mice were given a single intraperitoneal injection of tamoxifen (20 mg/ml in corn oil) at a dose of 0.25 mg/g body weight. Control mice that did not express Cre were also treated with tamoxifen. Tamoxifen treatment efficiently deleted *Myog* in skeletal muscle and allowed us to study the function of *Myog* during adult life. In order to obtain efficient deletion of *Myog*, high doses of tamoxifen were critical. In the process of treating the mice with tamoxifen and deleting their *Myog* locus, we observed a 15% mortality rate. Our experiments have shown that lower doses and fewer treatments of tamoxifen, which yield a lower mortality rate, do not efficiently delete *Myog* during adult life.

Section 7.3 – Voluntary cage wheel exercise

Plastic cage wheels were fitted with digital magnetic counters (Schwinn Bicycles) activated by wheel rotation and anchored into cages (Coast Cages model no. 36412, PetSmart) (Figure 26). The digital counters measure average running speed, maximum running speed, total distance, and trip distance. Mice were subjected to voluntary exercise for a maximum of six months. An arbitrary load of 1 kg was added to a wire that increased the rotational resistance of the wheel axis. The load was measured using a common fish weight scale.

Section 7.4 – Involuntary treadmill exercise

A six-lane Exer 3/6 Rodent Treadmill (Columbus Instruments) was used for involuntary exercise experiments. Up to six mice were tested simultaneously. Acclimatization was performed for three days prior to the experiment. Low-intensity acclimatization: zero degree incline, 30 min @ 10 m/min. Low-intensity exercise: zero degree incline, 30 min @ 10 m/min, 20 m/min until exhaustion. High-intensity acclimatization: 10 degree incline, 10 min @ 10 m/min, additional 2 m/min every 2 min until 20 min total exercise time is reached. High-intensity exercise: 10 degree incline, 10 min @ 10 m/min, additional 2 m/min every 2 min until exhaustion. Modified high-intensity acclimatization: none. Modified high-intensity exercise: 0 degree incline, 5 min @ 6 m/min, additional 1 m/min every 2 min until 10 m/min is reached, additional 2 m/min every 2 min until exhaustion. Mice were run until exhaustion in each experiment. Fatigue was operationally defined as the time at which the mouse is unable or refusing to maintain its running speed for 10 seconds despite encouragement by mild electrical stimulation. A stimulus grid located at the rear of the treadmill provided a physically harmless 0.2 mA stimulus. Electrical stimulation was discontinued when the mice reached fatigue. Under high-intensity exercise conditions, mice were subjected to this treatment 5-7 times per week for 1-2 months. Under low- and modified high-intensity exercise conditions, mice were subjected to this treatment only once.

Section 7.5 – Blood metabolite assays

Blood metabolites were measured immediately before and after exercise. Blood glucose and ketones were measured using a Precision Xtra Advanced Diabetes Management System

(Abbott Diabetes Care Inc.). Blood lactate was measured with a Lactate Pro blood lactate test meter (Arkray Inc.). Approximately 2 uL of blood was deposited onto the blood glucose, blood ketone, and blood lactate test strips, and the test strips were then inserted into their respective monitor for analysis.

Section 7.6 – Tissue harvest & histology

After mice were sacrificed, various muscle groups were harvested for RNA isolation and histology. Muscles for RNA isolation were placed into an appropriate volume RNAlater (Ambion) and stored at -80 C. Muscles for histology were snap frozen in LN2-cooled isopentane and stored at -80 C. Ten-micrometer fresh-frozen sections were made using a Leica Cryostat. Slides containing fresh-frozen sections were stored at -80 C.

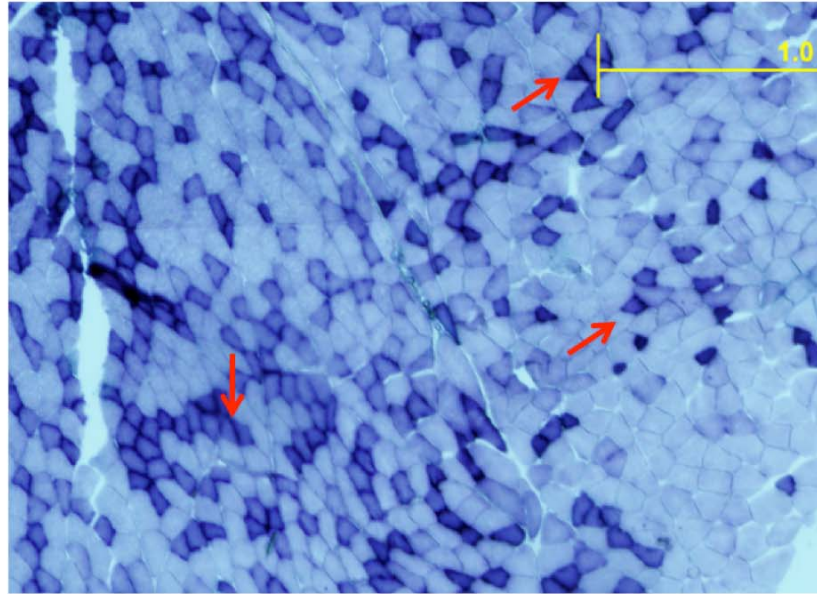
Section 7.7 – Succinate dehydrogenase assay

Fresh frozen muscle sections were treated as follows: Nitroblue tetrazolium (NBT) stock was prepared with 100mL 100mM phosphate buffer pH 7.6, 6.5 mg KCN, 185 mg EDTA, 100 mg NBT. Succinate stock was prepared as 500 mM sodium succinate. Incubation medium consisted of 10% succinate stock in NBT stock with 0.7 mg phenazine methosulphate. The incubation medium was prepared immediately prior to use and kept out of strong light. The reaction was completed within 5 minutes. The sections were then rinsed in distilled water, fixed in 4% PFA, dehydrated, cleared, and mounted. Modified from (Pette and Tyler, 1983). SDH activity was found to colocalize with myoglobin expression (Abcam ab77232) (Supplemental Figure 48).

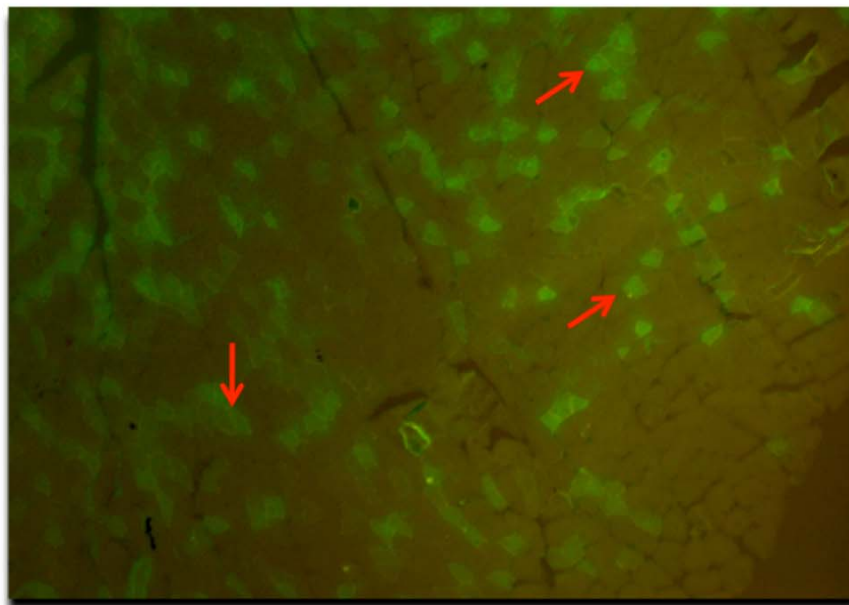
Figure 48 – Co-localized expression of myoglobin and succinate dehydrogenase activity.

Myoglobin protein, as shown by immunohistochemistry, is expressed in highly oxidative SDH-positive myofibers of the gastrocnemius. Serial sections are shown.

SDH Activity



Myoglobin IHC



Section 7.8 – Adenosine Triphosphate (ATP) staining protocol

The pH 4.3 ATP protocol was the most preferred and reliable method for distinguishing Type-I and Type-II fibers. Type-I fibers are visibly dark while Type II fibers are visibly light following this procedure. The following solutions are prepared prior to the staining procedure: 0.1 M sodium barbital, 0.18 M calcium chloride, 1% calcium chloride, barbital acetate solution (1.47 g sodium barbital and 0.97 g sodium acetate into 50 mL ddH₂O), 1 N NaOH, 0.1 N NaOH, 1 N HCl, 0.1 N HCl, “4.3 ATP” pre-incubation solution (5.0 mL barbital acetate solution, 10 mL 0.1 N HCl, 4.0 mL ddH₂O, adjust pH with 1 N HCl), ATP incubating solution (60 mg ATP powder, 6.0 mL 0.1 M sodium barbital, 21.0 mL ddH₂O, 3.0 mL 0.18 M calcium chloride, adjust pH with 1N NaOH), 50% ethanol, 70% ethanol, 80% ethanol, 95% ethanol, 2% ammonium sulfide (prepare immediately prior to use).

Staining procedure: Incubate fresh frozen sections in 4.3 solution for exactly 5 minutes at room temperature. Rinse with ddH₂O. Incubate with ATP solution for 25 minutes. Wash sections with 3 changes of 1% calcium chloride for a total of 10 minutes. Wash sections with 2% cobalt chloride for 10 minutes. Wash with 3-5 changes of a 1:20 solution of 0.1 M sodium barbital (in ddH₂O); wash should turn a faint blue color. Wash with 5 exchanges of ddH₂O. Wash with 2% ammonium sulfide for 20-30 seconds. Rinse with 5 changes of tap water. Dehydrate in ascending alcohols, clear in xylene, and mount only with Canada balsam. (Brooke and Kaiser, 1970a; Brooke and Kaiser, 1970b) Borrowed from <http://neuromuscular.wustl.edu/pathol/histol/atp.htm>

Section 7.9 – RNA isolation & RT-qPCR

RNA was isolated from semi-confluent satellite cell lines and hind limb muscle homogenates with the Invitrogen Trizol protocol. Tissue homogenization was performed with a Wheaton 1mL Dounce tissue grinder. Muscle samples were homogenized in Trizol directly from fresh or fresh-frozen muscle tissue. RNA was then used with the ABI RNA to cDNA kit for reverse transcription. SYBR RT-qPCR was performed with ABI Power-SYBR master mix and on the ABI 7500 Fast Real Time PCR system with version 2.0.1 software, and using the following default conditions: denaturation 95°C 10 minutes, 40 cycles [denaturation 95°C 15 seconds, annealing/extension 60°C 30 seconds], 5 minutes final extension. Taqman RT-qPCR assays were performed with ABI Taqman Master mix (FAM/ROX) and using default parameters. Proper dynamic range was determined for *Gapdh* and *Myog* Taqman primer/probes. All reactions were normalized to GAPDH expression. Unpaired 2-class t-tests were performed using Microsoft Excel 2007. Samples were analyzed, at minimum, in biological triplicate.

cDNA primer pairs used were:

<i>Gapdh</i> Fwd	5'-CCACCAACTGCTTAGCACC-3'
<i>Gapdh</i> Rev	5'-GCCAAATTCGTTGTCACACC-3'
<i>Myog</i> Fwd	5'-GAGACATCCCCCTATTTCTACCA-3'
<i>Myog</i> Rev	5'-GCTCAGTCCGCTCATAGCC-3'

ABI Taqman Primer/Probe Sets:

GAPDH Endogenous Control (FAM/MGB Probe)

Myog LoxP Custom Fwd: GGCCCGGGTAGGAGTAATTG

Myog LoxP Custom Rev: CCGTCGGCTGTAATTTGATTAGT

Myog LoxP Custom Probe: AAGGAGCAGATGAGACGG

Myogenin, Assay ID Mm00446194_m1
Myosin, heavy polypeptide 7, Assay ID Mm00600555_m1
Myosin, heavy polypeptide 4, Assay ID Mm01332541_m1
Myosin, 2A, Assay ID Mm00454982_m1
UCP2, Assay ID Mm00627599_m1
UCP3, Assay ID Mm00494077_m1
Cox8b, Assay ID Mm00432648_m1
Glut4, Assay ID Mm00436615_m1
CD36, Assay ID Mm01135198_m1
Acc2, Assay ID Mm01204691_m1
ppar-a, Assay ID Mm00627559_m1
ppar-g, Assay ID Mm00440945_m1
Cpt1, Assay ID Mm00550438_m1
Rfx7, Assay ID Mm01146805_m1
Nfatc2, Assay ID Mm00477776_m1
RhoBTB1, Assay ID Mm01143659_m1
Rhpn2, Assay ID Mm00518451_m1
Htra1, Assay ID Mm00479887_m1
Gpx3, Assay ID Mm00492427_m1
Zscan21, Assay ID Mm00442147_m1
Pcx, Assay ID Mm00500992_m1
Bmp5, Assay ID Mm00432091_m1
Pfkfb3, Assay ID Mm00504650_m1
Mpa2l, Assay ID Mm00843395_m1
Dpyd, Assay ID Mm00468111_m1

Bdh1, Assay ID Mm00558330_m1
AdamTS5, Assay ID Mm01344182_m1
CD24a, Assay ID Mm00782538_sH
Itga4, Assay ID Mm00439770_m1
Ptgis, Assay ID Mm00447271_m1
Sema3d, Assay ID Mm00712652_m1
Socs3, Assay ID Mm01249143_g1
Ampd1, Assay ID Mm01308676_m1
Casq2, Assay ID Mm00486742_m1
Fgf6, Assay ID Mm01183111_m1
Ldb3, Assay ID Mm00522021_m1
Lmod2, Assay ID Mm01165337_m1
Myf5, Assay ID Mm00435125_m1
Mrf4, Assay ID Mm00435126_m1
Myod1, Assay ID Mm0040387_m1

Section 7.10 – RNA quality control and gene chip hybridization

Using RNA isolated from the *Myog* wild-type control and *Myog*-deleted adult gastrocnemius muscle, quality control was first carried out by the microarray core.

Approximately 1 µg of each sample was submitted to insure the 28s and 18s ribosomal RNA bands were of sufficient relative intensity and that the RNA concentration and amount was sufficient. Once this was approved, each sample was submitted for hybridization. The Affymetrix 430 2.0 microarray platform was used for this analysis as it covers approximately 40,000 transcripts within the mouse genome.

Section 7.11 – Microarray data analysis

Genespring GX10 was used to analyze the raw microarray data. The 6 raw data sets were loaded into the program and each data set was labeled as being either control or experimental. Normalization was performed using the RMA algorithm. Unpaired two-class t-tests were performed without error stabilization or p-value correction and p-value cutoffs were set at $p < 0.05$. Genespring GX10 and Microsoft Excel 2007 were used for statistical analysis. From the filtered data set, all genes changing ≥ 1.4 fold were kept for further analysis.

Section 7.12 – Cell culture

Previously characterized adult muscle stem cells (Meadows et al., 2008) were maintained in Gibco F-10 Media supplemented with Clontech Tet-free FBS and Invitrogen Antibiotic-Antimycotic (ABAM). The cells were differentiated with DMEM supplemented with 2% Horse Serum and ABAM. Cells were stored in LN2 prior to use.

Section 7.13 – Cloning and retroviral integration of Myog-Ires-GFP into adult muscle stem cells

The RetroX Tet-On Advanced Inducible Expression System (Clontech) was used to create doxycycline-inducible-myogenin adult muscle stem cells. *Myog* cDNA was PCR-amplified with *Myog* cDNA primers (Section 7.1) from *Myog* full length cDNA (Open Biosystems Acc:BC068019), gel-purified, and cloned into pCR 2.1 Topo (Invitrogen). A IRES-GFP sequence was cut from a pIRES-hrGFP vector (Stratagene) with BstEII/XhoI and ligated

into Topo-*Myog*, yielding Topo-*Myog*-GFP. *Myog*-GFP was then cut out (BamHI/XbaI) and ligated into the MCS of pRetroX-Tight-Pur (dam- competent cells), yielding pRetroX-*Myog*-GFP. As the *Myog*^{flox/flox} adult muscle stem cells contain a neomycin cassette, originally used for selection during gene targeting, the neomycin cassette contained in pRetroX-Tet-On-Advanced was cut out (BstXI/RsrII) and replaced with a Blasticidin selection cassette. The Blasticidin selection cassette came from (pBlast49-hIGF1a). The resulting vector was named pRetroX-Advanced-Blast.

Packaging cells (EcoPack 2-293, Clontech) were next transfected with pRetroX-*Myog*-GFP, pRetroX-Tight-Luc (control), and pRetroX-Advanced-Blast. Viral supernatants were collected 48 hours after transfection. Muscle stem cells were infected with pRetroX-Adv-Blast in the presence of Blasticidin and approximately 30 stably infected colonies were selected. These colonies were next infected with pRetroX-Tight-Luc, and luciferase assays were performed in the presence and absence of doxycycline (500 ng/mL; 3 days) to determine which colonies exhibited the strongest luciferase induction. pRetroX-Adv-Blast satellite cells #5 exhibited strong luciferase induction, approximately 25-fold. The selected single stable muscle stem cells were next infected with pRetroX-*Myog*-GFP in the presence of puromycin. Based upon previous experiments with pRetroX-*Myog*-GFP to determine titer and colony forming unit (CFU) characteristics, 100 uL of a 1000-fold dilution of virus was added to 3 mL of media to keep copy numbers per cell to a minimum while yielding high infection efficiency. Approximately 30 double stable infected colonies were selected for further analysis. Using confocal microscopy to assay the induction of GFP expression in the presence and absence of doxycycline (500 ng/mL; 3 days), colonies numbered 1, 6, 8, 12, 21, 23, and 25 exhibited the least amount of background GFP expression and the strongest induction. RNA from these seven colonies (induced and non-induced) was harvested for RT-qPCR for *Myog* expression, which revealed colony #12 as showing the best induction of *Myog* and #23,25 the next best. 38 vials

of colony 12, 10 vials (each) of colonies 23 & 25, and 1 vial each of the remaining colonies were frozen in LN2. All infections were performed in the presence of 4 ug/mL of polybrene.

Section 7.14 – Doxycycline concentration curve

Double stable adult muscle stem cells (colony #12) were treated with 0, 50, 100, 150, 200, and 250 ng/mL of doxycycline under proliferative conditions. After 24 hours of doxycycline treatment, the cells were differentiated for 48 hours and treated with doxycycline for an additional 48 hours (72 hours total). Wild-type adult muscle stem cells were used as controls. RNA was then harvested using the Trizol method and RT-qPCR performed to determine the fold-induction of *Myog* associated with doxycycline concentration.

Section 7.15 – Immunofluorescence

Immunofluorescence was performed on adult muscle stem cells and embryonic myoblast cell lines plated on 2 or 4 well chamber slides, antibody probed, and imaged by an Olympus IX70 confocal microscope. Cells were first plated on 2 or 4 well chamber slides with a total cell count of either 10×10^4 or 5×10^4 cells per well, respectively. No-primary antibody controls were used for each cell line probed. The cells were given at least 24 hours to adhere to the slide (and differentiate if necessary) before beginning. The media was first aspirated and the chambers removed from each slide. The slides were rinsed in PBS and the cells were fixed with 4% paraformaldehyde (in PBS) for 30 minutes. The cells were then washed with PBS for 5 minutes 3-times and then permeabilized with PBST (0.5% Triton X-100 in PBS) for 10 minutes. Another 5 minutes 3-times PBS wash followed and the cells were then blocked in 2% BSA (in PBST) at room temperature for 1 hour. The primary antibody was then added at a dilution of 1:200 in

PBS (.5% BSA) for 1 hour. Primary antibodies used were against myogenin (sc-576) and GFP (Vitality hrGFP monoclonal antibody 240241, Stratagene). The cells were again washed with PBS for 5 minutes 3-times and the secondary antibody was then added at 1:400 (up to 1:200) dilution in PBS for 1 hour. Secondary antibodies used were Cy3 anti-mouse (Jackson Immuno), Cy5 anti-rabbit (Jackson Immuno), and Alexa488 anti-goat (Molecular Probes). After the secondary antibody incubation, the cells were washed with PBS for 10 minutes 3-times and kept out of direct light. Excess PBS was then dripped from the slides and 2 to 3 drops of Aqua-Mount added before the glass coverslip was carefully placed over the cells. The slides were stored in the dark at 4°C and imaged using a confocal microscope. Background intensity was first checked using the no-antibody control samples before analyzing the antibody-stained cells for signal.

Section 7.16 – Statistical analysis

All t-tests in this dissertation were two-tailed and unpaired, performed in Microsoft Excel 2007 or 2008. The superior adaptation to exercise training was performed using a box plot (BLiP) by Lei Feng (MD Anderson Biostatistics).

References

- Abdelmalki, A., Fimbel, S., Mayet-Sornay, M. H., Sempore, B., Favier, R., 1996. Aerobic capacity and skeletal muscle properties of normoxic and hypoxic rats in response to training. *Pflugers Arch.* 431, 671-9.
- Allen, D., Westerblad, H., 2004. Physiology. Lactic acid--the latest performance-enhancing drug. *Science.* 305, 1112-3.
- Allen, D. G., Lamb, G. D., Westerblad, H., 2008. Skeletal muscle fatigue: cellular mechanisms. *Physiol Rev.* 88, 287-332.
- Allen, D. L., Harrison, B. C., Maass, A., Bell, M. L., Byrnes, W. C., Leinwand, L. A., 2001. Cardiac and skeletal muscle adaptations to voluntary wheel running in the mouse. *J Appl Physiol.* 90, 1900-8.
- Asmussen, E., 1956. Observations on experimental muscular soreness. *Acta Rheumatol Scand.* 2, 109-16.
- Baldwin, K. M., Cooke, D. A., Cheadle, W. G., 1977. Time course adaptations in cardiac and skeletal muscle to different running programs. *J Appl Physiol.* 42, 267-72.
- Baldwin, K. M., Klinkerfuss, G. H., Terjung, R. L., Mole, P. A., Holloszy, J. O., 1972. Respiratory capacity of white, red, and intermediate muscle: adaptative response to exercise. *Am J Physiol.* 222, 373-8.
- Bender DA, M. P., Harper's Illustrated Biochemistry. In: B. D. Murray RK, Botham KM, Kennelly PJ, Rodwell VW, Weil PA, (Ed.), *Gluconeogenesis & the Control of Blood Glucose.* McGraw Hill, 2009.

- Berkes, C. A., Bergstrom, D. A., Penn, B. H., Seaver, K. J., Knoepfler, P. S., Tapscott, S. J., 2004. Pbx marks genes for activation by MyoD indicating a role for a homeodomain protein in establishing myogenic potential. *Mol Cell*. 14, 465-77.
- Berkes, C. A., Tapscott, S. J., 2005. MyoD and the transcriptional control of myogenesis. *Semin Cell Dev Biol*. 16, 585-95.
- Black, B. L., Olson, E. N., 1998. Transcriptional control of muscle development by myocyte enhancer factor-2 (MEF2) proteins. *Annu Rev Cell Dev Biol*. 14, 167-96.
- Blais, A., Tsikitis, M., Acosta-Alvear, D., Sharan, R., Kluger, Y., Dynlacht, B. D., 2005. An initial blueprint for myogenic differentiation. *Genes Dev*. 19, 553-69.
- Blake, D. J., Weir, A., Newey, S. E., Davies, K. E., 2002. Function and genetics of dystrophin and dystrophin-related proteins in muscle. *Physiol Rev*. 82, 291-329.
- Booth, F. W., Thomason, D. B., 1991. Molecular and cellular adaptation of muscle in response to exercise: perspectives of various models. *Physiol Rev*. 71, 541-85.
- Brooke, M. H., Kaiser, K. K., 1970a. Muscle fiber types: how many and what kind? *Arch Neurol*. 23, 369-79.
- Brooke, M. H., Kaiser, K. K., 1970b. Three "myosin adenosine triphosphatase" systems: the nature of their pH lability and sulfhydryl dependence. *J Histochem Cytochem*. 18, 670-2.
- Cao, Y., Kumar, R. M., Penn, B. H., Berkes, C. A., Kooperberg, C., Boyer, L. A., Young, R. A., Tapscott, S. J., 2006. Global and gene-specific analyses show distinct roles for Myod and Myog at a common set of promoters. *Embo J*. 25, 502-11.
- Carter, G. T., Abresch, R. T., Fowler, W. M., Jr., 2002. Adaptations to exercise training and contraction-induced muscle injury in animal models of muscular dystrophy. *Am J Phys Med Rehabil*. 81, S151-61.

- Chamberlain, J. S., Metzger, J., Reyes, M., Townsend, D., Faulkner, J. A., 2007. Dystrophin-deficient mdx mice display a reduced life span and are susceptible to spontaneous rhabdomyosarcoma. *Faseb J.* 21, 2195-204.
- Charge, S. B., Rudnicki, M. A., 2004. Cellular and molecular regulation of muscle regeneration. *Physiol Rev.* 84, 209-38.
- Chi, M. M., Hintz, C. S., McKee, D., Felder, S., Grant, N., Kaiser, K. K., Lowry, O. H., 1987. Effect of Duchenne muscular dystrophy on enzymes of energy metabolism in individual muscle fibers. *Metabolism.* 36, 761-7.
- Cole, R. P., 1982. Myoglobin function in exercising skeletal muscle. *Science.* 216, 523-5.
- Cossu, G., Molinaro, M., 1987. Cell heterogeneity in the myogenic lineage. *Curr Top Dev Biol.* 23, 185-208.
- Coyle, E. F., 2007. Physiological regulation of marathon performance. *Sports Med.* 37, 306-11.
- Davie, J. K., Cho, J. H., Meadows, E., Flynn, J. M., Knapp, J. R., Klein, W. H., 2007. Target gene selectivity of the myogenic basic helix-loop-helix transcription factor myogenin in embryonic muscle. *Dev Biol.* 311, 650-664.
- Dudley, G. A., Abraham, W. M., Terjung, R. L., 1982. Influence of exercise intensity and duration on biochemical adaptations in skeletal muscle. *J Appl Physiol.* 53, 844-50.
- Fischer, K. F., Lees, J. A., Newman, J. H., 1986. Hypoglycemia in hospitalized patients. Causes and outcomes. *N Engl J Med.* 315, 1245-50.
- Fitts, R. H., 1994. Cellular mechanisms of muscle fatigue. *Physiol Rev.* 74, 49-94.
- Fitts, R. H., Mechanisms of Muscular Fatigue. In: J. H. Poortmans, (Ed.), *Principles of Exercise Biochemistry*, Vol. 46. Karger, 2004, pp. 279-300.

- Fitts, R. H., and Widrick, J.J., Muscle mechanics: adaptations with exercise training. In: J. O. Holloszy, (Ed.), Exercise and Sport Sciences Reviews. Williams & Wilkins, New York, 1996, pp. 427-473.
- Frey, N., Frank, D., Lippl, S., Kuhn, C., Kogler, H., Barrientos, T., Rohr, C., Will, R., Muller, O. J., Weiler, H., Bassel-Duby, R., Katus, H. A., Olson, E. N., 2008. Calsarcin-2 deficiency increases exercise capacity in mice through calcineurin/NFAT activation. *J Clin Invest.* 118, 3598-608.
- Gibson, M. C., Schultz, E., 1983. Age-related differences in absolute numbers of skeletal muscle satellite cells. *Muscle Nerve.* 6, 574-80.
- Gladden, L. B., Lactate Transport and Exchange During Exercise. In: L. B. a. S. J. T. Rowell, (Ed.), *Handbook of Physiology.* Oxford University Press, New York, 1996, pp. 614-648.
- Gladden, L. B., 2000. Muscle as a consumer of lactate. *Med Sci Sports Exerc.* 32, 764-71.
- Gladden, L. B., 2008. A lactatic perspective on metabolism. *Med Sci Sports Exerc.* 40, 477-85.
- Gnaiger, E., 2009. Capacity of oxidative phosphorylation in human skeletal muscle: new perspectives of mitochondrial physiology. *Int J Biochem Cell Biol.* 41, 1837-45.
- Gordon, A. M., Homsher, E., Regnier, M., 2000. Regulation of contraction in striated muscle. *Physiol Rev.* 80, 853-924.
- Grady, R. M., Teng, H., Nichol, M. C., Cunningham, J. C., Wilkinson, R. S., Sanes, J. R., 1997. Skeletal and cardiac myopathies in mice lacking utrophin and dystrophin: a model for Duchenne muscular dystrophy. *Cell.* 90, 729-38.
- Hakimi, P., Yang, J., Casadesus, G., Massillon, D., Tolentino-Silva, F., Nye, C. K., Cabrera, M. E., Hagen, D. R., Utter, C. B., Baghdy, Y., Johnson, D. H., Wilson, D. L., Kirwan, J. P.,

- Kalhan, S. C., Hanson, R. W., 2007. Overexpression of the cytosolic form of phosphoenolpyruvate carboxykinase (GTP) in skeletal muscle repatterns energy metabolism in the mouse. *J Biol Chem.* 282, 32844-55.
- Hamilton, M. T., Booth, F. W., 2000. Skeletal muscle adaptation to exercise: a century of progress. *J Appl Physiol.* 88, 327-31.
- Hasty, P., Bradley, A., Morris, J. H., Edmondson, D. G., Venuti, J. M., Olson, E. N., Klein, W. H., 1993. Muscle deficiency and neonatal death in mice with a targeted mutation in the myogenin gene. *Nature.* 364, 501-6.
- Hayashi, S., McMahon, A. P., 2002. Efficient recombination in diverse tissues by a tamoxifen-inducible form of Cre: a tool for temporally regulated gene activation/inactivation in the mouse. *Dev Biol.* 244, 305-18.
- Heydemann, A., Huber, J. M., Demonbreun, A., Hadhazy, M., McNally, E. M., 2005. Genetic background influences muscular dystrophy. *Neuromuscul Disord.* 15, 601-9.
- Holloszy, J. O., Coyle, E. F., 1984. Adaptations of skeletal muscle to endurance exercise and their metabolic consequences. *J Appl Physiol.* 56, 831-8.
- Holloszy, J. O., Oscai, L. B., Don, I. J., Mole, P. A., 1970. Mitochondrial citric acid cycle and related enzymes: adaptive response to exercise. *Biochem Biophys Res Commun.* 40, 1368-73.
- Hughes, S. M., Chi, M. M., Lowry, O. H., Gundersen, K., 1999. Myogenin induces a shift of enzyme activity from glycolytic to oxidative metabolism in muscles of transgenic mice. *J Cell Biol.* 145, 633-42.
- Hughes, S. M., Taylor, J. M., Tapscott, S. J., Gurley, C. M., Carter, W. J., Peterson, C. A., 1993. Selective accumulation of MyoD and myogenin mRNAs in fast and slow adult

- skeletal muscle is controlled by innervation and hormones. *Development*. 118, 1137-47.
- Ishihara, A., Inoue, N., Katsuta, S., 1991. The relationship of voluntary running to fibre type composition, fibre area and capillary supply in rat soleus and plantaris muscles. *Eur J Appl Physiol Occup Physiol*. 62, 211-5.
- Jackman, R. W., Kandarian, S. C., 2004. The molecular basis of skeletal muscle atrophy. *Am J Physiol Cell Physiol*. 287, C834-43.
- Jitrapakdee, S., St Maurice, M., Rayment, I., Cleland, W. W., Wallace, J. C., Attwood, P. V., 2008. Structure, mechanism and regulation of pyruvate carboxylase. *Biochem J*. 413, 369-87.
- Kablar, B., Asakura, A., Krastel, K., Ying, C., May, L. L., Goldhamer, D. J., Rudnicki, M. A., 1998. MyoD and Myf-5 define the specification of musculature of distinct embryonic origin. *Biochem Cell Biol*. 76, 1079-91.
- Kassar-Duchossoy, L., Gayraud-Morel, B., Gomes, D., Rocancourt, D., Buckingham, M., Shinin, V., Tajbakhsh, S., 2004. Mrf4 determines skeletal muscle identity in Myf5:Myod double-mutant mice. *Nature*. 431, 466-71.
- Kiens, B., Essen-Gustavsson, B., Christensen, N. J., Saltin, B., 1993. Skeletal muscle substrate utilization during submaximal exercise in man: effect of endurance training. *J Physiol*. 469, 459-78.
- Knapp, J. R., Davie, J. K., Myer, A., Meadows, E., Olson, E. N., Klein, W. H., 2006. Loss of myogenin in postnatal life leads to normal skeletal muscle but reduced body size. *Development*. 133, 601-10.

- Kontrogianni-Konstantopoulos, A., Ackermann, M. A., Bowman, A. L., Yap, S. V., Bloch, R. J., 2009. Muscle giants: molecular scaffolds in sarcomerogenesis. *Physiol Rev.* 89, 1217-67.
- Kraemer, W. J., Patton, J. F., Gordon, S. E., Harman, E. A., Deschenes, M. R., Reynolds, K., Newton, R. U., Triplett, N. T., Dziados, J. E., 1995. Compatibility of high-intensity strength and endurance training on hormonal and skeletal muscle adaptations. *J Appl Physiol.* 78, 976-89.
- Lin, J., Wu, H., Tarr, P. T., Zhang, C. Y., Wu, Z., Boss, O., Michael, L. F., Puigserver, P., Isotani, E., Olson, E. N., Lowell, B. B., Bassel-Duby, R., Spiegelman, B. M., 2002. Transcriptional co-activator PGC-1 alpha drives the formation of slow-twitch muscle fibres. *Nature.* 418, 797-801.
- Mayne, C. N., Mokrusch, T., Jarvis, J. C., Gilroy, S. J., Salmons, S., 1993. Stimulation-induced expression of slow muscle myosin in a fast muscle of the rat. Evidence of an unrestricted adaptive capacity. *FEBS Lett.* 327, 297-300.
- Meadows, E., Cho, J. H., Flynn, J. M., Klein, W. H., 2008. Myogenin regulates a distinct genetic program in adult muscle stem cells. *Dev Biol.* 322, 406-14.
- Minchenko, O., Opentanova, I., Caro, J., 2003. Hypoxic regulation of the 6-phosphofructo-2-kinase/fructose-2,6-bisphosphatase gene family (PFKFB-1-4) expression in vivo. *FEBS Lett.* 554, 264-70.
- Moresi V., W. A. H., Meadows E., Flynn J.M., McAnally J., Shelton J.M., Backs J., Klein W.H., Richardson J.A., Bassel-Duby R., Olson E.N., 2010. Myogenin and class II HDACs trigger skeletal muscle atrophy by inducing E3 ubiquitin ligases. In Preparation.

- Nabeshima, Y., Hanaoka, K., Hayasaka, M., Esumi, E., Li, S., Nonaka, I., Nabeshima, Y., 1993. Myogenin gene disruption results in perinatal lethality because of severe muscle defect. *Nature*. 364, 532-5.
- Ohkawa, Y., Marfella, C. G., Imbalzano, A. N., 2006. Skeletal muscle specification by myogenin and Mef2D via the SWI/SNF ATPase Brg1. *Embo J*. 25, 490-501.
- Olson, E. N., Klein, W. H., 1994. bHLH factors in muscle development: dead lines and commitments, what to leave in and what to leave out. *Genes Dev*. 8, 1-8.
- Olson, E. N., Williams, R. S., 2000. Remodeling muscles with calcineurin. *Bioessays*. 22, 510-9.
- Owen, O. E., Morgan, A. P., Kemp, H. G., Sullivan, J. M., Herrera, M. G., Cahill, G. F., Jr., 1967. Brain metabolism during fasting. *J Clin Invest*. 46, 1589-95.
- Pedersen, T. H., Nielsen, O. B., Lamb, G. D., Stephenson, D. G., 2004. Intracellular acidosis enhances the excitability of working muscle. *Science*. 305, 1144-7.
- Pette, D., Tyler, K. R., 1983. Response of succinate dehydrogenase activity in fibres of rabbit tibialis anterior muscle to chronic nerve stimulation. *J Physiol*. 338, 1-9.
- Powers, S. K., Ji, L. L., Leeuwenburgh, C., 1999. Exercise training-induced alterations in skeletal muscle antioxidant capacity: a brief review. *Med Sci Sports Exerc*. 31, 987-97.
- Rawls, A., Morris, J. H., Rudnicki, M., Braun, T., Arnold, H. H., Klein, W. H., Olson, E. N., 1995. Myogenin's functions do not overlap with those of MyoD or Myf-5 during mouse embryogenesis. *Dev Biol*. 172, 37-50.
- Rodnick, K. J., Reaven, G. M., Haskell, W. L., Sims, C. R., Mondon, C. E., 1989. Variations in running activity and enzymatic adaptations in voluntary running rats. *J Appl Physiol*. 66, 1250-7.

- Rudnicki, M. A., Schlegelsberg, P. N., Stead, R. H., Braun, T., Arnold, H. H., Jaenisch, R., 1993. MyoD or Myf-5 is required for the formation of skeletal muscle. *Cell*. 75, 1351-9.
- Sabourin, L. A., Rudnicki, M. A., 2000. The molecular regulation of myogenesis. *Clin Genet*. 57, 16-25.
- Schiaffino, S., Sandri, M., Murgia, M., 2007. Activity-dependent signaling pathways controlling muscle diversity and plasticity. *Physiology (Bethesda)*. 22, 269-78.
- Schluter, J. M., Fitts, R. H., 1994. Shortening velocity and ATPase activity of rat skeletal muscle fibers: effects of endurance exercise training. *Am J Physiol*. 266, C1699-73.
- Schultz, E., Jaryszak, D. L., Valliere, C. R., 1985. Response of satellite cells to focal skeletal muscle injury. *Muscle Nerve*. 8, 217-22.
- Service, F. J., 1995. Hypoglycemic disorders. *N Engl J Med*. 332, 1144-52.
- Sexton, W. L., 1995. Vascular adaptations in rat hindlimb skeletal muscle after voluntary running-wheel exercise. *J Appl Physiol*. 79, 287-96.
- Tang, H., Goldman, D., 2006. Activity-dependent gene regulation in skeletal muscle is mediated by a histone deacetylase (HDAC)-Dach2-myogenin signal transduction cascade. *Proc Natl Acad Sci U S A*. 103, 16977-82.
- Tang, H., Macpherson, P., Marvin, M., Meadows, E., Klein, W. H., Yang, X. J., Goldman, D., 2009. A histone deacetylase 4/myogenin positive feedback loop coordinates denervation-dependent gene induction and suppression. *Mol Biol Cell*. 20, 1120-31.
- Venuti, J. M., Morris, J. H., Vivian, J. L., Olson, E. N., Klein, W. H., 1995. Myogenin is required for late but not early aspects of myogenesis during mouse development. *J Cell Biol*. 128, 563-76.
- Wallace, G. Q., McNally, E. M., 2009. Mechanisms of muscle degeneration, regeneration, and repair in the muscular dystrophies. *Annu Rev Physiol*. 71, 37-57.

- Wang, N., Hikida, R. S., Staron, R. S., Simoneau, J. A., 1993. Muscle fiber types of women after resistance training--quantitative ultrastructure and enzyme activity. *Pflugers Arch.* 424, 494-502.
- Wang, Y. X., Zhang, C. L., Yu, R. T., Cho, H. K., Nelson, M. C., Bayuga-Ocampo, C. R., Ham, J., Kang, H., Evans, R. M., 2004. Regulation of muscle fiber type and running endurance by PPARdelta. *PLoS Biol.* 2, e294.
- Wehling-Henricks, M., Oltmann, M., Rinaldi, C., Myung, K. H., Tidball, J. G., 2009. Loss of positive allosteric interactions between neuronal nitric oxide synthase and phosphofructokinase contributes to defects in glycolysis and increased fatigability in muscular dystrophy. *Hum Mol Genet.* 18, 3439-51.
- Windisch, A., Gundersen, K., Szabolcs, M. J., Gruber, H., Lomo, T., 1998. Fast to slow transformation of denervated and electrically stimulated rat muscle. *J Physiol.* 510 (Pt 2), 623-32.
- Wu, Z., Puigserver, P., Andersson, U., Zhang, C., Adelmant, G., Mootha, V., Troy, A., Cinti, S., Lowell, B., Scarpulla, R. C., Spiegelman, B. M., 1999. Mechanisms controlling mitochondrial biogenesis and respiration through the thermogenic coactivator PGC-1. *Cell.* 98, 115-24.
- Yalcin, A., Telang, S., Clem, B., Chesney, J., 2009. Regulation of glucose metabolism by 6-phosphofructo-2-kinase/fructose-2,6-bisphosphatases in cancer. *Exp Mol Pathol.* 86, 174-9.

Eric Meadows
Curriculum Vitae

Current Address

Department of Biochemistry and Molecular Biology
University of Texas MD Anderson Cancer Center
1515 Holcombe Blvd
Houston, TX 77030
Phone: 713-834-6264
Email: ermeadows@mdanderson.org

Home Address

2662 Skyview Grove Ct
Houston, TX 77047
Phone: 817-266-0423

Education

University of Texas Health Science Center, Houston, TX
Doctor of Philosophy, Biochemistry and Molecular Biology, In Progress

University of Texas Health Science Center, Houston, TX
Master of Science, Biochemistry and Molecular Biology, 2006

University of Texas at Arlington, Arlington, TX
Bachelor of Science, Biology, 2003

Research and Training

- | | |
|--------------|---|
| 2006-present | PhD Student, Graduate Training Program in Genes and Development, Laboratory of Dr. William Klein, University of Texas MD Anderson Cancer Center. |
| 2004-2006 | MS Student, Graduate Training Program in Genes and Development, Laboratory of Dr. William Klein, University of Texas MD Anderson Cancer Center. |
| 2003-2004 | Research Technician II, Laboratory of Dr. Eric Olson, Department of Molecular Biology, University of Texas Southwestern Medical Center at Dallas. |
| 2001-2003 | Student Intern, Laboratory of Dr. Eric Olson, Department of Molecular Biology, University of Texas Southwestern Medical Center at Dallas. |

Lab Techniques and Experience

- Most standard Molecular Biology techniques including plasmid preps, PCR, Western Blotting, Southern/Northern Blotting, etc.
- Experience in mouse husbandry and genotyping
- Experience crossing and maintaining *Drosophila* fly stocks.

Publications

Vega RB, Matsuda K, Oh J, Barbosa AC, Yang X, **Meadows E**, McAnally J, Pomajzl C, Shelton JM, Richardson JA, Karsenty G, Olson EN. Histone deacetylase 4 controls chondrocyte hypertrophy during skeletogenesis. *Cell*, 2004.

Vega RB, Harrison BC, **Meadows E**, Roberts CR, Papst PJ, Olson EN, McKinsey TA. Protein kinases C and D mediate agonist-dependent cardiac hypertrophy through nuclear export of histone deacetylase 5. *Mol. Cell. Biol.*, 2004.

Knapp JR, Davie JK, Myer A, **Meadows E**, Olson EN, Klein WH. Loss of myogenin in postnatal life leads to normal skeletal muscle but reduced body size. *Development*, 2006.

Davie JK, Cho JH, **Meadows E**, Flynn JM, Knapp JR, Klein WH. Target gene selectivity of the myogenic basic helix-loop-helix transcription factor myogenin in embryonic muscle. *Developmental Biology*, 2007.

Rishniw M, Fisher PW, Doran RM, **Meadows E**, Klein WH, Kotlikoff MI. Smooth muscle persists in the *muscularis externa* of developing and adult mouse esophagus. *Journal of Muscle Research and Cell Motility*, 2007

Meadows E, Cho JH, Flynn JM, Klein WH. Myogenin regulates a distinct genetic program in adult muscle stem cells. *Developmental Biology*, 2008.

Tang H, Marvin M, Macpherson P, Mardon G, **Meadows E**, Klein W, Yang WJ, Goldman D. An HDAC4/Myogenin positive feedback loop coordinates denervation-dependent gene induction and repression in adult skeletal muscle. *Mol Biol Cell*, 2008.

Moresi V, Williams A, **Meadows E**, Flynn J, McAnally J, Shelton J, Backs J, Klein W, Richardson J, Bassel-Duby R, Olson E. Myogenin and class II HDACs trigger skeletal muscle atrophy by inducing E3 ubiquitin ligases. In preparation.